



Addis Ababa University
Ababa Institute of Technology
School of Electrical and Computer Engineering

**Analysis of Blind Adaptive Equalization Techniques for Audio
Broadcast System**

by
Tewodros Amsalu
Advisor
Dr. -Ing. Dereje Hailemariam

A Thesis Submitted to the School of Graduate Studies of Addis Ababa
University in Partial Fulfillment of the Requirements for the Degree of
Masters of Science in Electrical Engineering

May, 2017
Addis Ababa, Ethiopia

Addis Ababa University
Addis Ababa Institute of Technology
School of Electrical and Computer Engineering
**Analysis of Blind Adaptive Equalization Techniques for Audio
Broadcast System**

Tewodros Amsalu

Approval by Board of Examiners

Chairman, School Graduate

Committee

Dr. -Ing. Dereje Hailemariam

Advisor

Internal Examiner

External Examiner

Signature

Signature

Signature

Signature

Declaration

I, the undersigned, declare that this thesis is my original work, has not been presented for a degree in this or any other university, and all sources of materials used for the thesis have been fully acknowledged.

Tewodros Amsalu

Name

Signature

Place: Addis Ababa

Date of Submission: _____

This thesis has been submitted for examination with my approval as a university advisor.

Dr.-Ing. Dereje Hailemariam

Advisor's Name

Signature

ABSTRACT

The wireless channel, in general, and the audio broadcasting range in particular is prone to time dispersion, which causes inter symbol interference (ISI). This dispersive channel must be compensated (equalized) by making a communication system adaptive to the time varying properties of the channel. Practically, in digital audio broadcasting training sequences may not be available to implement the adaptation, which makes blind adaptive equalization methods more appropriate for such application.

In this thesis the performance of three blind adaptive equalization techniques; namely, constant modulus algorithm (CMA), multi modulus algorithm (MMA) and fractionally spaced constant modulus algorithm (FS CMA) are investigated for application in audio broadcasting. This investigation is part of a joint project between Information Networks Security Agency (INSA) of Ethiopia and the Addis Ababa University (AAU) that intends to implement advanced digital receiver for a certain application. To capture the broadcasting environment three channel models are used. Moreover, 16-quadrature amplitude modulation (QAM) is considered for the simulation. Symbol error rate (SER), rate of convergence, stability, complexity and audibility are used as performance metrics.

The simulation result shows that FSCMA has much better SER performance than CMA & MMA which provide 1 to 1.5 SNR advantages over the other two methods. The three equalizers are able to recover the transmitted audio bit streams when the channel do not introduce phase shift; MMA being the only method capable of recovering phase shift. On convergence, once the algorithms converged they stay stable until the channel condition start to change. Finally, it was noted that the three equalizers are able to equalize the received input data faster than the sampling rate of the audio signal.

From all the simulation results, FS CMA has better or comparable performance than the CMA and MMA. Therefore, the thesis recommends FS CMA for implementation by INSA with the assumption that a separate unit will handle the phase recovery implementation.

ACKNOWLEDGMENTS

First and foremost I would like to thank my God for give me the strength to finish the thesis and without whom nothing is possible.

I would like to express my sincere gratitude to my adviser Dr. -Ing. Dereje Hailemariam for giving me the opportunity to work with him, his support and unreserved continuous follow up in order to complete this thesis.

I would also like to extend gratitude to my families and friends who provide me valuable feedback and support throughout the course of doing this thesis.

TABLE OF CONTENTS

ABSTRACT	iv
ACKNOWLEDGMENTS	v
TABLE OF CONTENTS	vi
LIST OF TABLES.....	x
LIST OF FIGURES.....	xi
ABBREVIATIONS.....	xiv
CHAPTER I: Introduction.....	1
1.1 Statement of the Problem	2
1.2 Objective	2
1.2.1 General Objective	2
1.2.2 Specific Objectives.....	2
1.3 Literature Review	3
1.4 Methodology	5
1.5 Scope and Limitation	6
1.5.1 Scope of the Thesis.....	6
1.5.2 Limitation of the Thesis.....	7
1.6 Contribution	7
1.7 Thesis Layout	7
CHAPTER II: Terrestrial Digital Audio Broadcasting System.....	8
2.1 Introduction.....	8
2.2 Digital Broadcasting Standards.....	10
2.2.1 Digital Audio Broadcasting	10
2.2.2 Integrated Services Digital Broadcasting–Terrestrial Sound Broadcasting	11
2.2.3 Digital Radio Mondiale	12
2.2.4 Other Standards.....	13
2.3 ATSC-T Standard.....	13

2.3.1 ATSC-T System Block Diagram.....	14
2.3.2 Source Coding and Compression.....	15
2.3.3 Service Multiplex and Transport.....	16
2.3.4 Radio Frequency Transmission	18
2.3.4.1 Transmission Characteristics for Terrestrial Broadcast	19
2.3.4.2 Data Organization	20
2.3.4.3 Channel Error Protection.....	22
2.3.4.4 Synchronization.....	24
2.3.2.5 Modulation.....	25
2.3.5 ATSC DTV Receiver.....	26
CHAPTER III: Wireless Communication Channel	28
3.1 Introduction.....	28
3.2 Small Scale Multipath Fading.....	30
3.2.1 Fading Effects Due to Multipath Time Delay Spread	32
3.2.1.1 Flat Fading	32
3.2.1.2 Frequency Selective Fading	32
3.2.2 Fading Effects Due to Doppler Spread.....	33
3.2.2.1 Fast Fading	33
3.2.2.2 Slow Fading.....	34
3.2.3 Rayleigh and Ricean Distributions	34
3.2.3.1 Rayleigh Fading Distribution	34
3.2.3.2 Ricean Fading Distribution	35
3.3 Broadcast Channel Models	35
3.3.1 Path loss models	35
3.3.1.1 Empirical path loss model.....	36
3.3.1.1.1 Recommendation ITU-R P.1546-5	36
3.3.1.1.2 The Okumura Model.....	36
3.3.1.1.3 Hata Model.....	37

3.3.1.2 Site-Specific Models for Path Loss	38
3.3.1.2.1 Ray-Tracing Technique.....	39
3.3.2 Impulse-Response Models	39
3.3.2.1 Statistical Models for Multipath Fading Channels.....	39
3.3.2.1.1 Two-Ray Rayleigh Fading Model	40
3.3.2.1.2 Saleh and Valenzuela Model	40
3.3.2.2 Deterministic Models of Time-Delay Spread	41
3.3.1.2.1 Ray Tracing for Time-Delay Spread	41
3.3.1.2.2 Virtual Reflection Points.....	41
3.3.2.3 Models Based on Measurement Results.....	42
3.3.1.1.1 Direct Pulse Measurements	42
3.3.1.1.2 Swept-frequency measurements	43
3.4 Channel Models used for the Simulation	43
3.4.1 Measured Channel Impulse Response	44
3.4.2 Joint Technical Committee Model.....	45
3.4.3 Exponential Channel Model	45
CHAPTER IV: Blind Adaptive Equalization	47
4.1 Introduction.....	47
4.2 Equalization in QAM Data Communication System	47
4.3 Equalizers Classification.....	49
4.4 Trained Equalizers	51
4.4.1 Linear Equalizer.....	51
4.4.1.1 Zero Forcing Equalizer	52
4.4.1.2 Minimum Mean Square Error Equalizer.....	53
4.4.2 Non Linear Equalizers	55
4.5 Blind Equalizers.....	55
4.5.1 Constant Modulus Algorithm	56
4.5.2 Multiple Module Algorithm	58

4.5.3 Fractionally Spaced CMA	59
4.6 Equalizers Performance Parameters	61
CHAPTER V: Simulation and Result	62
5.1 Simulation Steps and Parameters.....	62
5.2 Simulation Block Diagram	63
5.3 Simulation Results.....	67
5.3.1 Constant Module Algorithm Results.....	67
5.3.1.1 Stored channel impulse response.....	68
5.3.1.2 Joint Technical Committee Model.....	69
5.3.1.3 Exponential Decaying Channel	70
5.3.1.4 Additional CMA Performance Matrix	72
5.3.2 Multi Module Algorithm Result.....	74
5.3.2.1 Stored channel impulse response.....	75
5.3.2.2 Joint Technical Committee Model.....	75
5.3.2.3 Exponential Decaying Channel	77
5.3.2.4 Additional CMA Performance Matrix	79
5.3.3 Fractional Space Constant Module Algorithm Result	80
5.3.3.1 Stored channel impulse response.....	81
5.3.3.2 Joint Technical Committee Model.....	81
5.3.3.3 Exponential Decaying Channel	82
5.3.3.4 Additional CMA Performance Matrix	84
5.4 Summery	85
CHAPTER VI: Conclusion and Future Works.....	90
6.1 Conclusion	90
6.2 Future Works	91
REFERENCES.....	92
Appendix A: Raised Cosine Pulse Shaping Filter	98

LIST OF TABLES

Table	Page
Table 2.1: DAB & DAB+ System.....	11
Table 2.2: ISDB Terrestrial Sound Broadcasting System	12
Table 2.3: DRM System	13
Table 2.4: Parameters for VSB Transmission Modes	20
Table 3.1: JTC Channel Model Parameters for Outdoor Urban	45
Table 5.1: Simulation Parameters Summery	62
Table 5.2: Equalizers SER Ccompared to DAB ToA	86
Table 5.3: Equalizations Methods Performance Summery	89

LIST OF FIGURES

Figure	Page
Figure 2.1: ITU-R digital terrestrial television broadcasting model.....	14
Figure 2.2: Video coding in relation to the ATSC DTV system	15
Figure 2.3: Audio subsystem within the ATSC DTV system	16
Figure 2.4: A functional overview of the ATSC transport subsystem	18
Figure 2.5: 8-VSB transmitter block diagram, RF transmission system	20
Figure 2.6: VSB data frame without extra field sync	22
Figure 2.7: Randomizer polynomial	23
Figure 2.8: Trellis encoder	24
Figure 2.9: 8-VSB data segment	25
Figure 2.10: 8-VSB receiver block diagram	26
Figure 3.1: ISI Caused by Multi-Path Distortion.....	29
Figure 3.2: Fading channel manifestation.....	29
Figure 3.3: Multipath propagation in rural area.....	31
Figure 3.4: Direct pulse RF Channel measurement system.....	42
Figure 3.5: Frequency domain channel sounder.....	43
Figure 3.6: Stored channel impulse responses	44
Figure 3.7: Exponential decaying channel.....	46
Figure 4.1: Baseband representation of a QAM data communication system.....	48
Figure 4.2: Adaptive blind equalization system.....	49
Figure 4.3: Classification of adaptive equalizers	50
Figure 4.4: Structure of a linear transversal equalizer.....	52

Figure 4.5: FIR filter as an MMSE equalizer.....	54
Figure 4.6: Baseband Model for a Communication System with FSE.....	59
Figure 4.7: Vector representation for an FSE.....	61
Figure 5.1: Raised cosine pulse and its frequency response for beta 0.35.....	63
Figure 5.2: Simulation block diagram	64
Figure 5.3: Channels impulse response for raised cosine	65
Figure 5.4: Flow chart for audio and random bit stream simulation	66
Figure 5.5: CMA Implementation flow chart.....	67
Figure 5.6: CMA Equalizer for stored channel and random generated data	68
Figure 5.7: CMA Equalizer for stored channel response for an audio data	69
Figure 5.8: CMA Equalizer for JTC channel for random data source	69
Figure 5.9: CMA Equalizer for JTC channel with an audio file source	70
Figure 5.10: CMA Equalizer for exponential decaying channel.....	71
Figure 5.11: CMA Equalized signal at 4th iteration for different SNR.....	71
Figure 5.12: CMA Equalizer for exponentially decaying channel for audio data source.....	72
Figure 5.13: CMA Equalizer for a complex channel at 10 dB SNR.....	73
Figure 5.14: CMA Equalizer using phase recovery loop.....	73
Figure 5.15: MMA Simulation flow chart.....	74
Figure 5.16: MMA Equalizer for stored channel response for random data source	75
Figure 5.17: MMA Equalizer for JTC channel taken with random data source.....	76
Figure 5.18: MMA Equalizer for JTC channel at 13.5 dB for an audio data source.....	76
Figure 5.19: MMA Equalizer for exponentially decaying channel	77
Figure 5.20: MMA Equalized for different SNR	78
Figure 5.21: MMA Equalizer for exponentially decaying channel for audio	78

Figure 5.22: MMA phase recovery for exponentially decaying channel	79
Figure 5.23: FS CMA Simulation flow chart.....	80
Figure 5.24: FS CMA Equalizer for randomly generated data source	81
Figure 5.25: FS CMA Equalizer for randomly generate source in JTC channel.....	82
Figure 5.26: FS CMA Equalization for JTC channel for audio Source.....	82
Figure 5.27: FS CMA in exponentially decaying channel for randomly generated source.....	83
Figure 5.28: FS CMA Equalization at different SNR.....	83
Figure 5.29: FS CMA Equalizer for a complex channel at 10 dB SNR.....	84
Figure 5.30: FS CMA with phase recovery loop for exponentially decaying channel.....	85
Figure 5.31: SER v Iteration for CMA, MMA & FS CMA at 10 dB, complex impulse response channel	86
Figure 5.32: BER v Iteration/SNR for CMA, MMA & FS CMA for JTC channel	87
Figure 5.33: SER at different step size for JTC channel at 13.5 dB	88
Figure A.1: Raised cosine impulse & frequency reponse.....	99

ABBREVIATIONS

8-VSB	Vestigial sideband modulation with 8 discrete amplitude levels
16-VSB	Vestigial sideband modulation with 16 discrete amplitude levels
A/D	Analog to digital converter.
AAC	Advanced Audio Coding
AAU	Addis Ababa University
AC	Audio Compression
AM	Amplitude Modulation
ATM	Asynchronous Transfer Mode.
ATSC DTV	Advanced Television Systems Committee Digital Television
AWGN	Additive White Gaussian Noise
BST-OFDM	Band Segmented structure orthogonal frequency-division multiplexing
CELP	Code Excited Linear Predictive
CM	Constant Modulus
CMA	Constant Module Algorithm
COFDM	Coded Orthogonal frequency-division multiplexing
DAB	Digital Audio Broadcasting
DFE	Decision Feedback Equalization
DQPSK	Differential phase-shift keying
DRM	Digital Radio Mondiale
DTMB	Digital Terrestrial Television Multimedia Broadcasting
DTx	Distributed Transmission
DVB	Digital Video Broadcasting
DVB-T	Digital Video Broadcasting Terrestrial
E8-VSB	Enhanced 8-VSB
ERP	Effective Radiated Power

ETSI	European Telecommunications Standards Institute
FDTD	Finite Difference Time Domain
FEC	Foreword Error Correction
FIR	Finite Impulse Response
FM	Frequency Modulated
FS CMA	Fractional Space Constant Module Algorithm
FSE	Fractionally Spaced Equalizer
HDTV	High Definition Television
HE AAC	High Efficiency Advanced Audio Coding
HOS	Higher Order Statistics
HVXC	Harmonic Vector Excitation
IBOC	In-Band On-Channel
IEC	International Electrotechnical Commission
IF	Intermediate Frequency
INSA	Information Networks Security Agency
ISDB	Integrated Services Digital Broadcasting
ISDB-T	Integrated Services Digital Broadcasting Terrestrial
ISDB-TSB	Integrated Services Digital Broadcasting–Terrestrial Sound Broadcasting
ISI	Inter Symbol Interference
ISO	International Organization for Standardization.
ITU	International Telecommunication Union
JTC	Joint Technical Committee
LMS	Least Mean Square
LOS	Line of Sight
LW	Long Wave
MCMA	Modified Constant Modulus Algorithm
MFNs	Multiple Frequency Networks
MLSE	Maximum Likelihood Sequence Estimation
MMA	Multi Module Algorithm
MP2	MPEG 1-Layer 2

MPC	Multi Path Component
MPEG	Moving Picture Experts Group
MPEG-2-TS	MPEG-2 Transport Stream
MW	Medium Wave
OFDM	Orthogonal frequency-division multiplexing
PDF	Probability Density Function
PLL	Phase Lock Loop
PRBS	Pseudo Random Binary Sequence
PRS	Pseudo Random Sequence
PSIP	Program and System Information Protocol
QAM	Quadrature Amplitude Modulation
QPSK	Quadrature Phase Shift Keying
RCA	Reduced Constellation Algorithm
RF	Radio Frequency
RS	Reed Solomon
S/N	Signal to Noise Ratio
SDTV	Standard Definition Television
SFNs	Single Frequency Networks
SGD	Stochastic Gradient Descent
SW	Short Wave
ToA	Threshold of Audibility
TS	Transport Stream
TSE	T-Spaced Equalization
VHF	Vary High Frequency
VRP	Virtual Reflection Points

CHAPTER I

Introduction

The introduction of digital broadcasting brings a considerable improvement in the quality of received audio/video signal and more channel content offerings. Nevertheless, there is a continuous demand for improved services which in turn, requires supporting high data rate through band limited channel [1]. This brings its own complications to meet the demand for improved services specifically given that the channel is constantly varying multi path that causes inter symbol interference (ISI).

In the same way to other type of broadcasting systems, audio broadcasting systems are exposed to ISI. Hence, the audio signal processing at receivers must address the ISI problem. Among the different methods used to mitigate ISI equalizations are one of the available techniques. Due to constantly varying characteristic of wireless broadcasting channels the equalizers must adaptively track the channel time varying characteristics [1].

Adaptive equalization can be classified into training-based or blind equalization. In training-based equalization a particular training sequence available both at the transmitter and receiver is transmitted in proper synchronism for the purpose of initial training of equalizer's weights. However, in many wireless digital audio broadcasting systems the transmission of training sequence is very costly in terms of data throughput [2] especially when there is high mobility. Blind adaptive equalization methods mitigate the ISI without the need for training sequences; this makes these equalizers preferable over the training-based equalizers for broadcasting environment [2].

Blind equalizers exploit known statistical properties of the transmit signal to estimate both channel and data. The equalizers' coefficients are adjusted in such a way that certain

statistical properties of the equalizers' outputs match known statistical properties of the transmit signal. There are variants of blind equalization methods used in various applications; some of the methods frequently named in literatures include: constant modulus algorithm (CMA), multi modulus algorithm (MMA), blind decision feedback equalizer and fractionally spaced constant modulus algorithm (FS CMA). Audio broadcasting system are one of the area where blind adaptive equalization techniques are ideal solution to address the problem of ISI, thus the thesis will focus on it.

1.1 Statement of the Problem

As indicated channel condition for audio broadcasting system is constantly varying, which requires in depth analysis to understand it first and then identify and implement optimal blind adaptive equalizers to mitigate its effects. The performance of the different blind adaptive equalization methods varies depending on the application and environment in which the algorithms are implemented. Information Networks Security Agency (INSA) of Ethiopia is working with the Addis Ababa University (AAU) on an industrial project that aims to implement optimal blind adaptive equalizations to mitigate ISI effects for digital audio broadcasting application for a certain application. Hence, the motivation of the thesis is identifying an optimal blind adaptive equalization method to mitigate ISI for audio broadcasting system and thus, address the need of the industry.

1.2 Objective

1.2.1 General Objective

The main objective of the thesis is to identify and implement selected adaptive blind equalization techniques for an application in digital audio broadcast system.

1.2.2 Specific Objectives

The following are the specific objectives expected from the thesis:

- Understand the effect of multipath wireless channels on received audio signals in broadcasting systems. Appropriate channel models are also identified.

- Understand blind adaptive equalization methods, with specific focus on broadcasting systems, used to mitigate the problem of ISI prone channels.
- Study and implement the selected blind equalization techniques; namely, CMA, MMA and FS CMA using Matlab.
- Analyze the performance of the selected equalization techniques in terms symbol error rate (SER), rate of convergence, stability and complexity as the metrics and recommend one optimal technique.

1.3 Literature Review

The concept of training less blind equalizer is first recommended by Y. Sato in 1975 [3]. The original Y. Sato method was converted into a class of algorithms having some desired convergence characteristic by Benveniste et al. [4]. The breakthrough algorithm, CMA, for blind equalization was discovered independently by Godard [5] and Treichler et al. [6].

CMA is the most popular and robustness blind adaptive equalization method [7]. CMA uses gradient descent-based equalization algorithm, which exploits the constant modularity of the transmitted signal to adapt the equalizer parameters or weights. Any deviation of the received signal amplitude from the constant module is considered as a distortion introduced by the channel [8]. While CMA provides reliable convergence, the CMA cost function does not track the phase shift in the constellation; as a consequence the equalizer output signal suffers from an arbitrary phase shift. Hence, in steady-state operation phase shift recovery system is required after the equalizer output that can recover the phase shift back to the right position. The phase recovery system increases the complexity to system [7-11].

Indicating successful equalization result the CMA blind equalization method is recommended for quadrature amplitude modulation (QAM) techniques by analyzing the performance of the algorithm for 16 and 64-QAM modulated signal in a linear band-limited channel condition [12, 13].

The modified constant modulus algorithm (MCMA) that accomplishes blind equalization and carrier phase recovery simultaneously is proposed by Oh and Chin [14]. Independently, Yang et al. also proposed a modified CMA called the multi modulus algorithm [2, 15].

Yang et al. combined the reliable convergence and simple implementation benefits of the reduced constellation algorithm (RCA) and CMA, respectively, to introduce the MMA. In addition, MMA provides more flexibility, better suited to take advantage of the symbol statistics of certain types of signal constellations, and does not need the addition of a phase recovery system in steady-state in steady-state operation [2].

The phase recovery capability of MMA gives the algorithm much attention and coverage for implementation. A mathematical analysis of the MMA, which can perform joint blind equalization and carrier recovery for QAM signal constellations including analytic verification of a discrete-time first-order phase-locked loop hidden inside the MMA, is presented in [10]. The analysis results indicate that the MMA has implicitly incorporates a phase-tracking loop, which enable automatically carrier phase recovery and remove ISI simultaneously [10]. The performance gain on the reduction in complexity from the phase recovery capability and better data rate are the factor consider in the recommendation of MMA equalizations method for QAM modulation [16].

A practical CMA based joint Fractionally Spaced Equalization (FSE) and timing recovery solution for blind equalization and timing recovery is proposed for fast-fading and frequency selective wireless communication channels with a differential modulation employed to deal with any arbitrary carrier offset[17]. It is indicated that the proposed equalization method has good performance than T-Spaced Equalization (TSE) techniques in terms of mean square error (MSE) and BER performance in wireless fading channels [17].

A convergence analysis of Godard/CMA FSEs that proves the important advantages provided by the FSE structure is also presented in [18], the analysis result indicate that the result of the analysis changes the belief that fractionally spaced CMA equalizers with

complex inputs is a straightforward extension with similar results of CMA. It is also indicated that the use of FSE allows the exploitation of the channel diversity that supports two important conclusions of great practical significance: a finite-length channel satisfying a length-and-zero condition allows Godard/CMA FSE to be globally convergent, and the linear FSE filter length need not be longer than the channel delay spread [18]. The robustness of FSE CM cost function minima in the presence of additive channel noise is also analyzed and shown that the noise introduces a smoothing effect on the FSE CM cost function, which sets as a constraint on the output noise enhancement [19].

In review of the literatures it is solid clear that various research works has already been done to mitigate ISI using blind equalization methods. However, in my survey the papers do not cover in depth the different channel models of broadcasting environment and the different available equalization methods to address the specific case of audio broadcasting ISI problem.

1.4 Methodology

The thesis is based on books, articles and journals written on the subject. The work started with studying the different equalization methods for mitigating ISI with high focus on the blind equalization methods. After thoroughly understanding selected blind equalization methods a programmable flow chart is developed for each of the selected equalization method.

The simulation of the equalizer methods started with CMA using randomly generated bit streams with simple channel impulse response of $[0.8, 0.2]$, after confirming that simulation able to recover the randomly bits the work of apply the equalizer to an audio broadcast system started.

In order to apply the equalization to audio broadcast system, books and literatures written on audio broadcasting and wireless channels are used. Using the information in the reference, the channel models which represent the broadcasting environment at large is

selected and then representative channels from each of the selected channel models are taken from the books and literature.

The application of the simulation to audio signal is done using uncompressed *.wav audio file. As the audio file is already sampled it is directly imported to the Matlab program (*.m file) and then quantized, changed to bit stream and modulated before it pass through the selected multipath channel.

The audio signal is recover first by passing the received signal through the equalizer, matched filter, demodulated, inverse quantized and then the audio signal is reconstructed using the sampling rate read from the *.wav file.

Finally, the same process is applied for MMA and FS CMA equalization method and then their performance is compared using the result found from the Matlab simulation.

1.5 Scope and Limitation

1.5.1 Scope of the Thesis

The scope of the thesis covers simulation and performance analysis of CMA, MMA and FS CMA adaptive blind equalization methods and the recommendation of one of these methods for audio broadcasting. The performance analyses and recommendation are based on SER, rate of convergence, stability and complexity using 16-QAM modulation. The simulation is done using entirely the Matlab simulation tool.

The thesis uses channels defined on books and literature for the broadcasting channel models without any adaptation or change.

In the simulation some functionalities of the receiver decoder are included these blocks are out of the scope of the thesis included in the simulation to validate the proper operation of the equalizers and lightly covered in the thesis.

Finally, the simulation only considers the effects of multipath & additive white Gaussian noise (AWGN) signal degradation caused by other type of interferences are included.

1.5.2 Limitation of the Thesis

The thesis is entirely based on simulation; hence, it does not include a demonstration in a real communication environment and limited to random bits and an audio file.

Even though, there are numbers of blind equalization methods the thesis covers only CMA, MMA and FS CMA blind equalization methods. Hence, the recommendation is limited to these methods.

At last, in real broadcasting environment multipath and AWGN may not be the only interfaces affecting the transmitted signal at the receiver.

1.6 Contribution

The contribution of this thesis is in the area of blind adaptive equalization method and audio signal recovery. Specific contributions of the work are in the following areas.

- Performance investigation of the adaptive blind equalization specifically for audio broadcasting system.
- Investigation of the audio data recovery capability of the considered adaptive blind equalization algorithms for different channel types.
- Assessing the impact of randomizer in improving the adaptive blind equalization algorithms audio signal recovery.

1.7 Thesis Layout

The thesis is organized in such a way that it gives a clear flow and understanding of the subject matter. The second and third Chapters will provide an overview of terrestrial digital broadcasting system and broadcasting communication channels respectively and then in the fourth Chapter adaptive equalization techniques used to mitigate channel distortion is presented. In the fifth Chapter the simulation and results for the CMA, MMA and FS CMA equalization technique is presented. Finally on the sixth Chapter the conclusion and future work part is covered.

CHAPTER II

Terrestrial Digital Audio Broadcasting System

2.1 Introduction

The success story of radio and television was originally based on terrestrial transmission; although at the end of the twentieth century other distribution forms like cable and satellite had significantly overrun the terrestrial platform in many countries. There are still many regions around the globe where terrestrial broadcasting constitutes the primary means to deliver radio and television programmes to the listeners and viewers [20].

When it comes to technological development, analogue terrestrial broadcasting is under pressure due to two fundamental problems. Firstly, with the advent of digital media such as smart phone and audio file format like Moving Picture Experts Group 1(MPEG-1) and MPEG-2 Audio Layer 3(MP3) provides customers to get used to high audio and video quality. Moreover, the lacks of spectrum do not allow to provide a greater variety of programmes. Hence, more efficient spectrum usages became an important issue and achieved by the development of digital terrestrial broadcasting systems [20-22].

Digital broadcasting increases the capacity of transmission networks by improving spectrum efficiency. Typical spectrum efficiency gains are expected in the range of 5 - 15 times, depending on the digital transmission standard, modulation scheme, network configuration (e.g. compression, code rate, guard interval, etc.), service bitrate allocation and frequency planning. Moreover, digital broadcasting has additional primary objectives of high transmission quality, and a large enough data capacity to allow for a sufficient number of attractive programs [22].

Today, we live in a world of digital communication systems and services. Essential parts of the production processes in digital audio broadcasting houses were changed to digital ones, beginning with the change from conventional analogue audio tape to digital recording on magnetic tape or hard disk, digital signal processing in mixing desks and digital transmission links in distribution processes. Consequently, broadcast transmission systems now tend to change from conventional analogue transmission to digital [2]. The main advantages of a digital audio broadcasting over the analog system are [2, 23]:

- High quality audio services.
- Both audio and data services (such as text information, news, graphics, still or moving pictures) can be received using the same receiver.
- Well standardized system layout and a wide range of receiving equipment including fixed (stationary), mobile and portable radio receivers.
- Efficient use of the available radio frequency spectrum.
- Provides flexible bit rates (between 8 and 384 Kbit/s) and multiplex configuration. These provide service providers to change program or data service without interruption and also change quality of service without interruption.
- Transmitter networks can be designed as single frequency networks. This provides all transmitters to operate at the same frequency which provides great economy with regard to frequency efficiency.
- Low transmitting power.
- High robustness against multipath reception.
- Larger coverage area than current amplitude modulation (AM) and frequency modulation (FM) systems. Due to the available option to extend the coverage with the addition of more transmitters at the same frequency.

2.2 Digital Audio Broadcasting Standards

The development of digital broadcasting system has led to technical specifications for a myriad of system components, ranging from the description of coding algorithms to that of modulation procedures, transmission parameters, hardware components, device interfaces, protocols and techniques for interactive channels and software platforms [1].

Different digital multimedia broadcasting standards were developed and used in different parts of the world. In the next sections some of these standards are briefly covered.

2.2.1 Digital Audio Broadcasting

Eureka-147 digital audio broadcasting (DAB) was the first adopted digital sound-broadcasting standard [20]. Eureka 147 is widely applied in Europe, Canada and part of Asia. The E-147 DAB specification allows for any channel center frequency between 30 MHz and 3 GHz that is divisible by 16 Hz but the recommended DAB frequencies are L-band (1,452–1,492 MHz) or very high frequency (VHF) Band III(175–240 MHz), and VHF band I (47–67MHz)[24]. Its 1.5 MHz bandwidth can accommodate a maximum of about 1.2 Mbps of data. DAB employs both 48 kHz and 16-bit sampling rates for audio playback. The signal is then compressed with MPEG 1-Layer 2 (MP2) technology. The system allows a flexible range of frequencies between 64–192 kbps for mono channels. Generally speaking, a 1.5 MHz channel can carry up to six 256 kbps stereo channels plus Program Associated Data that describe the program being transmitted and other information such as the name of the song, the artist and the genre of music [24].

The newer DAB+, on the other hand, employs High Efficiency Advanced Audio Coding, version 2 (HE AAC v.2), or sometimes known as MPEG-4 Part 14 (MP4), The sweet spot (which is the bit rate at which the encoding algorithms work best) is 64 kbps per channel and 96 kbps can be used for even higher audio quality. The more efficient in audio coding thus allows DAB+ to carry 18 or even more channels in one mux [24].

The E-147 DAB specification includes four modes for transmission. Each mode allows the same throughput of data, uses the same modulation scheme for each carrier quadrature

phase shift keying (QPSK), and the same radio frequency(RF) channel bandwidth, and different guard intervals, 246 μ s, 123 μ s, 62 μ s and 31 μ s for Mode I, II, III & IV, respectively (Table 2.1).

Standard	Modulation Method	Frequencies	Guard Interval (μ s)	Bit rate	Sampling Frequency	Compression
DAB	OFDM and DQPSK	30 MHz - 3 GHz	246, 123, 62 and 31 for Mode I, II,III & IV	8, 16, 24, 40 or 144 kbit/s	24 kHz, 48kHz	MPEG 1-Layer 2 (MP2)
DAB+	OFDM and DQPSK	30 MHz - 3 GHz	246, 123, 62 and 31 for Mode I, II,III & IV	8, 16, 24, 40 or 144 kbit/s	24 kHz, 48kHz	AAC v.2/MP4

Table 2.1: DAB and DAB+ system [24].

The modes that are designed for use at higher frequencies have fewer and more widely-spaced carriers, so they can better cope with the Doppler effects that become more severe as broadcast frequency increases. These modes have shorter guard intervals and symbol lengths in order to keep the channel capacity the same even though the number of carriers is now less. The shorter guard intervals mean the maximum allowable transmitter spacing is less for transmitters operating within SFN [24]. This is a severe restriction in case of systems with short latency time and high bandwidth efficiency requirements. Using an equalizer the ISI distortions can be compensated and a perfect reconstruction can be achieved without the need for guard interval [23].

2.2.2 Integrated Services Digital Broadcasting–Terrestrial Sound Broadcasting

The Integrated Services Digital Broadcasting – Terrestrial Sound Broadcasting (ISDB – T_{SB}) system was developed in Japan. ISDB – T_{SB} audio services are broadcast in VHF band III in Japan. The spectrum between 188MHz and 192 MHz has been allocated for this purpose. The ISDB – T_{SB} transmission is built around an MPEG-2 transport stream capable of carrying a number of audio-compression algorithms, including MPEG-2 AAC. As

an MPEG-2 transport stream is used, it is easy to insert low-bit rate video or data services if required. As many different services as are required can be sent in the same program stream [24, 25].

Standard	Modulation Method	Frequency	Guard Interval	Bit Rate	Sampling Frequency	Compression
ISDB-Tsb	BST-OFDM, coherent QPSK, 16QAM and 64QAM	188 MHz and 192 MHz	1/4, 1/8, 1/16, 1/32 of active symbol duration	44 kbps	32 kHz, 44.1Khz or 48kHz	MPEG-2, MPEG-2 AAC

Table 2.2: ISDB Terrestrial Sound Broadcasting System [24].

The ISDB – T_{SB} services have three transmission modes options. The three mode of operation have four available guard intervals options. The guard interval are 1/4, 1/8, 1/16, 1/32 of active symbol duration. When we use the 1/4 option we are losing 1/4 the transmitting space.

2.2.3 Digital Radio Mondiale

The Digital Radio Mondiale (DRM) consortium was founded by international broadcasters and equipment manufacturers in 1998 to develop a digital sound broadcasting system for use at frequencies below 30 MHz. These frequencies have been traditionally used for narrowband amplitude modulation (AM) broadcasting. They are largely used for local, national, and international services in the medium wave and long wave bands, and for international broadcasting in the short wave bands. These bands have propagation characteristics that allow coverage of large areas and rugged terrain, but the primitive AM modulation has no protection against noise [24].

DRM can deliver FM-comparable sound quality on frequencies below 30 MHz (long wave, medium wave and short wave), which allow for very-long-distance signal propagation. In the VHF bands, the term "DRM+" is used. DRM+ is able to use available broadcast spectrum between 30 and 300 MHz; generally this means band I (47 to 68 MHz),

band II (87.5 to 108 MHz) and band III (174 to 230 MHz). DRM has been designed to be able to re-use portions of existing analogue transmitter facilities such as antennas, feeders, and, especially for DRM30, the transmitters themselves avoiding major new investment [26].

Standard	Modulation Method	Freq.	Guard Interval (ms)	Bit rate	Sampling Frequency	Compression
DRM	COFDM 16, and 64 QAM	<30 MHz	2.66, 5.33, 5.33, and 7.33 for Mode I, II,III & IV	4.5, 5, 9, 10, 18, or 20 kHz	24 kHz, 48kHz	HVXC and CELP for low bit rate, MPEG AAC HE for high bit rate

Table 2.3: DRM system[24, 26].

2.2.4 Other Standards

There are standard for audio and video broadcasting such as Digital Video Broadcasting (DVB), Advanced Television Systems Committee (ATSC) digital television (DTV), Integrated Services Digital Broadcasting (ISDB) and Digital Terrestrial Television Multimedia Broadcasting (DTMB). The standard defined by Advanced Television Systems Committee (ATSC) is one of the broadcasting standards which exclusively indicate the use of equalizer for mitigating channel distortion. The ATSC Digital TV Standards include digital audio and data broadcasting in addition to the digital television standards. In the next section an overview of ATSC digital television (DTV) system is presented in order to provide an insight where adaptive blind equalization method can be implemented in practical world.

2.3 ATSC-T Standard

In the terrestrial DTV standard of the ATSC, 8-vestigialside band (8-VSB) modulation was adopted as a modulation standard in the United States [27]. ATSC DTV Standards include digital high definition television (HDTV), standard definition television (SDTV), data broadcasting, multichannel surround-sound audio, and satellite direct-to-home broadcasting [28].

Receivers for broadcast DTV service are designed to recover the signal under the greatest possible range of transmission impairments. They must also condition the decoded video data for the scanning format (e.g., interlaced or progressive) and row and column pixel count of the display. In these matters, digital receivers offer new signal recovery and processing opportunities—a lower received signal to noise ratio (S/N) requirement for essentially error-free decoding, multipath reduction, and decoupling of the display scanning functions from the actual transmitted signal [29].

The innovations in equalization, automatic gain control, interference cancellation, and carrier and timing recovery improve signal reception and create product performance differentiation [24].

2.3.1 ATSC-T System Block Diagram

A basic block diagram representation of the ATSC-T system is shown in Figure 2.1. According to this model, the system can be seen to consist of three subsystems [30]. In the next three sections each of the three subsystems covered in detail

- Source coding and compression;
- Service multiplex and transport;
- RF transmission.

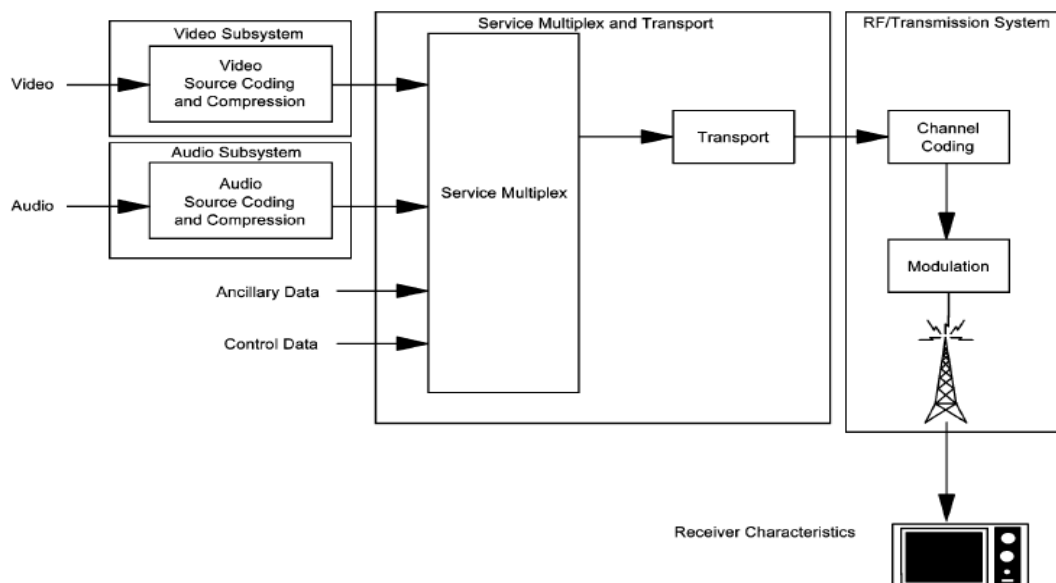


Figure 2.1: ITU-R digital terrestrial television broadcasting model [30].

2.3.2 Source Coding and Compression

Source coding and compression refers to the bit rate reduction methods, also known as data compression, appropriate for application to the video, audio, and ancillary digital data streams. The term “ancillary data” includes control data, conditional access control data, and data associated with the program audio and video services, such as closed captioning, the payload identification code, and the time code. The purpose of the coder is to minimize the number of bits needed to represent the audio and video information [30].

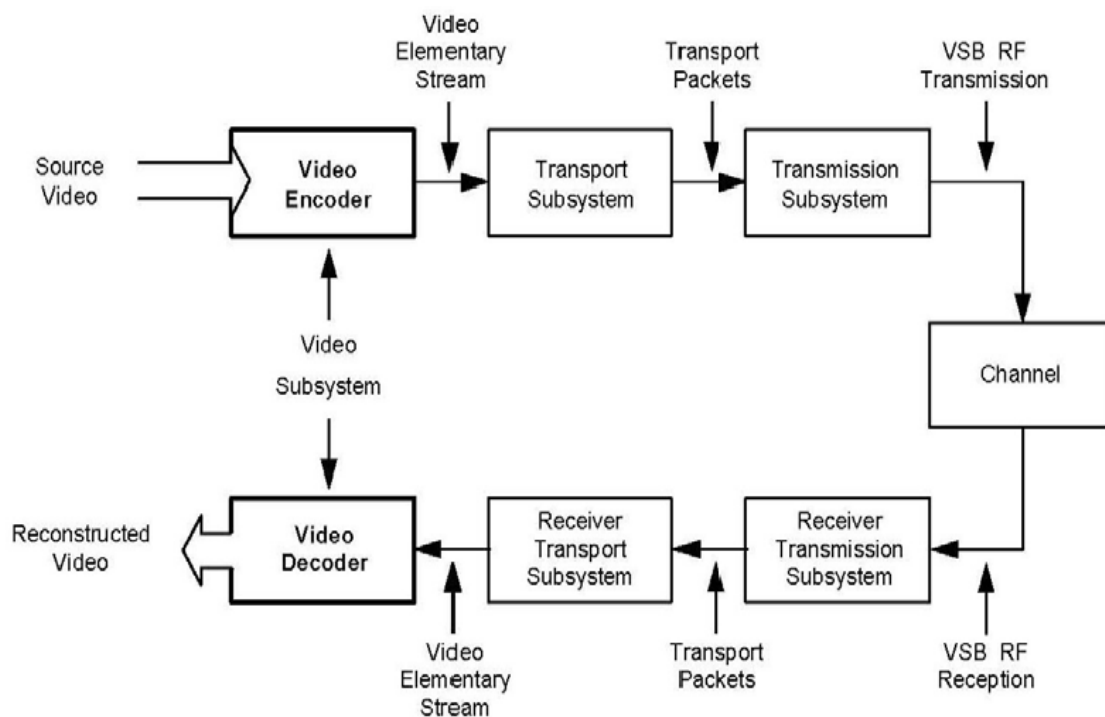


Figure 2.2: Video coding in relation to the ATSC DTV system [24].

- Video Source coding and compression:** The digital television system employs the MPEG-2 video stream syntax for the coding of video [24]. Figure 2.2 shows the flow of video signals in the ATSC DTV system. Analog video signals, when presented to the system, are digitized and sent to the encoder for compression, and then the compressed data passes through the transport and transmission subsystems before the compressed data transmitted over a communications channel to the receiver. On the received decoder module, the compressed signal is decompressed and reconstructed for display (after passing through transport and transmission

subsystem of the receiver) [24]. The transport and transmission subsystem are covered in a separate sections.

- **Audio Source coding and compression:** the Digital Audio Compression three (DAC-3) standard is used for coding of audio signals. As illustrated in Figure 2.3, the audio subsystem comprises the audio encoding/decoding function and resides between the audio inputs/outputs and the transport subsystem. An audio encoder is responsible for generating an audio elementary stream, which is an encoded representation of the baseband audio input signals. The flexibility of the transport system allows multiple audio elementary streams to be delivered to the receiver. At the receiver, the transport subsystem is responsible for selecting which audio stream to deliver to the audio subsystem. The audio subsystem is responsible for decoding the audio elementary stream back into baseband audio.

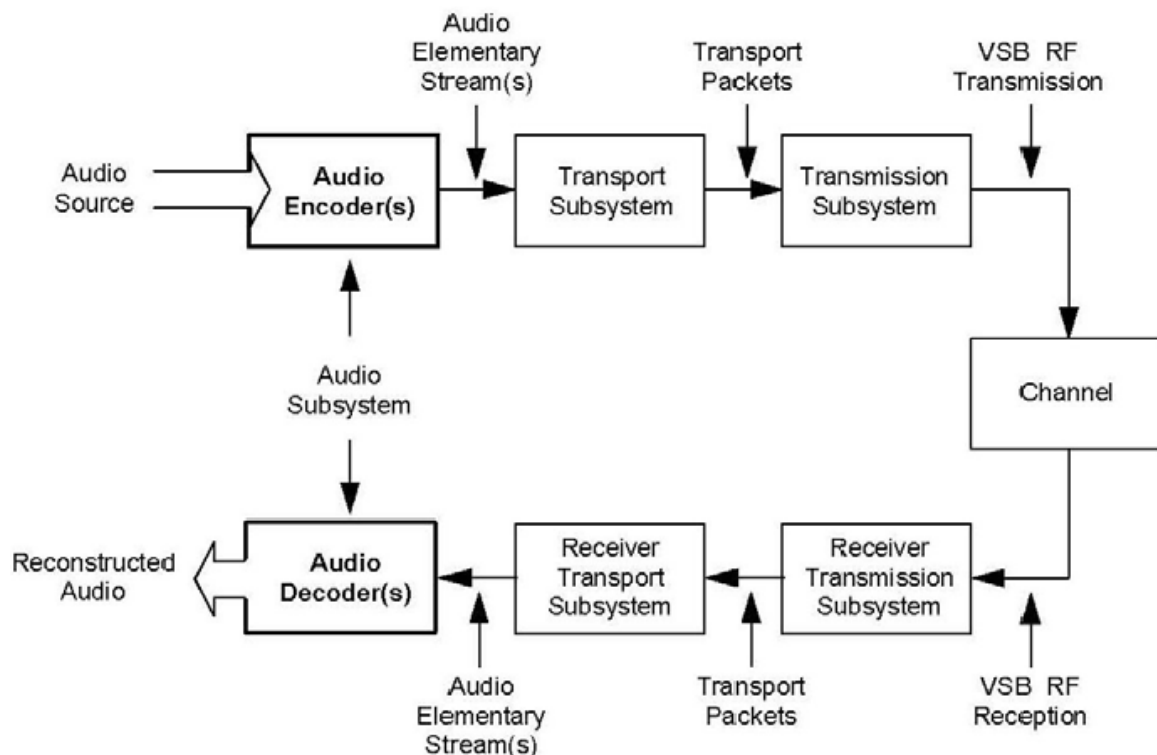


Figure 2.3: Audio subsystem within the ATSC DTV system [24].

2.3.3 Service Multiplex and Transport

Service multiplex and transport subsystem has two subsystems: service multiplexing and transportation. The multiplexing system combines the video, audio, and ancillary data

stream into a single data stream using appropriate methods which enables demultiplexing, and the transport system converts the digital data stream into “packets” of information by including the means of uniquely identifying each packet or packet type [24].

In developing the transport mechanism, interoperability among digital media, such as terrestrial broadcasting, cable distribution, satellite distribution, recording media, and computer interfaces, was a prime consideration. The digital television system employs the MPEG-2 transport stream syntax for the packetization and multiplexing of video, audio, and data signals for digital broadcasting systems (ISO/IEC 13818-1)[30].

In the simplified block diagram representation of audio & video subsystems shown in Figures 2.2 and 2.3 the “Service multiplex and transport” is best illustrated by transport subsystem shown in Figure 2.4.

In typical implementations of transport subsystem shown in Figure 2.4, the video and audio encoders and the ATSC transport multiplexer each create output bit streams in the transport stream (TS) format. The TS format provides a mechanism to encapsulate and multiplex coded video, coded audio, and generic data into a unified bit stream. It includes timing information in the form of time stamps in order to enable the real-time reproduction and precise synchronization of video, audio, and data (as necessary)[24].

The transmit site’s transport subsystem is responsible for formatting the coded bit streams and multiplexing the different components of the program for transmission. The receiver’s transport subsystem does the inverse function, recovering the coded bit streams to pass them to the appropriate decoder and for the corresponding error signaling [24].

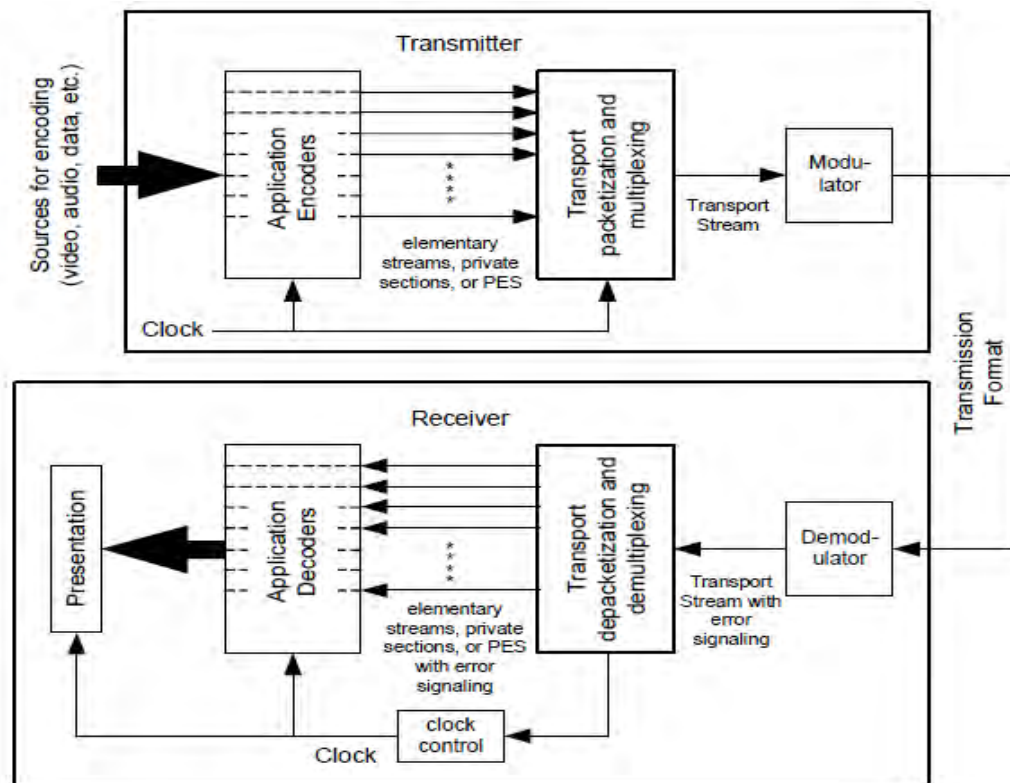


Figure 2.4: A functional overview of the ATSC transport subsystem [24].

The transport multiplexer (also known as a mux) is responsible for receiving the compressed video bit stream, compressed audio bit streams, Program and System Information Protocol(PSIP) bit stream, associated data (synchronous, asynchronous, and synchronized) bit streams, and independent data bit streams, packaging them up into a single multi stream transport, and ensuring that streams that require synchronization among them are correctly aligned and do not exceed established bit rate or buffer size parameters, and then deliver (in a real-time stream of bits) the multi stream transport to a channel modulator or other network interface[24].

2.3.4 Radio Frequency Transmission

The RF transmission system, as shown in Figure 2.1, refers to channel coding and modulation. The channel coder based RS, interleaver and trellis encoder takes the data bit stream and adds additional information that can be used by the receiver to reconstruct the data from the received signal which, due to transmission impairments, may not accurately represent the transmitted signal [30]. In order to protect against burst and random errors,

the packet data is interleaved before transmission and convolutional and Reed-Solomon forward error correction (FEC) codes are added [24].

The modulation (or physical layer) uses the digital data stream information to modulate the transmitted signal [30]. The modulation subsystem offers two modes: an 8-VSB mode for terrestrial broadcasting and a 16-VSB mode intended for cable applications[24].

Digital signals suffer from all the degradations, distortions, and impairments that impact analog signals. The degradation includes such linear distortions as amplitude variations across the frequency spectrum of the channel, envelope delay distortion, and multi path [30].

The ATSC standard indicates that distortions caused by the transmission channel can be treated conceptually by developing a model of the channel and then applying its inverse to the signal. The determination of the channel model and the creation of a filter having characteristics inverse to those of the channel are the functions of an adaptive equalizer.

2.3.4.1 Transmission Characteristics for Terrestrial Broadcast

The ATSC broadcasting system includes the standard (Main) and mobile/handheld systems. The functional block diagram of the main service RF transmission system is shown in Figure 2.5. Incoming data is randomized and then processed for FEC in the form of RS coding (20 RS parity bytes are added to each MPEG-2 packet), one-sixth data field interleaving and two-thirds rate trellis coding, the data organization is presented in the next section. The randomization and FEC processes are not applied to the synchronization byte of the transport packet, which is represented in transmission by a Data Segment Sync signal. Following randomization and forward error correction processing, the data packets are formatted into data frames by the multiplexer for transmission and data segment sync and data field sync are added when the signal pass through the multiplexer. [30].

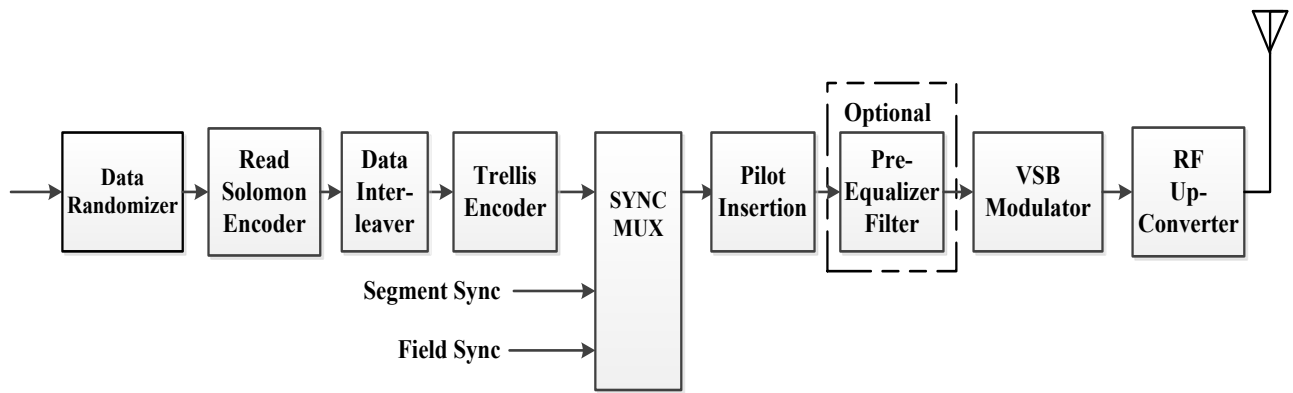


Figure 2.5: 8-VSB transmitter block diagram, RF transmission system [30].

Parameter	Terrestrial Mode
Channel bandwidth	6 MHz
Guard bandwidth	11.5 percent
Symbol rate	10.76... M symbols/s
Trellis FEC	2/3 rate
Reed-Solomon FEC	T = 10 (207,187)
Segment length	832 symbols
Segment sync	4 symbols per segment
Frame sync	1 per 313 segments
Payload data rate	19.39 Mbps
Analog co-channel rejection	Analog rejection filter in receiver
Pilot power contribution	0.3 dB
C/N threshold	~ 14.9 dB

Table 2.4: Parameters for VSB Transmission Modes [33].

2.3.4.2 Data Organization and data rate

Figure 2.6 shows how the data are organized for transmission. Each Data Frame consists of two Data Fields, each containing 313 Data Segments. The first Data Segment of each Data Field is a unique synchronizing signal (Data Field Sync) and includes the training sequence used by the equalizer in the receiver. The remaining 312 Data Segments each carry the equivalent of the data from one 188-byte transport packet plus its associated RS-FEC

overhead. The actual data in each Data Segment comes from several transport packets because of data interleaving. Each Data Segment consists of 832 symbols. The first 4 symbols are transmitted in binary form and provide segment synchronization. This Data Segment Sync signal also represents the sync byte of the 188-byte MPEG-2-compatible transport packet 2. The remaining 828 symbols of each Data Segment carry data equivalent to the remaining 187 bytes of a transport packet and its associated RS-FEC overhead. These 828 symbols are transmitted as 8-level signals and therefore carry three bits per symbol. Thus, $828 \times 3 = 2484$ bits of data are carried in each Data Segment, which exactly matches the requirement to send a protected transport packet [30]:

$$187 \text{ data bytes} + 20 \text{ RS parity bytes} = 207 \text{ bytes}$$

$$207 \text{ bytes} \times 8 \text{ bits/byte} = 1656 \text{ bits}$$

$$\text{Two-thirds rate trellis coding requires } \frac{3}{2} \times 1656 \text{ bits} = 2484 \text{ bits}$$

The exact symbol rate is given by equation 2.1 below[30]:

$$S_r(\text{MHz}) = 4.5/286 \times 684 = 10.76 \dots \text{ MHz} \quad (2.1)$$

The numbers in the formula for the ATSC symbol rate in 6 MHz systems are related to NTSC scanning and color frequencies.

The particular numbers used are:

- 4.5 MHz = the center frequency of the audio carrier offset in NTSC
- $4.5 \text{ MHz}/286$ = the horizontal scan rate of NTSC
- 684: this multiplier gives a symbol rate for an efficient use of bandwidth in 6 MHz.

The frequency of a Data Segment is given in Equation 2.2 below[30]:

$$f_{seg} = S_r/832 = 12.94 \dots \times 10^3 \text{ Data Segments/s} \quad (2.2)$$

The Data Frame rate is given in Equation 2.3 below[30]:

$$f_{frame} = f_{seg}/626 = 20.94 \dots \frac{\text{frames}}{\text{s}} \quad (2.3)$$

This yields the following gross data rate:

$$\text{Gross Data Rate} = 3 \text{ bit/Symbol} \times 10.76 \text{ M Symbols/s} = 32.2867 \text{ M bit/s}$$

The net data rate is then:

$$\begin{aligned} \text{Net Data Rate} &= 188/208 * 2/3 * 312/313 * (\text{Gross Data Rate}) \\ &= 19.39265846 \text{ Mbit/s;} \end{aligned}$$

The above equations are based on the following parameter values:

- 8VSB = 3 bit/symbol
- Reed-Solomon = 188/208
- Code rate = 2/3 (trellis)
- Field sync = 312/313

Therefore the symbol rate, gross data rate and the net data rate of ATSC system is 10.76 MHz., 32.2867 M bit/s and 19.39 Mbit/s respectively. The other parameters for VSB transmission modes are summarized in Table 2.4.

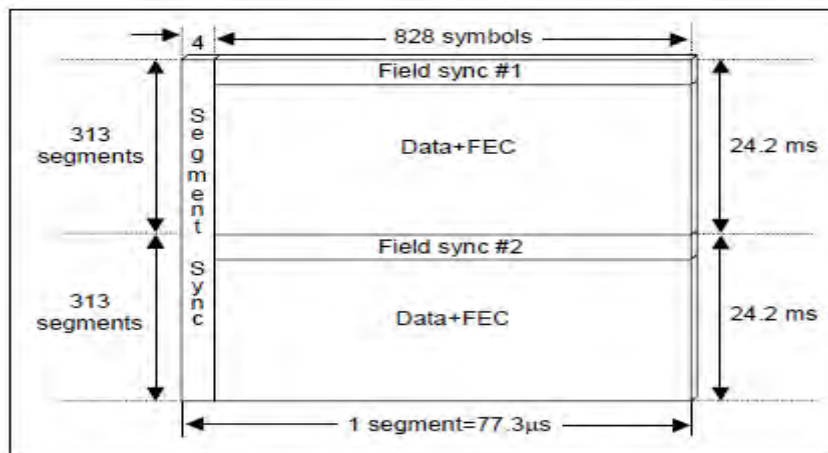


Figure 2.6: VSB data frame without extra field sync [30].

2.3.4.3 Channel Error Protection

As indicated in Figure 2.2, the main channel protection in ATSC T RF transmission system consists of RS encoding, interleaving and 4-state trellis encoding. Bellow we will discuss these three methods

- **Data Randomizer:** The data randomizer, Figure 2.7 is used to break up any long sequences of 1s or 0s contained in the transport stream. The data randomizer XORs the incoming data bytes with a pseudo random binary sequence (PRBS) which contains a 16-bit feedback shift register. The data randomizer is reset to defined

initialization word at a defined time during the field sync interval. The sync information (e.g. data field sync, data segment sync) is not randomized and is used, among other things, for receiver-to-modulator coupling. At the receiver end, there is a complementary PRBS generator and randomizer, i.e., of exactly the same design and running exactly in synchronism with the generator/randomizer at the transmitter end [31].

When there are long sequences of 1s or 0s, there is no change in the 8-VSB symbols and therefore no clock information. This would cause synchronization problems in the receiver and, during the transmission of long sequences of 1s or 0s, produce discrete spectral lines in the transmission channel. This effect is cancelled by randomizing, which causes energy dispersal, i.e. it creates an evenly distributed power density spectrum [31].

The randomizer generator polynomial and initialization is shown in Figure 2.7. The initialization (pre-load) to 0xF180 (load to 1) occurs during the Data Segment Sync interval prior to the first Data Segment [30]. The generator polynomial is given by [30]:

$$G_{(16)}(X) = X^{16} X^{13} X^{12} X^{11} X^7 X^6 X^3 X + 1 \quad (2.4)$$

The initialization (pre load) occurs during the field sync interval

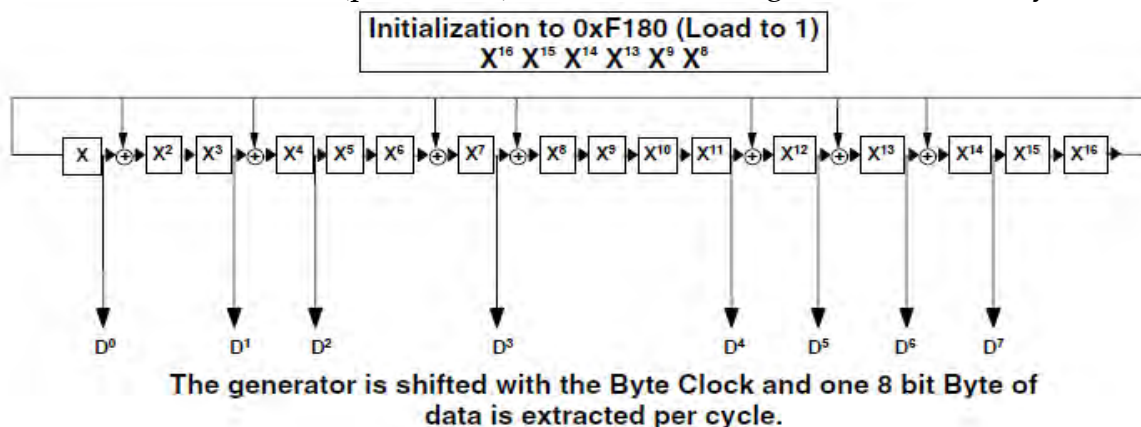


Figure 2.7: Randomizer polynomial [30].

- **Reed Solomon encoder:** Reed Solomon codes, the code is capable of correcting any combination of t or fewer errors, where t can be expressed as [31]:

$$t = \left\lfloor \frac{n - k}{2} \right\rfloor \quad (2.5)$$

Where k is the number of data symbols being encoded, and n is the total number of code symbols. An ATSC RS encoder uses 20 error protection bytes to the 188-byte TS packet ($k=188$ byte, $n=20$ byte+188byte). The 20 error protection bytes allow up to 10 errored bytes per TS packet to be corrected at the receiver end. If more than 10 errored bytes are contained in a TS packet, Reed-Solomon error correction fails, and the transport stream packet concerned is marked as errored [31].

- **Data interleaver:** The Reed-Solomon encoder RS is followed by a data interleaver, which changes the time sequence of the data, i.e. it scrambles the data according to a known algorithm specified in the ATSC standard. The receiver has a corresponding deinterleaver algorithm to put the segments back in their original sequence. [31].
- **Trellis Encoder:** The ATSC system employs a trellis encoder with two signal paths as shown in Figure 2.8. From the incoming bit stream, one bit is taken to a precoder with a code rate of 1, and the second bit to a trellis encoder with a code rate of 1/2. This yields an overall code rate of 2/3. The three data streams generated by the precoder and the trellis encoder are fed to a symbol mapper, which outputs the 8-level VSB baseband signal [31].

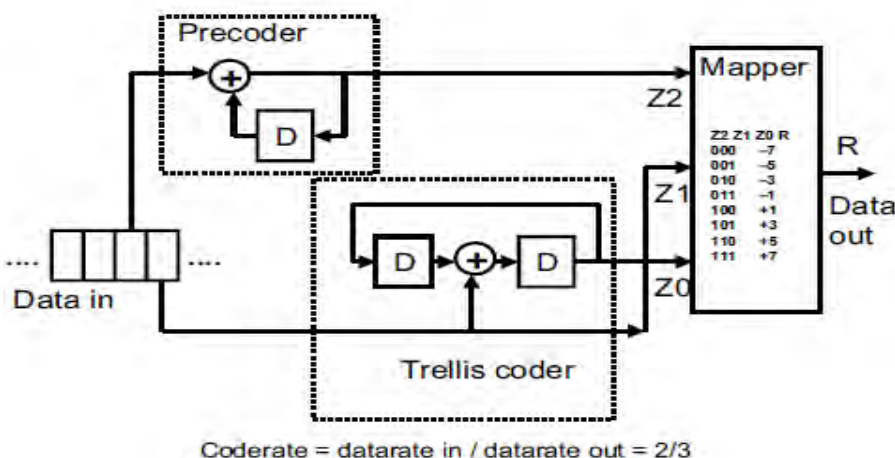


Figure 2.8: Trellis encoder [24].

2.3.4.4 Synchronization

ATSC uses two types of synchronization signals; namely, the Data Segment Synchronization and Data Field Synchronization, Figure 2.5. The synchronization signals are added when the encoded trellis passed through the multiplexer and is used, among other things, for receiver to-modulator coupling [31]. In the next subsection an overview of these synchronization signals is presented.

- Data Segment Sync:** A two-level (binary) 4-symbol Data Segment Sync is added into the 8-level digital data stream at the beginning of each Data Segment. A complete segment consists of 832 symbols: 4 symbols for Data Segment Sync, and 828 data plus parity symbols. The same sync pattern occurs regularly at 77.3 μ s intervals, and is the only signal repeating at this rate. Unlike the data, the four symbols for Data Segment Sync are not Reed-Solomon or trellis encoded, nor are they interleaved. The Data Segment Sync has '1001' pattern [30], as shown in Figure 2.9.

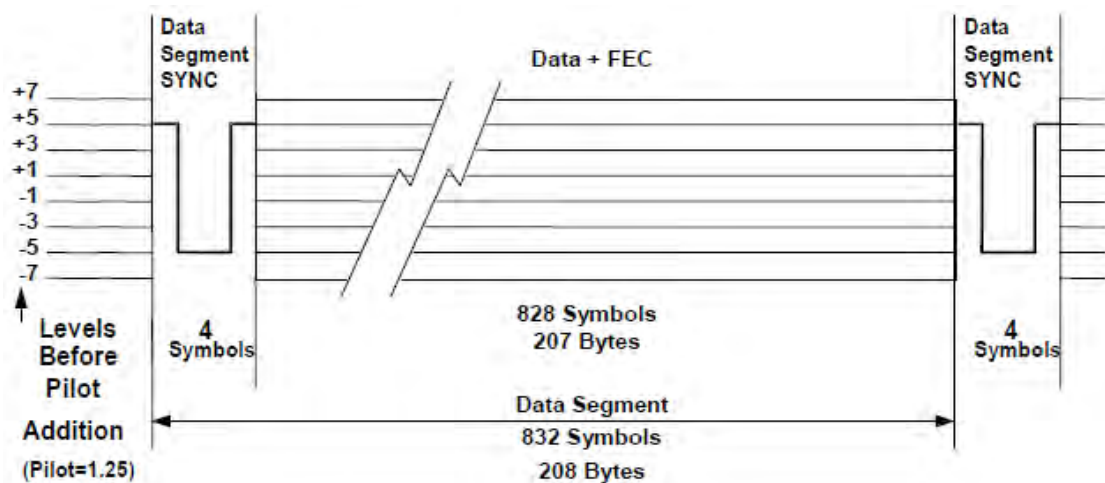


Figure 2.9: 8-VSB data segment [30].

- Data Field Sync:** The data are not only divided into Data Segments, but also into Data Fields, each consisting of 313 segments. Each Data Field has 24.2 ms length and start with one complete Data Segment of Data Field Sync [30].

2.3.4.5 Modulation

The 8-level vestigial sideband (8-VSB) modulation is used in ATSC DTV. The VSB modulator converts the output of the trellis decoder into the nominal signal levels of (-7, -5,

$-3, -1, 1, 3, 5, 7$). The 8-VSB is capable of transmitting three bits ($2^3=8$) per symbol. In ATSC, each symbol includes two bits from the MPEG transport stream which are trellis modulated to produce a three-bit figure. The resulting signal is then band-pass filtered with a raised cosine Nyquist filter to remove redundancies in the side lobes, and then shifted up to the broadcast frequency [30,32].

2.3.5 ATSC DTV Receiver

The receiver block diagram of the 8-VSB DTV system is shown in Figure 2.6.

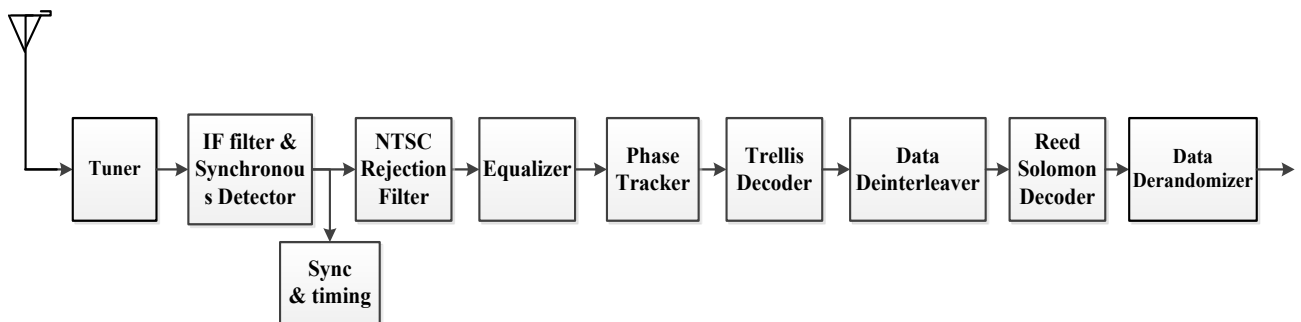


Figure 2.10: 8-VSB receiver block diagram [30].

- **Tuner:** The tuner is a high-side injection, double-conversion type with a first IF frequency of 920 MHz. The tuner input has a band-pass filter that limits the frequency range to 50–810 MHz, rejecting all other non-television signals that may fall within the image frequency range of the tuner (beyond 920 MHz). In addition, a broadband tracking filter rejects other television signals, especially those much larger in signal power than the desired signal power [33].
- **Equalizer:** The equalizer/echo-suppressor compensates for linear channel distortions, such as tilt, and the spectrum variations caused by echoes. These distortions can come from the transmission channel or from imperfect components within the receiver [33]. A separate chapter on adaptive blind equalizer is covered on chapter IV.
- **Phase Tracker:** The term “phase tracker” is a generic term applied to three servo loops—namely, a phase tracking loop, an amplitude-tracking loop and an offset-tracking loop. The phase-tracking loop is an additional decision-feedback loop which

degenerates phase noise that is not degenerated by the IF PLL operating on the pilot. Accordingly, two concatenated loops, rather than just one loop, degenerate phase noise in the demodulated DTV signal before its synchronous equalization [33].

- **Trellis Detector:** To help protect the trellis decoder against short burst interference, such as impulse noise or NTSC co-channel interference, 12-symbol-code intra segment interleaving is employed in the transmitter. The receiver uses 12 trellis decoders in parallel, where each trellis decoder sees every 12th symbol. This code de-interleaving has all the same burst noise benefits of a 12-symbol-code de-interleaver, but also minimizes the resulting code expansion (and hardware) when the NTSC rejection comb filter is active [33].
- **Data Deinterleaver:** At the receiver end, the de-interleaver restores the original time sequence of the data. With interleaving, even long burst errors can be corrected as they are distributed over several frames and can thus be handled more easily by the Reed-Solomon decoder [31].
- **Reed Solomon Decoder:** The trellis-decoded byte data is sent to the $t = 10$ RS decoder. The RS decoder receiver uses parity bytes to perform byte-error location and byte-error correction on a segment-by-segment basis [33].
- **Data Derandomizer:** The derandomizer accepts the error-corrected data bytes from the RS decoder, and applies the same PRS randomizing code to the data. The PRS code can be generated the same way as in the transmitter, using the same PRS generator feedback and output taps. Since the PRS is locked to the reliably recovered Data Field Sync (and not to some code word embedded within the potentially noisy data), it is exactly synchronized with the data, and performs reliably [33].

CHAPTER III

Wireless Propagation Channel Models

3.1 Introduction

A wireless propagation channel is the medium linking the transmitter and receiver. Its' properties determine the information-theoretic capacity; is the ultimate performance limit factor in wireless communications; and also determines how specific wireless systems behave. Wireless channels differ from wired channels by multipath propagation i.e., the existence of a multitude of propagation paths from transmitter and receiver, where the signal can be reflected, diffracted, or scattered along its way. One way to understand the wireless channel is to consider all those different propagation phenomena and how multipath component (MPC) are created by these phenomena [34].

The interference of the different MPCs creates not only fading but also delay dispersion. Delay dispersion means that if we transmit a signal of duration T , the received signal will have a longer duration. Naturally, this leads to ISI [34].

When the transmitted signal has a bandwidth greater than the coherent bandwidth of the channel; in the time domain, the transmitted symbol period is shorter than the multipath time delay spread result in time dispersion [35]. In other words, the impulse response of the channel is not a single delta pulse but rather a sequence of pulses each of which has a distinct arrival time in addition to having a different amplitude and phase. These multipath components interfere with subsequently transmitted pulses, Figure 3.1 and this effect is called ISI.

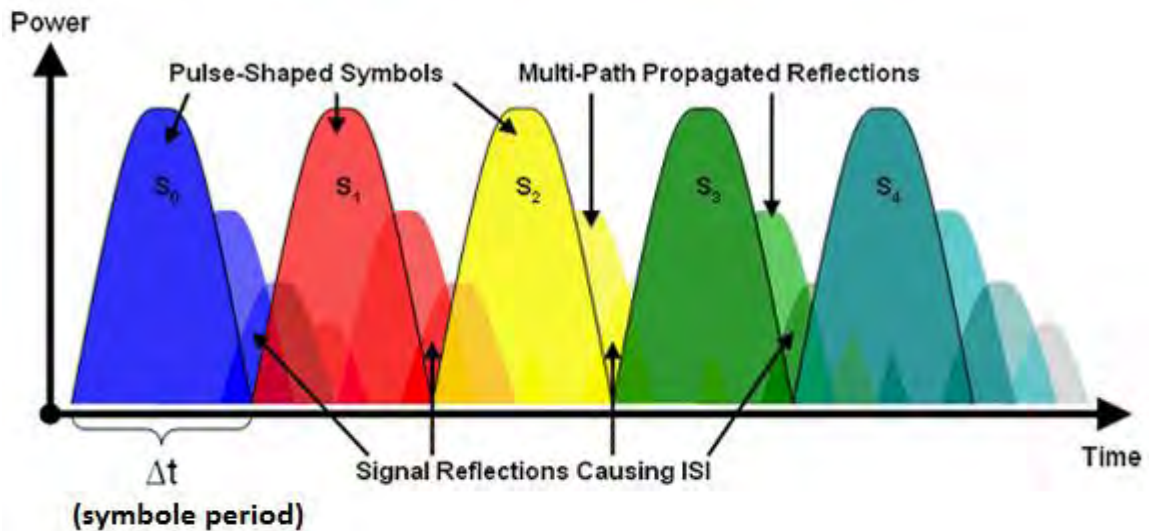


Figure 3.1: ISI Caused by Multi-Path Distortion [36].

The three-stage frequently used models to describe the impact of the radio channel are [37]:

- Large-scale path loss;
- Medium-scale shadowing;
- Small-scale multipath fading.

In general the type of fading experienced by a signal propagating through a radio channel depends on the nature of the transmitted signal, as well as on the characteristics of the channel. Different transmitted signals will undergo different types of fading, according to the relationship among the signal parameters, such as the path loss, the bandwidth (BW), the symbol period and the channel parameters (such as the root mean square(rms) delay spread and the Doppler spread). The different types of fading are summarized in Figure 3.2.

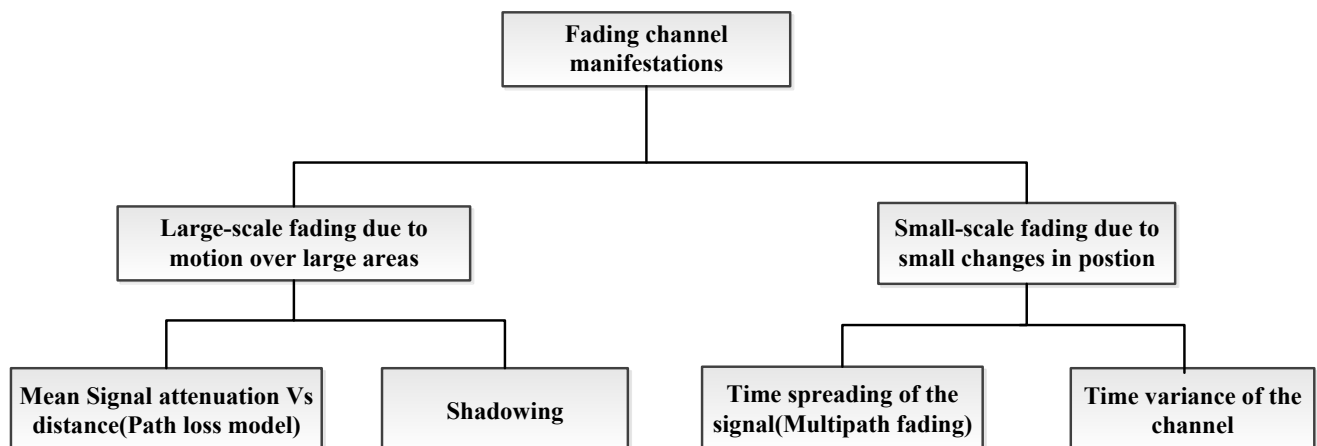


Figure 3.2: Fading channel manifestation [38].

Large Scale Fading: Large-scale attenuation or path loss model is associated with loss of the received power due to the large distance between the transmitter and the receiver and is mainly affected by absorption, reflection, refraction and diffraction. The path loss, P_L of the channel as the dB value of the linear path loss or, equivalently, the difference in dB between the transmitted, P_t and received, P_r signal power is defined as [39]:

$$P_L[\text{dB}] = 10 \log_{10} \frac{P_t}{P_r} \text{ dB} \quad (3.1)$$

Large-scale fading is caused by shadowing due to variations in both the terrain profile and the nature of the surroundings. In deeply shadowed conditions, the received signal strength at a receiver can drop well below that of free space. Shadowing happens mainly due to the presence of obstacles blocking the line of-sight (LOS) between the transmitter and the receiver. The main mechanisms of signal transmission involved in shadowed receiver are reflection and scattering of the radio signal.

Small Scale Fading: Multipath fading is associated with multiple reflected copies of the transmitted signal due to scattering from various objects arriving at the receiver at different time instants. The thesis focus on the adaptive blind equalization technique for mitigating distortion caused by multipath hence in the next section multipath fading is covered in more detail.

3.2 Small-scale Multipath Fading

In wireless communications, multipath is the propagation phenomenon that results in radio signals reaching the receiving antenna by two or more paths. Causes of multipath include atmospheric ducting, ionospheric reflection and refraction, and reflection from water bodies and terrestrial objects such as mountains and buildings [40].

The effects of multipath include constructive and destructive interference, and phase shifting of the signal. The number of the possible propagation paths is very large especially in cities due to the large numbers of reflector and scatters. As shown in Figure 3.3, each of the paths has a distinct amplitude, delay (runtime of the signal), direction of departure from

the transmitter, and direction of arrival; most importantly, the components have different phase shifts with respect to each other [34].

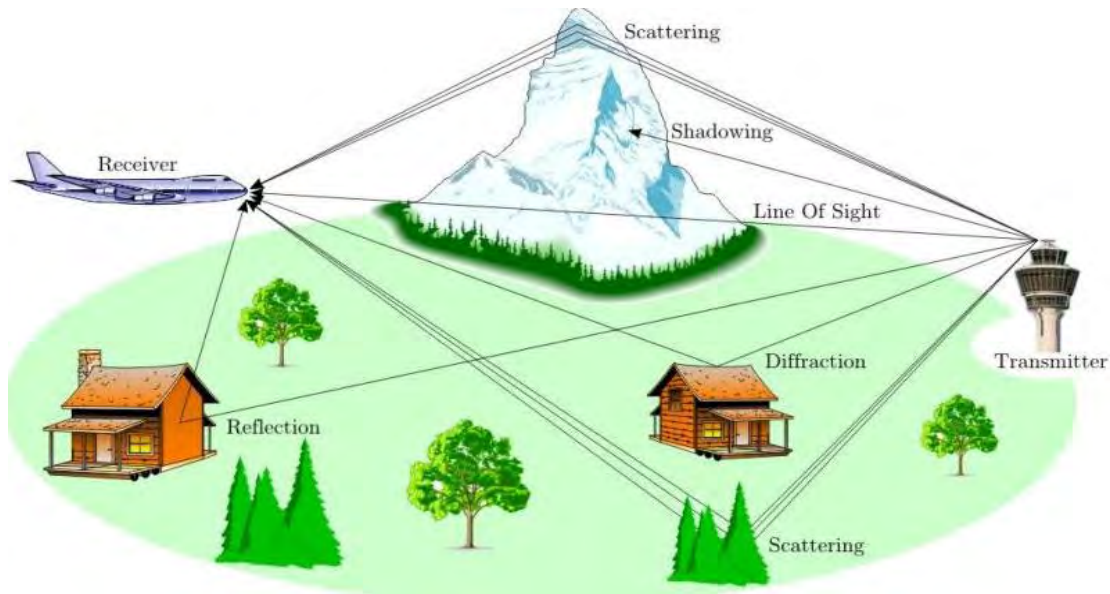


Figure 3.3: Multipath propagation in rural area [41].

The following are the most important multipath fading effects:

1. Rapid changes in signal strength over a small travel distance or time interval.
2. Random frequency modulation due to varying Doppler shifts on different multipath signals.
3. Time dispersion or echoes caused by multipath propagation delays.

One way to represent the impulse response of a multipath channel is to use a discrete number of impulses of the tapped delay line model [38]. If the input signal is a unit impulse, $\delta(t)$, the output will be the channel impulse response, which can be written as[42]:

$$h(t) = \sum_{n=0}^N A_n(t) \delta(t - \tau_n) \exp^{-j\varphi_n} \quad (3.2)$$

Where A_n , τ_n and φ_n are the attenuation, delay in time of arrival, and phase corresponding to path n , respectively

The channel impulse response can thus be characterized by N time delayed impulses, each represented by an attenuated and phase shifted version of the original transmitted impulse. Although multipath interference seriously degrades the performance

of communication systems, little can be done to eliminate it [42]. A mitigation technique must be used to achieve better quality of service.

3.2.1 Fading Effects Due to Multipath Time Delay Spread

Time dispersion due to multipath causes the transmitted signal to undergo either flat or frequency selective fading.

3.2.1.1 Flat Fading

If a channel has a constant gain and linear phase response over a bandwidth which is greater than the bandwidth of the transmitted signal, then the received signal will undergo flat fading. In flat fading, the multipath structure of the channel is such that the spectral characteristics of the transmitted signal are preserved at the receiver. However the strength of the received signal changes with time, due to fluctuations in the gain of the channel caused by multipath [35]. A signal undergoes flat fading if[35]:

$$B_S \ll B_C \quad (3.3)$$

and

$$T_S \gg \sigma_\tau \quad (3.4)$$

Where T_S the reciprocal bandwidth (e.g., symbol period) and B_S is the bandwidth of the transmitted signal, σ_τ and B_C are the rms delay spread and coherence bandwidth, respectively, of the channel [35].

3.2.1.2 Frequency Selective Fading

If the channel possesses a constant-gain and linear phase response over a bandwidth that is smaller than the bandwidth of transmitted signal, then the channel creates frequency selective fading on the received signal. Under such conditions the channel impulse response has a multipath delay spread which is greater than the reciprocal bandwidth of the transmitted message waveform. When this occurs, the received signal includes multiple versions of the transmitted waveform which are attenuated (faded) and delayed in time, and hence the received signal is distorted. Frequency selective fading is due to time

dispersion of the transmitted symbols within the channel. Thus the channel induces ISI [35]. A signal undergoes frequency selective fading if[35]:

$$B_S > B_C \quad (3.5)$$

and

$$T_S < \sigma_\tau \quad (3.6)$$

3.2.2 Fading Effects Due to Doppler Spread

The Doppler Effect causes the received frequency of a source to differ from the sent frequency if there is motion that is increasing or decreasing the distance between the source and the receiver the Doppler Effect is readily observable as variation in the pitch of sound between a moving source and a stationary observer [43].

When the distance between the source and receiver of electromagnetic waves is increasing, the frequency of the received wave forms is lower than the frequency of the source wave form. When the distance is decreasing, the frequency of the received wave form will be higher than the source wave form. Depending on how rapidly the transmitted baseband signal changes as compared to the rate of change of the channel, a channel may be classified either as a fast fading or slow fading channel [43].

3.2.2.1 Fast Fading

In a fast fading channel, the channel impulse response changes rapidly within the symbol duration. That is, the coherence time of the channel is smaller than the symbol period of the transmitted signal. This causes frequency dispersion (also called time selective fading) due to Doppler spreading, which leads to signal distortion. In frequency domain, signal distortion due to fast fading increases with increasing Doppler spread [35]. A signal undergoes fast fading if[35]:

$$T_S > T_C \quad (3.7)$$

and

$$B_S < B_C \quad (3.8)$$

3.2.2.2 Slow Fading

In a slow fading channel, the channel impulse response changes at a rate much slower than the transmitted baseband signal $s(t)$. In this case, the channel may be assumed to be static over one or several reciprocal bandwidth intervals. In the frequency domain, this implies that the Doppler spread of the channel is much less than the bandwidths of the baseband signal [35]. Therefore, a signal undergoes slow fading if[35]:

$$T_S \ll T_C \quad (3.9)$$

and

$$B_S \gg B_C \quad (3.10)$$

3.2.3 Rayleigh and Ricean Distributions

In order to get an understanding of the fading channel, it is important to study the distribution of the envelope of the received signal. A few possible choices of the statistical distributions for modeling the envelope are presented below.

3.2.3.1 Rayleigh Fading Distribution

In mobile radio channels, the Rayleigh distribution is commonly used to describe the statistical time varying nature of the received envelope of a flat fading signal, or the envelope of an individual multipath component [35].

When there are many objects in the environment that scatter the radio signal before it arrives at the receiver. The central limit theorem holds that, if there is sufficiently much scatter, the channel impulse response will be well-modelled as a Gaussian process irrespective of the distribution of the individual components. If there is no dominant component to the scatter, then such a process will have zero mean and phase evenly distributed between 0 and 2π radians. The envelope of the channel response will therefore be Rayleigh distributed [44]. The Rayleigh distribution has a probability density function (pdf) given by[35]:

$$p(r) = \begin{cases} \frac{r}{\sigma^2} \exp\left(-\frac{r^2}{2\sigma^2}\right) & 0 \leq r < \infty \\ 0 & r < 0 \end{cases} \quad (3.11)$$

Where σ is the rms value of the received voltage signal before envelope detection, and σ^2 is the time-average power of the received signal before envelope detection.

3.2.3.2 Ricean Fading Distribution

When there is a dominant stationary (nonfading) signal component present, such as a line-of-sight propagation path, the small-scale fading envelope distribution is Ricean. In such a situation, random multipath components arriving at different angles are superimposed on a stationary dominant signal. At the output of an envelope detector, this has the effect of adding a dc component to the random multipath [35]. The Ricean distribution is given by[35]:

$$p(r) = \begin{cases} \frac{r}{\sigma^2} \exp\left(-\frac{r^2 + A^2}{2\sigma^2}\right) I_0\left(\frac{Ar}{\sigma^2}\right) & \text{for } A \geq 0 \text{ and } r \geq 0 \\ 0 & \text{for } r < 0 \end{cases} \quad (3.12)$$

The parameter A denotes the peak amplitude of the dominant signal and $I_0(\cdot)$ is the modified Bessel function of the first kind and zero-order.

3.3 Broadcast Channel Models

Channel models are used to predict path loss and to characterize the impulse response of the propagating channel. The path loss is associated with the design of transmitter, as it tells us how much a transmitter needs to radiate to service a given region. Channel characterization, on the other hand, deals with the fidelity of the received signals, and has to do with the nature of the waveform received at a receiver. Channel models can be categorized into path loss models and impulse response models [42].

3.3.1 Path loss models

Generally, there are two main models for characterizing path loss empirical models, and site-specific models. The former are based on the statistical characterization of the

received signal. They are easier to implement, require less computational effort, and are less sensitive to the environment's geometry. The latter have a certain physical basis, and require a vast amount of data regarding geometry, terrain profile, locations of building and of furniture in buildings, and so on. These deterministic models require more computations, and are more accurate [42].

3.3.1.1 Empirical path loss model

Most wireless communication systems operate in complex propagation environments that cannot be accurately modeled by free-space path loss. A number of path loss models have been developed over the years to predict path loss in typical wireless environments mainly based on empirical measurements over a given distance in a given frequency range and a particular geographical area or building.

In practice, most simulation studies use empirical models that have been developed based on measurements taken in various real environments. The following are the most common empirical methods in use:

3.3.1.1.1 Recommendation ITU-R P.1546-5

The ITU channel recommendation is for point-to-area radio propagation predictions for terrestrial services in the frequency range 30 MHz to 3 000 MHz. It is intended for use on radio circuits over land paths, sea paths and/or mixed land-sea paths up to 1 000 km length for effective transmitting antenna heights less than 3 000 m. The method is based on interpolation/extrapolation from empirically derived field-strength curves as functions of distance, antenna height, frequency and percentage time [45].

3.3.1.1.2 The Okumura Model

Okumura's model is one of the most widely used models for signal prediction in urban areas. This model is applicable for frequencies in the range 150 MHz to 1920 MHz (although it is typically extrapolated up to 3000 MHz) and distances of 1 km to 100 km [35]. It can be used for base station antenna heights ranging from 30 m to 1000 m.

To determine path loss using Okumura's model, the free space path loss between the points of interest is first determined, and then the value of $A_{mu}(f, d)$ (as read from the Okumura curves) is added to it along with correction factors to account for the type of terrain. The model can be expressed as [35].

$$L_{50}(dB) = L_F + A_{mu}(f, d) - G(h_{te}) - G(h_{re}) - G_{AREA} \quad (3.13)$$

Where L_{50} is the 50th percentile (i.e., median) value of propagation path loss, L_F is the free space propagation loss, $A_{mu}(f, d)$ is the median attenuation relative to free space, $G(h_{te})$ is the base station antenna height gain factor, $G(h_{re})$ is the mobile antenna height gain factor, and G_{AREA} is the gain due to the type of environment.

$A_{mu}(f, d)$ and G_{AREA} can be read from median attenuation relative to free space and correction factor curves. Okumura found that $G(h_{te})$ varies at a rate of 20 dB/decade and $G(h_{re})$ varies at a rate of 10 dB/decade for height less than 3 m. $G(h_{te})$ and $G(h_{re})$ can be calculated using[35]:

$$G(h_{te}) = 20 \log\left(\frac{h_{te}}{200}\right) \quad 1000\text{m} < h_{te} < 30\text{m} \quad (3.14)$$

$$G(h_{re}) = 10 \log\left(\frac{h_{re}}{3}\right) \quad h_{re} \leq 0\text{m} \quad (3.15)$$

$$G(h_{re}) = 20 \log\left(\frac{h_{re}}{3}\right) \quad 10\text{m} < h_{re} < 0\text{m} \quad (3.16)$$

Where h_{te} and h_{re} are base station effective antenna height and a mobile antenna height respectively.

3.3.1.1.3 Hata Model

The Hata model is an empirical formulation of the graphical path loss data provided by Okumura, and is valid from 150 MHz to 1500 MHz. Hata presented the urban area propagation loss as a standard formula and supplied correction equations for application to other situations. The standard formula for median path loss in urban areas is given by[35]:

$$L_{50}(urban)(dB) = 69.55 + 26.16 \log(f_c) - 13.82 \log(h_{te}) - a(h_{re}) + (44.9 - 6.55 \log(h_{te})) \log(d) \quad (3.17)$$

Where f_c is the frequency (in MHz) from 150 MHz to 1500 MHz, h_{te} is the effective transmitter (base station) antenna height (in meters) ranging from 30 m to 200 m, h_{re} is the

effective receiver (mobile) antenna height (in meters) ranging from 1 m to 10 m, d is the transmitter to receiver separation distance (in km), and $a(h_{re})$ is the correction factor for effective mobile antenna height which is a function of the size of the coverage area. For a small to medium sized city, the mobile antenna correction factor is given by [35]:

$$a(h_{re}) = (1.1 \log(f_c) - 0.7)h_{re} - (1.56 \log(f_c) - 0.8) \text{ dB} \quad (3.18)$$

and for large city, it is given by

$$a(h_{re}) = 8.29[\log(1.54h_{re})]^2 - 1.1 \text{ dB for } f_c \leq 300 \text{ MHz} \quad (3.19)$$

$$a(h_{re}) = 3.2[\log(11.75h_{re})]^2 - 4.97 \text{ dB for } f_c \geq 300 \text{ MHz} \quad (3.20)$$

In Hata model to obtain the path loss in a suburban area the standard formula in equation (3.15) is modified as[35]:

$$L_{50}(\text{dB}) = L_{50}(\text{urban}) - 2 \left[\log\left(\frac{f_c}{28}\right) \right]^2 - 5.4 \quad (3.21)$$

and for path loss in open rural areas, the formula is modified as[35]:

$$L_{50}(\text{dB}) = L_{50}(\text{urban}) - 4.78[\log(f_c)]^2 - 18.33 \log(f_c) - 40.98 \quad (3.22)$$

3.3.1.2 Site-Specific Models for Path Loss

Site-specific propagation models, also called deterministic models, are based on the theory of electromagnetic-wave propagation. Unlike statistical models, site-specific propagation models do not rely on extensive measurements, but on knowledge of greater detail of the environment, and they provide accurate predictions of the signal propagation [42].

In theory, the propagation characteristics of electromagnetic waves could be computed exactly by solving Maxwell's equations. Unfortunately, this approach requires very complex mathematical operations and requires considerable computing power [42]. Ray tracing Technique, finite difference time domain (FDTD) models, moment-method models and artificial neural-network models are some of the available site specific path loss models. In the next section we will see briefly the ray tracing technique

3.3.1.2.1 Ray-Tracing Technique

Classical ray tracing determines all rays that can go from one transmitter (TX) location to one receiver (RX) location [34].

The method operates in two steps:

1. First, all rays that can transfer energy from the TX location to the RX location are determined. This is usually done by means of the image principle. Rays that can get to the RX via a reflection show the same behavior as rays from a virtual source that is located where an image of the original source (with respect to the reflecting surface) would be located.
2. In a second step, attenuations (due to free space propagation and finite reflection coefficients) are computed, thus providing the parameters of all MPCs.

3.3.2 Impulse-Response Models

The path loss is a parameter that can predict the power level of the system, and the coverage, it is necessary to model the effects of multipath delay. In the next sections the models for multipath are discussed.

3.3.2.1 Statistical Models for Multipath Fading Channels

Several multipath models have been suggested to explain the observed statistical nature of a wireless channel. The following are some of the statistical models for multipath fading channels

- Two-Ray Rayleigh Fading Model
- Saleh and Valenzuela Model
- Log-Normal at Any Distance

In the next section the first two ray two of these models

3.3.2.1.1 Two-Ray Rayleigh Fading Model

A commonly used multipath model is an independent Rayleigh fading 2-ray model [35]. This model considers two paths (one main path corresponding to a zero lag and one secondary path that typically has a fixed pre specified delay) with independently distributed Rayleigh amplitudes and phases [46]. The impulse response of the model is represented as [35].

$$h_b(t) = \alpha_1 \exp(j\varphi_1) \delta(t) + \alpha_2 \exp(j\varphi_2) \delta(t - \tau) \quad (3.23)$$

Where α_1 and α_2 are independent and Rayleigh distributed, φ_1 and φ_2 are independent and uniformly distributed over $[0, 2\pi]$, and τ is the time delay the two rays. By setting α_2 equal to zero, the special case of a flat Rayleigh fading channel is obtained as[35]:

$$h_b(t) = \alpha_1 \exp(j\varphi_1) \delta(t) \quad (3.24)$$

By varying τ for α_2 different from zero, it is possible to create a wide range of frequency selective fading effects.

3.3.2.1.2 Saleh and Valenzuela Model

Saleh and Valenzuela developed a simple multipath model for indoor channels based on measurement results. The model assumes that the multipath components arrive in clusters. The amplitudes of the received components are independent Rayleigh random variables with variances that decay exponentially with cluster delay as well as excess delay within a cluster. The corresponding phase angles are independent uniform random variables over $[0, 2\pi]$. The clusters and multipath components within a cluster form Poisson arrival processes with different rates. The clusters and multipath components within a cluster have exponentially distributed inter arrival times. The formation of the clusters is related to the building structure, while the components within the cluster are formed by multiple reflections from objects in the vicinity of the transmitter and the receiver [35].

3.3.2.2 Deterministic Models of Time-Delay Spread

The deterministic category encompasses all models that describe the propagation channel for a specific transmitter location, receiver location, and environment. Deterministic channel models are site-specific, as they clearly depend on the location of transmitter, receiver, and the properties of the environment [47]. These models use the geographical and morphological information from a database for a deterministic solution of Maxwell's equation or some approximation [34]. Ray tracing & virtual reflection points (VRP) models are techniques which are used to determine time delay spread.

3.3.2.2.1 Ray Tracing for Time-Delay Spread

In theory, the ray-tracing technique can determine almost all multipath components, including their amplitudes, time delays, and phases, and the technique is effective in predicting the time-delay spread. A detailed knowledge of the environment is required when applying a ray-tracing method [38].

Since the phase of each ray arriving at a receiver varies significantly with distance and cannot be accurately predicted, it will be impossible to achieve agreement with either the instantaneous measured shape or the value of the rms delay spread for a single individual measurement. The comparison between measured and modeled results should be used for average values in a small area around the actual receiver position. A seven-ray and a 25-ray model consider only single or double reflections, respectively, and were used to simulate propagation in a room. The rms delay spread was predicted, and agreed well with that calculated from measurements [38].

3.3.2.2.2 Virtual Reflection Points

This is similar to a seven-ray model, but in an outdoor environment. It assumed some VRF's, located at the intersection points along the LOS on streets and at building walls. It did not consider the effects of traffic and moving humans. The predicted results for the rms delay spreads were verified by measurements [38].

3.3.2.3 Models Based on Measurement Results

Because of the importance of determining the time-delay spread for wireless communications, a number of wideband channel-sounding techniques have been developed. These techniques may be classified as

- Direct pulse measurements;
- Swept-frequency measurements.
- Spread-spectrum sliding correlator measurements and

In the next section direct pulse measurements and swept frequency measurements is presented briefly

3.3.2.3.1 Direct Pulse Measurements

A simple channel sounding approach is the direct RF pulse system. This technique allows one to determine the power delay profile of an RF channel. A direct pulse system is essentially a wideband pulsed bistatic radar, transmitting a pulse of width τ seconds, and uses a receiver with a wide bandpass filter ($BW = 1/2\tau\text{Hz}$). The pulse is repeated every second or fraction of a second so that it may be averaged at the receiver. The received signal is amplified, detected with an envelope detector, and displayed and stored on a high speed oscilloscope. This gives an immediate measurement of the square of the channel impulse response convolved with the probing pulse. If the oscilloscope is set on averaging mode, then this system can provide a local average power delay profile [48]. A block diagram of the direct pulse system is shown in Figure 3.4.

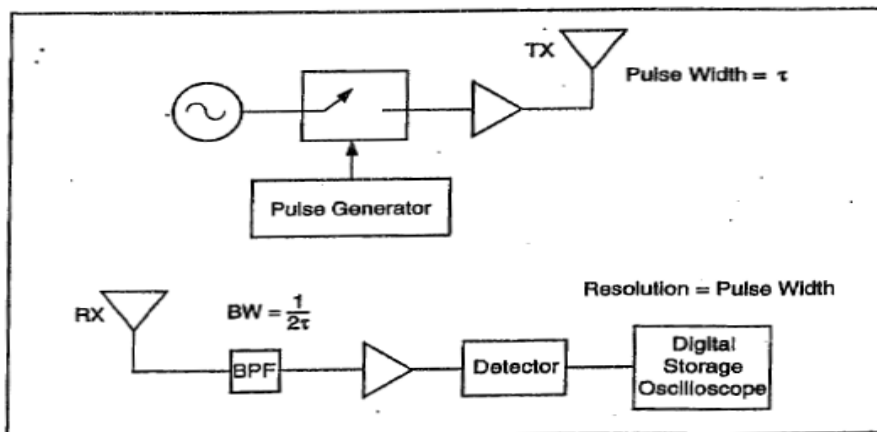


Figure 3.4: Direct pulse RF Channel measurement system [48].

3.3.2.3.2 Swept-frequency measurements

Because of the dual relationship between the time domain and the frequency domain, it is possible to measure the channel impulse response using frequency domain techniques. Figure 3.5 shows a frequency domain channel sounder. A vector network analyzer controls a synthesized frequency sweeper, and an S-parameter test set is used to monitor the frequency response of the channel. The sweeper scans a particular frequency band stepping through discrete frequencies. Due to the Fourier transform, the number and spacing of these frequency steps impact the time resolution of the impulse response measurement. For each frequency step, the S-parameter test set transmits a known signal level at port 1 and monitors the received signal level at port 2. These signals allow the analyzer to determine the complex response (i.e., transmissivity $S_{21}(\omega)$) of the channel over the measured frequency range. The transmissivity response is a frequency domain representation of the channel impulse response, and is converted to the time domain using inverse discrete Fourier transform (IDFT) processing, giving a band-limited version of the impulse response [48].

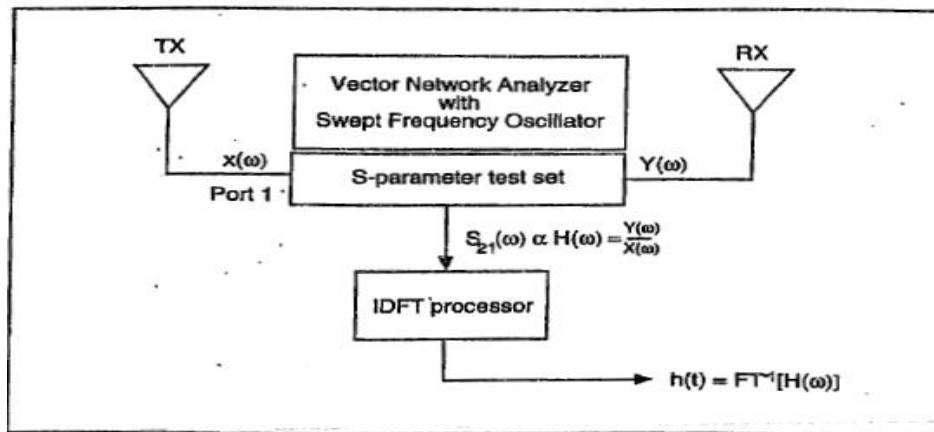


Figure 3.5: Frequency domain channel sounder [48].

3.4 Channel Models used for the Simulation

The channel behavior is described by its long-term and short-term fading characteristics where the former often depends on the geometrical location of a user in a wireless network and the latter defines the time-variant spatial channels [47]. For design,

simulation and planning of wireless systems the propagation channels model of the environment is required [34].

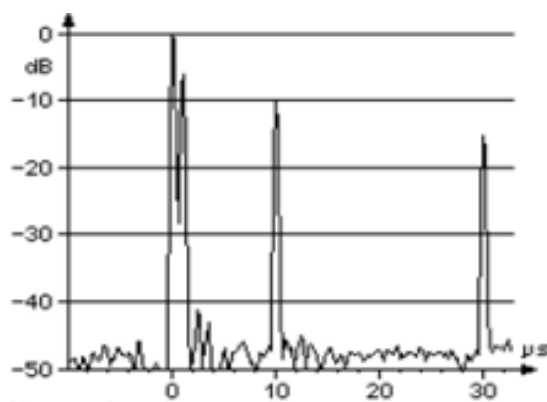
There are two main applications of channel models [34]:

- For the design, testing, and type approval of wireless systems
- The designers of wireless networks are interested in optimizing a given system in a certain geographical region.

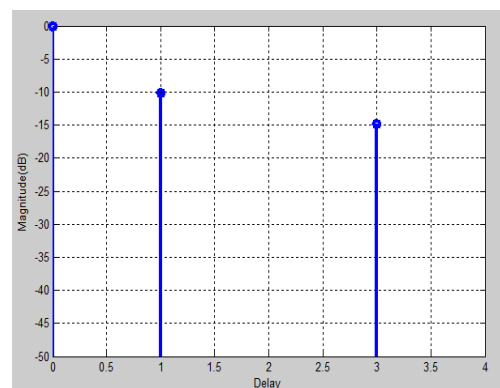
A combination of multipath channel and AWGN channel models are used for the simulation in this thesis. The AWGN are included due to the effect of noise is significant in multipath channel. The multipath channels are selected considering the three modeling methods in use for designing, testing, type approval and optimization of wireless system. The modeling methods are stored channel impulse responses, deterministic channel models and stochastic channel models. The following three multipath channels are used for the analysis of the adaptive blind equalization methods.

3.4.1 Measured Channel Impulse Response

The channel shown in Figure 3.6(a) is taken from [31], it is measured using via Inverse Fast Fourier Transform (IFFT). The measurement indicate that three impulse are detected with the maximum of the channel response [0 -10, -50, and -15] in dB at time interval of 0, 10, 20, and 30 μ seconds when converted to decimal the channel response becomes [1 .31 0 .18]. The response of the channel used for simulation is shown in Figure 3.6 (b) in logarithmic scale.



(a) Channel taken from reference[31]



(b) channel used for the simulation

Figure 3.6: Stored channel impulse responses.

3.4.2 Joint Technical Committee Model

A comprehensive multipath propagation model recommended by the Joint Technical Committee (JTC) for simulation of radio propagation is used as one of the channel for the simulation. The recommendation is for different areas of both indoor and outdoor channels. The JTC wideband multipath propagation channel model parameters for outdoor urban area are summarized in Table 3.1. This channel model is taken as one of the channel model used for the simulation.

Taps	Relative Delay(ns)	Average Power(dB)	Average Power (Decimal)
1	0	0	0
2	100	-3.6	0.660693
3	200	-7.2	0.436516
4	300	-10.8	0.288403
5	500	-18.0	0.125893
6	700	-25.2	0.054954

Table 3.1: JTC Channel Model Parameters for Outdoor Urban [49]

3.4.3 Exponential Channel Model

The exponential channel model is the ideal channel model for software simulation and performance comparisons due it is easy to generate and it is a reasonably accurate model of the real world [9]. This model provides a good compromise between simplicity and reality.

Theoretically, an infinite number of taps exist in the exponential model; however, the magnitude of the taps decays rapidly. Therefore, truncating the taps at some point is reasonable. This point is determined by the sampling frequency f and the rms delay spread τ . In other words, the channel can be represented by a FIR model.

The exponential channel model (IEEE 802.11b model) defined for wireless local area network (WLAN) is used for the simulation. The impulse response of the channel is given by [50]:

$$h(k) = N\left(0, \frac{1}{2}\sigma_k^2\right) + j.N\left(0, \frac{1}{2}\sigma_k^2\right) \text{ for } k = 0, 1, \dots, k_{max} \quad (3.25)$$

Where

$k_{max} = 10\tau_{rms}/T_s$, τ_{rms} delay spread and T_s sampling period and truncated to FIR

$$\sigma_k^2 = \sigma_0^2 \beta^k \quad (3.26)$$

$$\sigma_0^2 = (1 - \beta)/(1 - \beta^{k_{max}+1}), \text{ normalized average power} \quad (3.27)$$

$$\beta = e^{-T_s/\tau_{rms}} \quad (3.28)$$

The channel model is normalized in an expected value sense as.

$$\begin{aligned} E\{\sum_{k=0}^{k_{max}} |h_k|^2\} &= \sum_{k=0}^{k_{max}} \sigma_k^2 = \sigma_0^2 \sum_{k=0}^{k_{max}} e^{-kT_s/\tau_{rms}} \\ &= \sigma_0^2 (1 - e^{-T_s/\tau_{rms}})/(1 - e^{-(k_{max}+1)T_s/\tau_{rms}}) \end{aligned} \quad (3.29)$$

$$\begin{aligned} \text{The average power can made to 1 by selecting } \sigma_0^2 &= (1 - \\ e^{\frac{-(k_{max}+1)T_s}{\tau_{rms}}}) &/ (1 - e^{-T_s/\tau_{rms}}) \end{aligned} \quad (3.30)$$

** The $N\left(0, \frac{1}{2}\sigma_k^2\right)$ can be genated from the random variable with zero mean and $\frac{1}{2}\sigma_k^2$ variance.

Sample exponentially decaying channel impulse response is shown in Figure 3.7.

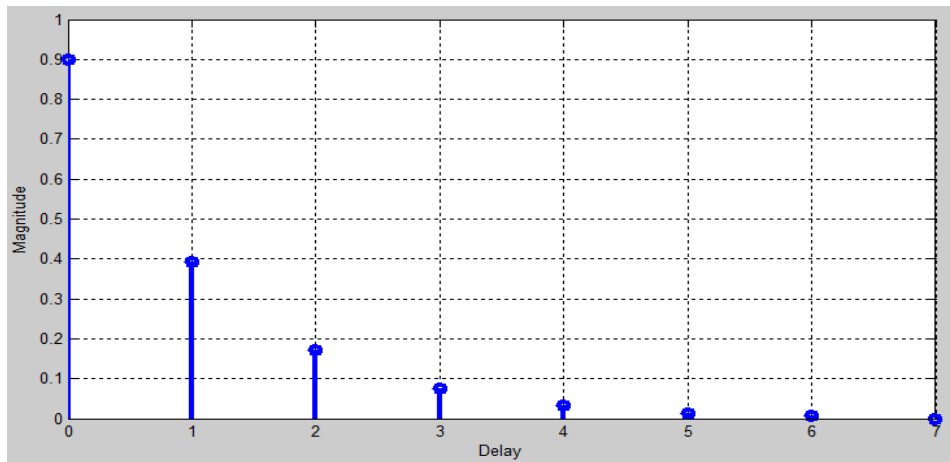


Figure 3.7: Exponential decaying channel

CHAPTER IV

Adaptive Equalization

4.1 Introduction

For bandwidth-efficient communication systems operating in high ISI environments, compensation of the amplitude and phase distortions introduced by the channel is essential to achieve reliable communication [11]. An application of adaptive filter called channel equalization is one of the techniques used to compensate the distortion caused by the multipath channel. In a broad sense, the term equalization can be used to describe any signal processing operation that minimizes ISI [35].

Generally the wireless channel is unknown and time varying hence the equalizer used to compensate the distortion caused by the channel must adapt to the changes in the channel. An adaptive equalizer provides a simple practical device capable of both learning and inverting the distorting effects of the channel. In adaptive equalizers the filter tap weight are updated by the equalizer at each training session or iteration of blind equalizer unlike the non-adaptive where the equalizer tap weight are fixed. The basic concept used to update the equalizer tap weight depends on equalizer type, in the section 4.3 detail classification of equalizer is presented

4.2 Equalization in QAM Data Communication System

In data communication, digital signals are transmitted by the sender through an analog channel to the receiver. The complex baseband model for a typical quadrature amplitude modulated(QAM) data communication system is shown in Figure 4.1, it consists

of an unknown linear time-invariant (LTI) channel $h(t)$ which represents all the interconnections between the transmitter and the receiver at baseband[51].

The baseband-equivalent transmitter generates a sequence of complex-valued random input data $a(n)$, each element of which belongs to a complex alphabet A (or constellation) of QAM symbols. The data sequence $a(n)$ is sent through a baseband equivalent complex LTI channel whose output $x(n)$ is observed by the receiver. The function of the receiver is to estimate the original data $a(n)$ from the received signal $x(n)$.

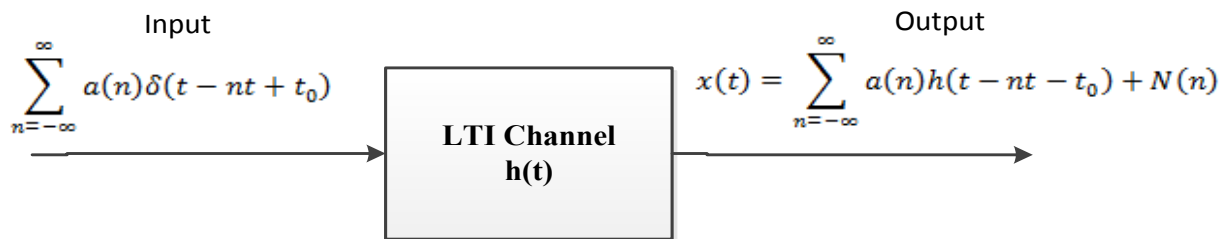


Figure 4.1: Baseband representation of a QAM data communication system.

For a causal and complex-valued LTI communication channel with impulse response $h(t)$, the input/output relationship of the QAM system can be written as[51]:

$$x(t) = \sum_{n=-\infty}^{\infty} a(n)\delta(t - nT + t_0) + N(t), \quad a(n) \in A \quad (4.1)$$

Where T is the symbol period. Typically the channel noise $N(t)$ is assumed to be stationary, Gaussian, and independent of the channel input $a(n)$.

Assuming perfect timing recovery the channel output sampled at the known symbol rate T is given by Equation (4.2)[51].

$$x(nT) = \sum_{k=-\infty}^{\infty} a(k)h(nT - kT + t_0) + N(nT), \quad (4.2)$$

Using the notations[51]

$$x(n) = x(nT), N(n) = N(nT), \text{ and } h(n - k) = h((n - k)T + t_0) \quad (4.3)$$

the relationship in Equation (4.2) can be written as[51]

$$x(n) = \sum_{k=-\infty}^{\infty} a(k)h(n - k) + N(n) \quad (4.4)$$

When the channel is non-ideal, the impulse response $h(n)$ is nonzero for $n \neq 0$. Consequently, undesirable signal distortion is introduced in the channel output $x(n)$ which

depends on multiple symbols in $\{\mathbf{a}(n)\}$. This phenomenon, known as ISI, can severely distort the transmitted signal [51]. A simple memoryless decision device acting on $\mathbf{x}(n)$ may not be able to recover the original data sequence under strong ISI. Channel equalization has proven to be an effective means of significant ISI removal.

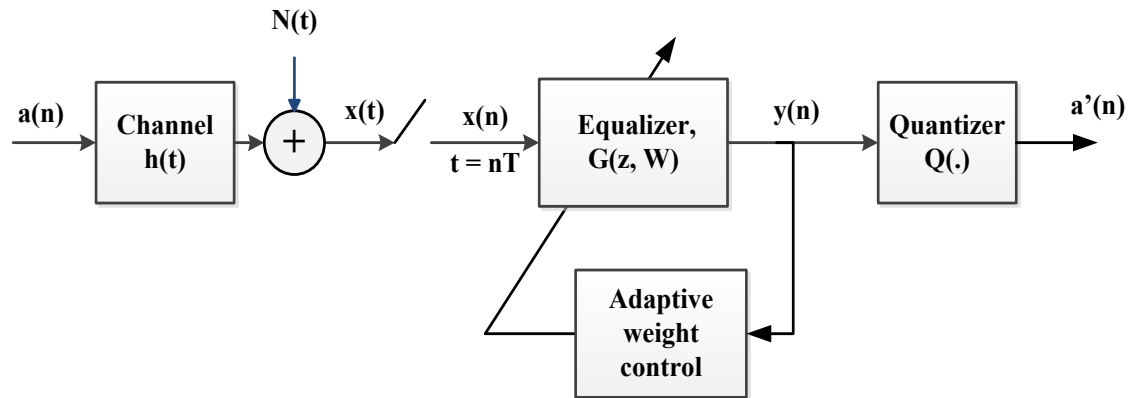


Figure 4.2: Adaptive blind equalization system [51].

Figure 4.2 shows the combined communication system with adaptive equalization. In this system, the equalizer $\mathbf{G}(z, \mathbf{W})$ is a linear FIR filter with parameter vector \mathbf{W} designed to remove the distortion caused by channel ISI. The goal of the equalizer on the receiver side is to generate an output signal $\mathbf{y}(n)$ that can be quantized to yield a reliable estimate of the channel input data as[51]:

$$\hat{a}(n) = Q(y(n)) = a(n - \delta) \quad (4.5)$$

Where $Q(x)$ is the quantization function and δ is a constant integer delay. Typically any constant but finite amount of delay introduced by the combined channel and equalizer is acceptable in communication systems [51].

Instead of identifying the channel and then inverting it to recover the source signal, a more direct approach is to find an equalizer along with optimal the equalizer coefficients to recover the source signal. From this point of view, a number of techniques have been proposed [51]. In the next sections we will see the different available equalization methods.

4.3 Equalizers Classification

In general adaptive equalizers can be classified as supervised (trained) equalizers and unsupervised (blind) equalizers [52], Figure 4.3 show a typical classification of equalizers.

In trained equalizers, the filter tap weights are initially set using a training sequence of data symbols known both to the transmitter and receiver. These training based equalizers are effective and widely used in application such as global system for mobile communications (GSM) [11, 53]. However, there are applications where training may not be feasible, for example, in equalizer implementations of digital handsets devices [54]. When the communications environment is highly non-stationary, it may even become grossly impractical to use training sequences. A blind equalizer, on the other hand, does not require a training sequence to be sent for start-up or restart of the receiver. Rather, the blind equalization algorithms use a priori knowledge regarding the statistics of the transmitted data sequence as opposed to an exact set of training sequences known both to the transmitter and receiver [54].

The trained equalizers can also be sub categorized as symbol-by-symbol (SBS) or sequence estimators (SE). SBS equalizers remove ISI from each symbol and then detect each symbol individually [39]. SBS equalizers further subdivided into two general categories linear and nonlinear equalization. These categories are determined from how the output of an adaptive equalizer is used for subsequent control (feedback) of the equalizer. In the next sections we will see in more detail the trained and blind equalization method [39].

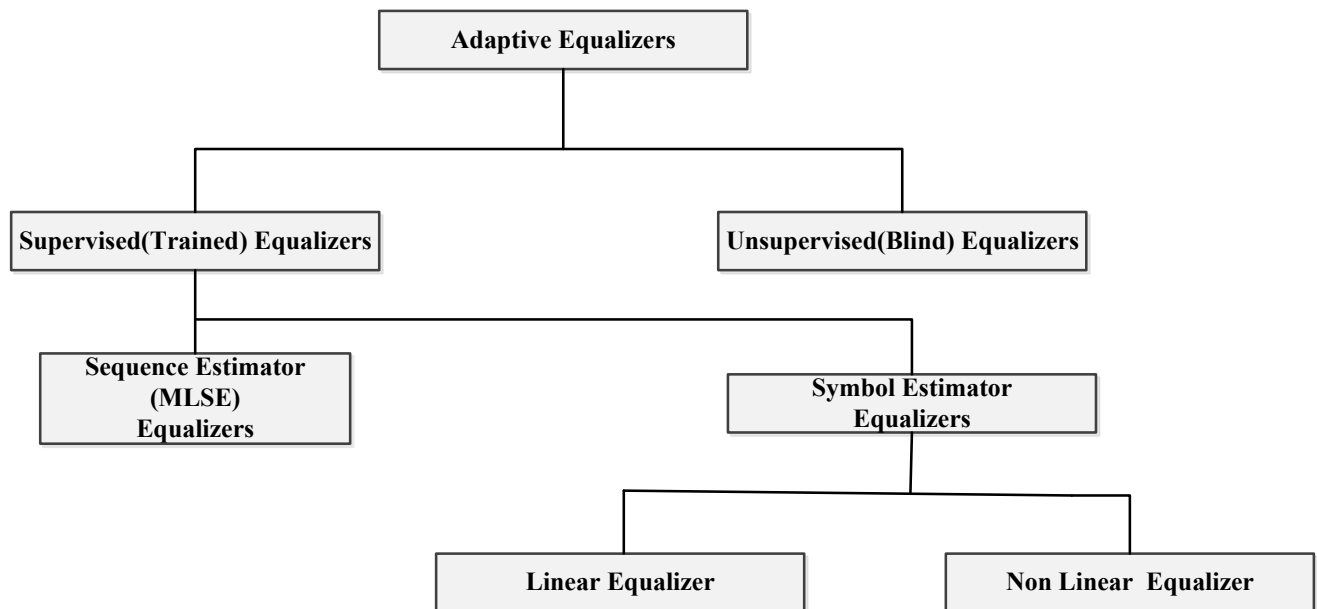


Figure 4.3: Classification of adaptive equalizers [55].

4.4 Trained Equalizers

The general operating modes of an adaptive trained equalizer include training and tracking. First, a known, fixed-length training sequence is sent by the transmitter so that the receiver's equalizer may average to a proper setting utilizing recursive algorithm to evaluate the channel and estimate filter coefficients to compensate for the channel. The training sequence is designed to permit an equalizer at the receiver to acquire the proper filter coefficients in the worst possible channel conditions so that when the training sequence is finished, the filter coefficients are near the optimal values for reception of user data [35]. Immediately following the training sequence the user data is sent.

The reliance of the trained adaptive equalizer on a training sequence requires that the transmitter cooperates by (often periodically) resending the training sequence for the equalizer to track the changing channel [51]. As a consequence, the adaptive equalizer is continually changing its filter characteristics over time [35].

As indicated in the previous section the trained equalizers are classified into two general categories linear and nonlinear equalization. We will see these categories in more detail in the next sections.

4.4.1 Linear Equalizer

A linear equalizer can be implemented as a finite impulse response (FIR) filter (also called the transversal filter). In such equalizer, the current and past values of the received signal are linearly weighted by the filter coefficient and summed to produce the output, as shown in Figure 4.4 [35]. The linear equalizer can also be implemented as lattice filter.

Mathematically the output of this transversal filter before decision making can be expressed as[35]:

$$\hat{d}_k = \sum_{n=-N_1}^{N_2} (C_n^*) y_{k-n} \quad (4.6)$$

Where (C_n^*) represents the tap weights, \hat{d}_k the equalizer output at time index k, y_i is the input received signal at time $t_0 + iT$, t_0 is the equalizer starting time, and $N = N_1 + N_2 + 1$ the numbers of taps used in the forward and reverse portions.

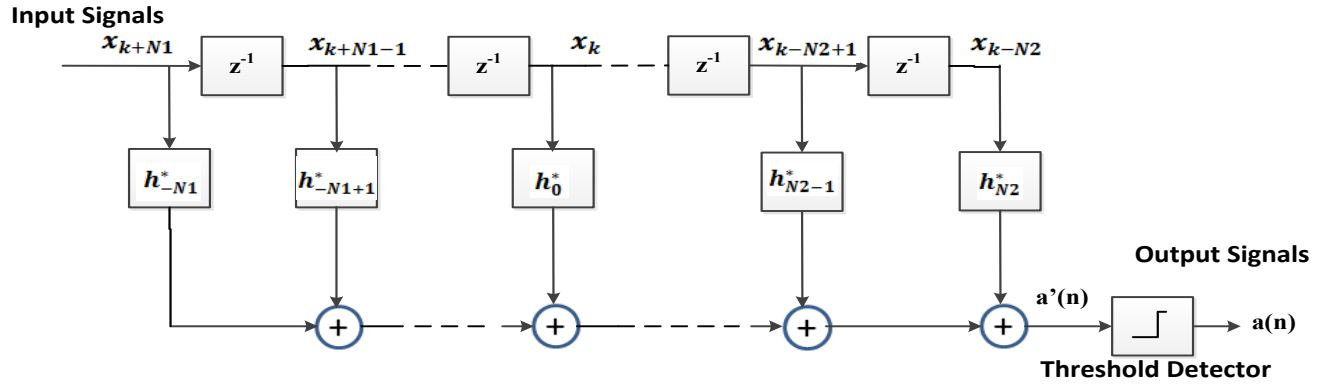


Figure 4.4: Structure of a linear transversal equalizer [35].

The following are some of the linear equalization methods available and we will see this equalization method in more detail.

1. Zero forcing(ZF) equalizer
2. Minimum Mean Square Error (MMSE) Equalizer

4.4.1.1 Zero Forcing Equalizer

The ZF equalizer adjusts the equalizer coefficients by forcing the samples of the combined channel and equalizer impulse response to zero at all but one of the sample points in the tapped delay line filter if there is no noise [35].

The ZF equalizer eliminates the ISI introduced by the channel and the impulse response of the combined channel and the equalizer is defined mathematically as [55]:

$$h_E(kT_s + D) = \begin{cases} 1, & k = 0 \\ 0, & k \neq 0 \end{cases} \quad (4.7)$$

Where T_s is symbol period and D is the delay period. By taking the Fourier transform of Equation (4.7) the ZF response can be expressed as[55]:

$$H_E(f) = H(f)G_{ZF}(f) = 1 \quad |f| \leq \frac{1}{2T_s} \quad (4.8)$$

$$G_{ZF}(f) = \frac{1}{H(f)} \quad (4.9)$$

Where $H(f)$ is the frequency response of the channel, and $G_{ZF}(f)$ is the ZF equalizer frequency response. The ZF equalizer can also be expressed as[55]:

$$G_{ZF}(z) = \frac{1}{H(z)} \quad (4.10)$$

The ZF equalizer defined by Equation (4.10) may not be implementable as a FIR. Specifically, it may not be possible to find a finite set of coefficients w_{-L}, \dots, w_L such that [35].

$$w_{-L}z^L + \dots + w_Lz^{-L} = \frac{1}{H(z)} \quad (4.11)$$

In this case we find the set of coefficients $\{w_i\}$ that best approximates the ZF equalizer.

The ZF equalizer has the disadvantage that the inverse filter may excessively amplify noise at frequencies where the folded channel spectrum has high attenuation.

4.4.1.2 Minimum Mean Square Error Equalizer

The ZF equalizer, although removes ISI, may not give the best error performance for the communication system because it does not take into account noises in the system [56]. In real world noise exist and a different equalizer that takes noises into account is the MMSE equalizer. It is based on the mean square error (MSE) criterion.

Without knowing the values of the information symbols a_k beforehand, each symbol \hat{a}_k can be model as a random variable. With the assumption that the information sequence \hat{a}_k is wide-sense stationary (WSS), and a choice of linear equalizer $H_E(z)$ to minimize the MSE between the original information symbols a_k and the output of the equalizer \hat{a}_k . The MSE is given by[56]:

$$MSE = E[e_k^2] = E[(a_k - \hat{a}_k)^2] \quad (4.12)$$

Where e_k is the error at the k^{th} symbol.

Using FIR filter of order $2L + 1$ shown in Figure 4.5 as the equalizer a delay of L symbols is incurred at the output of the FIR filter. Then Equation (4.12) can written as[56]:

$$MSE = E \left[\left(a_k - \sum_{j=-L}^L \tilde{a}_{k-j} h_{Ej} \right)^2 \right] \quad (4.13)$$

$$= E \left[(a_k - \hat{\mathbf{A}}_k^T \mathbf{h}_E)^2 \right], \quad (4.14)$$

$$\text{Where } \hat{\mathbf{A}}_k = [\hat{a}_{k+L}, \dots, \hat{a}_{k-L}]^T, \quad (4.15)$$

$$\mathbf{h}_E = [h_{E-L}, \dots, h_{E_L}]^T, \quad (4.16)$$

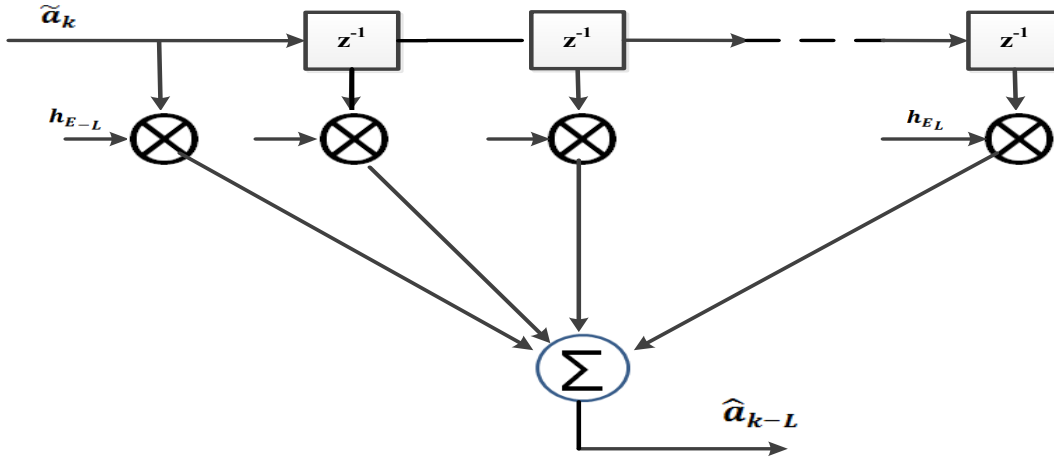


Figure 4.5: FIR filter as an MMSE equalizer

The MSE is minimized by suitable choices of h_{E-L}, \dots, h_{E-L} which can be found by differentiating with respect to each h_{E_j} and setting the result to zero. The MSE is achieved at[56]:

$$E[\hat{\mathbf{A}}_k(a_k - \hat{\mathbf{A}}_k^T \mathbf{h}_E)] = 0, \quad (4.17)$$

Rearranging, Equation (4.17) can be written as

$$\mathbf{R} \mathbf{h}_E = \mathbf{d}, \quad (4.18)$$

Where

$$\mathbf{R} = E[\hat{\mathbf{A}}_k \hat{\mathbf{A}}_k^T], \quad (4.19)$$

$$\mathbf{d} = E[a_k \hat{\mathbf{A}}_k], \quad (4.20)$$

If \mathbf{R} and \mathbf{d} are available, then the MMSE equalizer can be found by solving the linear matrix Equation (4.18). The linear MMSE equalizer can also be found iteratively. As MSE is a quadratic function of \mathbf{h}_E the gradient of the MSE with respect to \mathbf{h}_E gives the direction to change \mathbf{h}_E for the largest increase of the MSE. In our notation, the gradient is $-2(\mathbf{d} - \mathbf{R} \mathbf{h}_E)$. To decrease the MSE, \mathbf{h}_E must be update in the direction opposite to the gradient. This is the steepest descent algorithm: At the k^{th} step, the vector $\mathbf{h}_E(k)$ is updated as[56]:

$$\mathbf{h}_E(k) = \mathbf{h}_E(k-1) + \mu[\mathbf{d} - \mathbf{R} \mathbf{h}_E(k-1)] \quad (4.21)$$

Where μ is a small positive constant that controls the rate of convergence.

In many applications, \mathbf{R} and \mathbf{d} are unknown in advance. However, the transmitter can transmit a training sequence that is known a priori by the receiver. With a training sequence, the receiver can estimate \mathbf{R} and \mathbf{d} . Alternatively, with a training sequence, we can

replace \mathbf{R} and \mathbf{d} at each step in the steepest descent algorithm by the rough estimates $\sim \hat{\mathbf{A}}_k \hat{\mathbf{A}}_k^T$ and $a_k \hat{\mathbf{A}}_k$, respectively. The algorithm becomes[56]:

$$\mathbf{h}_E(k) = \mathbf{h}_E(k-1) + \mu[a_k - \hat{\mathbf{A}}_k^T \mathbf{h}_E(k-1)] \hat{\mathbf{A}}_k \quad (4.22)$$

This is a stochastic steepest descent algorithm called the least mean square (LMS) algorithm

4.4.2 Non Linear Equalizers

Nonlinear equalizers are used in applications where the channel distortion is too severe for a linear equalizer to handle. Linear equalizers do not perform well on channels which have deep spectral nulls in the passband. In an attempt to compensate for the distortion, the linear equalizer places too much gain in the vicinity of the spectral null, thereby enhancing the noise present in those frequencies.

The following are some of the nonlinear equalization techniques available [35]:

1. Decision Feedback Equalization (DFE)
2. Maximum Likelihood Symbol Detection
3. Maximum Likelihood Sequence Estimation (MLSE)

4.5 Blind Equalizers

In general, the blind equalization techniques can be classified according to their signals statistical properties exploitation. There are two known approaches used by blind equalized namely:

- Statistical approach and,
- Stochastic gradient descent(SGD) approach

The SGD approach iteratively minimizes a chosen cost function over all possible choices of the equalizer coefficients, while the statistical approach uses sufficient stationary statistics collected over a block of received data for channel identification or equalization [51]. A limitation of statistical methods is that they require the channel to be constant over a block of received data, which is not possible in real-world wireless fading channels. Hence SGD are mostly used to adapt in wireless fading channels [17].

The statistical approach exploits higher order statistics (HOS) or cyclostationary statistical information directly. The following are some of the equalizers categorized in this group.

1. Blind MMSE DFE
2. MMSE
3. Blind MLSE
4. Blind Equalization by Sampled PDF Fitting
5. Adaptive Blind Equalization through Quadratic PDF Matching

Now a day's many digital communication schemes transmit constant modulus (CM) signals. Hence, several iterative SGD based blind equalization algorithms exploiting this precious information, namely, the constant modulus criterion, have been developed and have gained a widespread use in different communication systems [57].

The following are some of the available SGD based equalization techniques.

1. CMA
2. MMA
3. Fractionally spaced CMA and
4. Variable step size CMA

In next sections, the three most commonly known and widely used constant modulus based blind adaptive algorithms: CMA, MMA and fractionally spaced CMA are presented in detail and these algorithms are used for the performance analysis of adaptive blind equalizers for audio broadcasting system in this thesis. Due to time limitation the thesis is not able to extend the analysis to include additional equalization techniques.

4.5.1 Constant Modulus Algorithm

CMA uses the constant modularity of the signal as the desired property. CMA assumes that the input to the channel is a modulated signal that has constant module such as 4-QAM, and 8-PSK at every instant in time. Any deviation of the received signal constant module from the constant value is considered a distortion introduced by the channel. The

distortion is mainly caused by band-limiting or multi-path effects in the channel. Both these effects result in ISI and thus distort the received signal [11].

CMA attempts to accomplish this objective by forcing the output of the adaptive filter (equalizer) to be of constant module. CMA can also be used for higher order QAM signals where the amplitude of the modulated signal is not the same at every instant [11].

For channel input signal that has a constant modulus, the CMA equalizer penalizes output samples $y(n)$ that do not have the desired constant modulus characteristics [51]. The cost function of CMA is given by Equation (4.23)[51]:

$$J_2(k) = E[(|y(k)|^2 - R_2)^2] \quad (4.23)$$

Where $y(k)$ is the equalizer's instantaneous output and R_2 is called constant modulus and the constant modulus is defined mathematically as[51]:

$$R_2 = \frac{E[|a(k)|^4]}{E[|a(k)|^2]} \quad (4.24)$$

Where $a(k)$ is the instantaneous transmitted symbols.

The N-tap weighted equalizer's output is given by[51]:

$$y(k) = W^T X \quad (4.25)$$

Where X the input sequence for the equalizer and W the equalizer weight which can be found using[51]:

$$X(k) = [x(k), x(k-1), \dots, x(k-N+1)]^T \quad (4.26)$$

$$W(k) = [w_0(k), w_1(k-1), \dots, w_{N-1}(k-N+1)]^T \quad (4.27)$$

The equalizer weight is updated using[51]:

$$W(k+1) = W(k) - \mu \nabla J_2(W(k)) \quad (4.28)$$

Using the SGD algorithm Equation (4.28) is simplified to[51]:

$$W(k+1) = W(k) - \mu e(k) X^*(k) \quad (4.29)$$

Where $e(k)$ is the instantaneous error and given by[51]:

$$e(k) = y(k)(|y(k)|^2 - R_2) \quad (4.30)$$

4.5.2 Multiple Module Algorithm

The MMA equalization technique exploits the constant modality of signal by minimizing the dispersion of real and imaginary parts, $y_R(n)$ and $y_I(n)$ of $y(n)$ separately and embedded in its cost function instead of minimizing the dispersion of the magnitude of the equalizer output $y(n)$. Unlike CMA, the MMA cost function ignores the cross term $y_R(n)y_I(n)$ between the in-phase and quadrature components in the CMA cost function. As a result, the MMA cost function is not a two-dimensional cost function. It can be considered as the sum of two one-dimensional cost functions, which minimize the dispersion of $y_R(n)$ and $y_I(n)$ around separate contours. However, by considering the real and imaginary parts of the equalizer output in the cost function, it carries the information of the channel phase-distortion [58].

The MMA penalizes the dispersion of $y_R(k)$ and $y_I(k)$ around separate straight contours. The cost function minimized by MMA is defined as [10]:

$$J_{MMA}(w) = J_R(w) + J_I(w) \quad (4.31)$$

Where $J_R(w)$ and $J_I(w)$ are the cost function for the real and imaginary part and given by [10]:

$$J_R(w) = E[(|y_R(w)|^2 - R_{2,R}^2)] \quad (4.32)$$

$$J_I(w) = E[(|y_I(w)|^2 - R_{2,I}^2)] \quad (4.33)$$

Where $R_{2,R}$ and $R_{2,I}$ are the constant module for the real and imaginary parts respectively and can be calculated using [10]:

$$R_{2,R} = \frac{E[|a_R(k)|^4]}{E[|a_R(k)|^2]}, \quad R_{2,I} = \frac{E[|a_I(k)|^4]}{E[|a_I(k)|^2]} \quad (4.34)$$

The equalizer weight is updated using [10]:

$$W(k+1) = W(k) - \mu \nabla J_{MMA}(W(k)) \quad (4.35)$$

Using SGD algorithm Equation (4.35) is simplified to

$$W(k+1) = W(k) - \mu e(k)X^*(k) \quad (4.36)$$

Where the $e(k)$ is calculated from the real and imaginary error as [10]:

$$e(k) = e_R(k) + e_I(k) \quad (4.37)$$

Where

$$e_R(k) = y_R(k)(|y_R(k)|^2 - R_{2,R}) \text{ and,} \quad (4.38)$$

$$e_I(k) = y_I(k)(|y_I(k)|^2 - R_{2,I}) \quad (4.39)$$

Then the output of the equalizer can be found using[10]:

$$y(k) = W^T X \quad (4.40)$$

Where X the input sequence for the equalizer and W the equalizer weight which can be found using[10]

$$X(k) = [x(k), \quad x(k - 1), \dots, x(k - N + 1)]^T \quad (4.41)$$

$$W(k) = [w_0(k), \quad w_1(k - 1), \dots, w_{N-1}(k - N + 1)]^T \quad (4.42)$$

4.5.3 Fractionally Spaced CMA

Conventional equalizers have tap spacing's that are spaced with respect to the symbol rate [59]. In fractionally spaced equalizer (FSE), the tap spacing of the equalizer is a fraction of the transmitted symbol period. As the output of the equalizer has the same rate as the input symbol rate, the output of the FSE needs to be calculated once in every symbol period. In this situation, the FSE can be modeled as a parallel combination of a number of baud spaced equalizers. This parallel combination of baud spaced equalizers is known as the Multi-Channel Model of FSE [60].

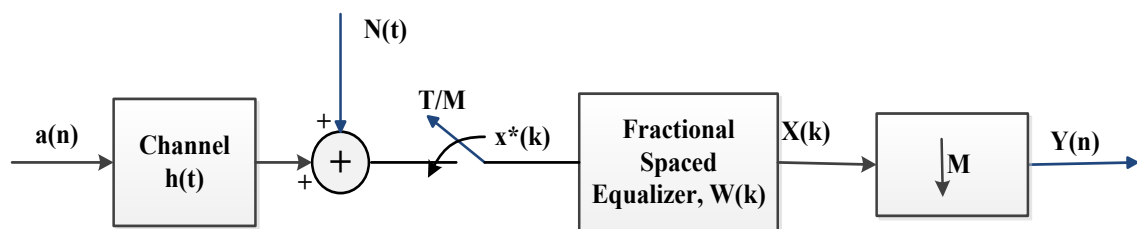


Figure 4.6: Baseband Model for a Communication System with FSE[13]

The FSE is an FIR filter and the tap spacing of this filter is T/M , where M is the oversampling factor. As the sample period of the input sequence is the same as the tap spacing of the filter, the input sequence to the FSE, $x(t)$, in Figure 4.6 needs to be sampled at intervals T/M apart. Then the expression in Equation (4.1) for the discrete time equivalent signal $x(k \cdot T/M)$ is given by Equation (4.43) [60].

$$x\left(k\frac{T}{M}\right) = \sum_{k=-\infty}^{\infty} y(n)h\left(k\frac{T}{M} - n\frac{T}{M} - t_0\right) + N\left(k\frac{T}{M}\right) \quad (4.43)$$

For notational simplicity, the oversampled channel output $x\left(k\frac{T}{M}\right)$ can be divided into M linearly independent subsequences[60]:

$$x^i(n) \cong x\left[\left(nM + i\right)\frac{T}{M}\right] = x\left(nT + i\frac{T}{M}\right), i = 1, \dots, M \quad (4.44)$$

Define K as the effective channel length based on

$$h_0^i = 0, \text{ for some } 1 < i < M \quad (4.45)$$

$$h_K^i = 0, \text{ for some } 1 < i < M \quad (4.46)$$

By denoting the sub-channel transfer function as[60]:

$$H_i(z) = \sum_{k=0}^K h_k^{(i)} z^{-k} \quad \text{where } h_k^{(i)} \cong h\left(kT + i\frac{T}{M} + t_0\right) \quad (4.47)$$

the M subsequences can be written as

$$x^i(n) = H_i(z)a(n) + w\left(nT + i\frac{T}{M}\right), i = 1, \dots, M \quad (4.48)$$

Thus, these M subsequences can be viewed as stationary outputs of M discrete FIR channels with a common input sequence $a(n)$ as shown in Figure 4.7.

The vector representation of the FSE is shown in Figure 4.7. One equalizer filter is provided for each subsequence $x^i(n)$. In fact, the actual equalizer is a vector of filters[60]:

$$W_i(z) = \sum_{k=0}^L w_{i,k} z^{-k} \quad i = 1, \dots, M \quad (4.49)$$

Where L is the equalizer length

The M filter outputs $\{y^i(n)\}$ are summed to form the stationary equalizer output[60]:

$$y(n) = W^T X(n) \quad (4.50)$$

Where

$$W = [w_{1,0} \dots w_{1,m} \dots w_{p,0} \dots w_{p,m}]^T \quad (4.51)$$

$$X = [x^1(n) \dots x^1(n-m) \dots x^p(n) \dots x^p(n-m)]^T \quad (4.52)$$

Given the equalizer output and parameter vector, the adaptive blind CMA equalization discussed in section (4.6) applied to the FSE to get the adaptive blind FSE CMA.

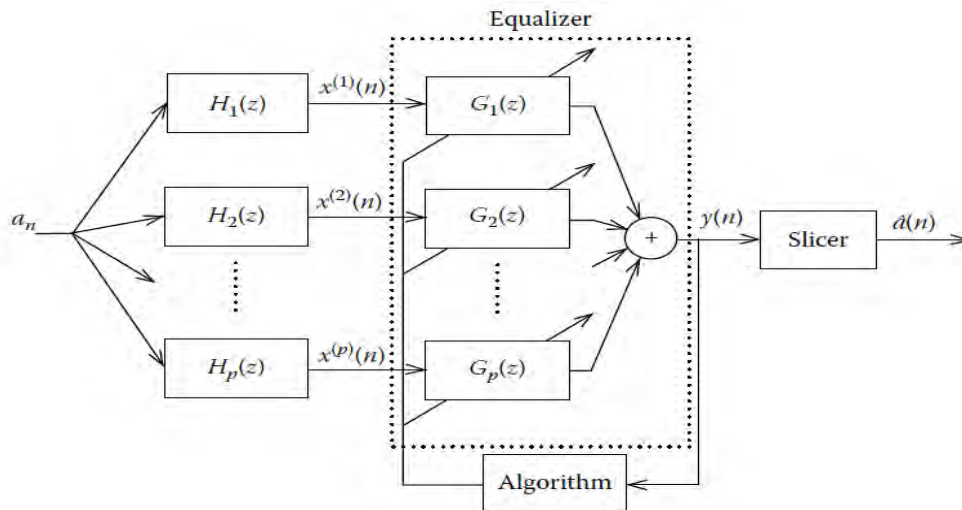


Figure 4.7: Vector representation for an FSE [51].

4.6 Equalizers Performance Parameters

The performance of equalizers depended on the specific algorithm used to update the equalizer coefficients and track the channel variation. A wide range of algorithms are available to adapt the equalizer coefficients and the performance of an algorithm is determined by various factors which include [35]:

- **Rate of convergence:** - This is defined as the number of iterations required for the algorithm, in response to stationary inputs, to converge close enough to the optimum solution. A fast rate of convergence allows the algorithm to adapt rapidly to a stationary environment of unknown statistics. Furthermore, it enables the algorithm to track statistical variations when operating in a nonstationary environment [35].
- **Misadjustment:-** For an algorithm of interest, this parameter provides a quantitative measure of the amount by which the final value of the MSE, averaged over an ensemble of adaptive filters, deviates from the optimal minimum MSE[35].
- **Computational complexity:-** The computation time depends on the number of operations required for one complete iteration of the algorithm along with the amount of memory needed to store the mathematical calculations.
- **Numerical properties:-** When an algorithm is implemented numerically, inaccuracies are produced due to round-off' noise and representation errors in the computer. These kinds of errors influence the stability of the algorithm [35].

CHAPTER V

Simulation and Results

Matlab-based simulation is used to investigate the performances of the CMA, MMA & FS CMA adaptive blind algorithms. The simulation of these algorithms as they apply to broadcasting environment is presented for typical channels which can broadly represent the audio propagation channel; moreover a modulation technique suitable for audio broadcasting system is used for the simulation. Finally the simulation result for the evaluation metrics is summarized and compared with broadcasting standard.

5.1 Simulation Steps and Parameters

In order to perform the simulation, parameters required for the simulation must be clearly identified and defined. The parameters used for the simulation are summarized in Table 5.1.

Seq. No	Parameter	Value
1	Modulation	16-QAM
2	SNR	10 to 35 dB
3	Equalizer length	16
4	Step size	0.0001 to 0.001
5	Input data	Random bits and *.wav file
6	Raised cosine roll of factor	0.35
7	Audio file sampling rate	48 k Hz
8	Duty cycle	1
9	Randomizer polynomial	8 character hexadecimal

Table 5.1: Simulation Parameters Summery

5.2 Simulation Block Diagram

The block diagram of the blind adaptive equalization technique simulation is showing in Figure 5.2. The detail flow chart for the simulation of each block of the adaptive equalizer methods are presented in Appendix B.

Source: - the data source for the simulation, there are two data types used for the simulation namely a randomly generate bits and an audio file sampled at 48 kHz.

Quantization:-it is applied for the audio signal data source and used to convert each sample of the audio signal into 16 bit.

Randomization:-in the audio signal there are continues zero's and one's, the primary purpose of the randomizer included in the simulation is to break up these zeros and once, even though it can also be used for encryption.

Digital Modulation:- 16-QAM digital modulation technique is used to convert the information sequence to signal waveforms.

Pulse shaping filter:- a raised cosine filter with roll off factor of 0.35 is used, additional information can be found at Appendix A.

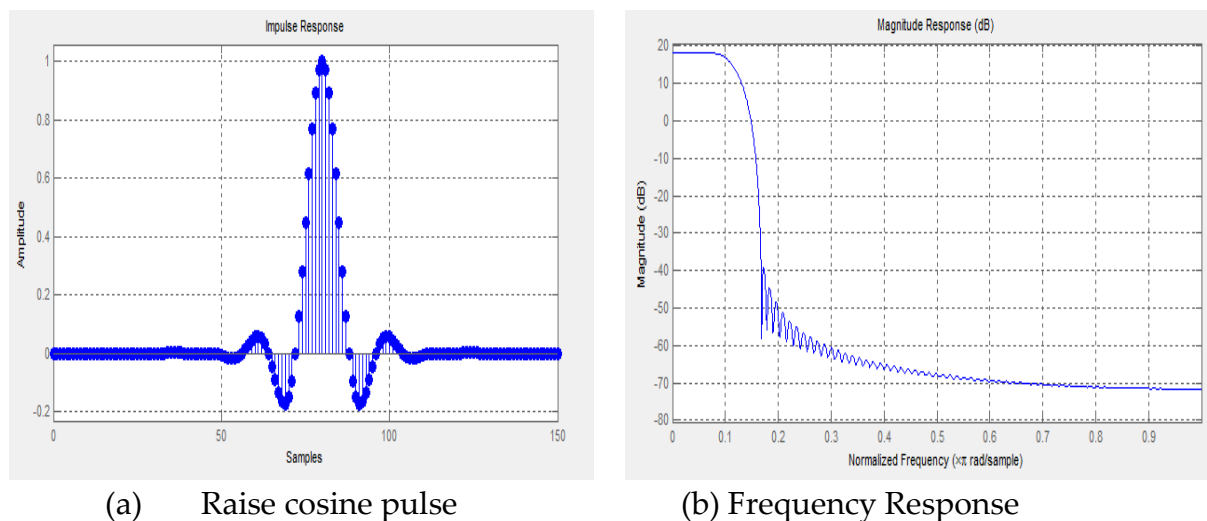


Figure 5.1: Raised cosine pulse and its frequency response for beta 0.35

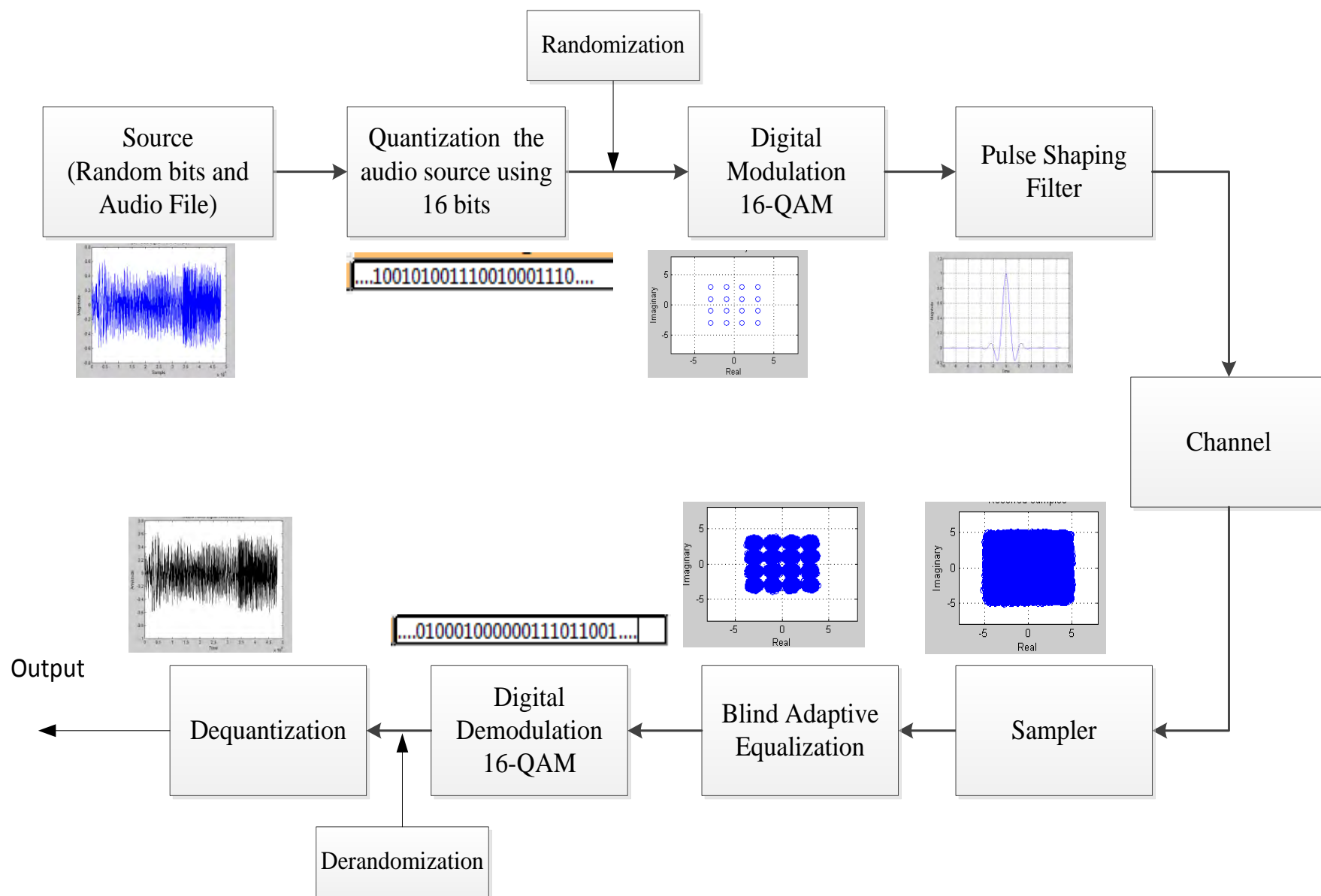


Figure 5.2: Simulation block diagram

Channel: - three channel models are used for the simulation; the multipath components of the channels for raised cosine pulse are plotted in Figure 5.3.

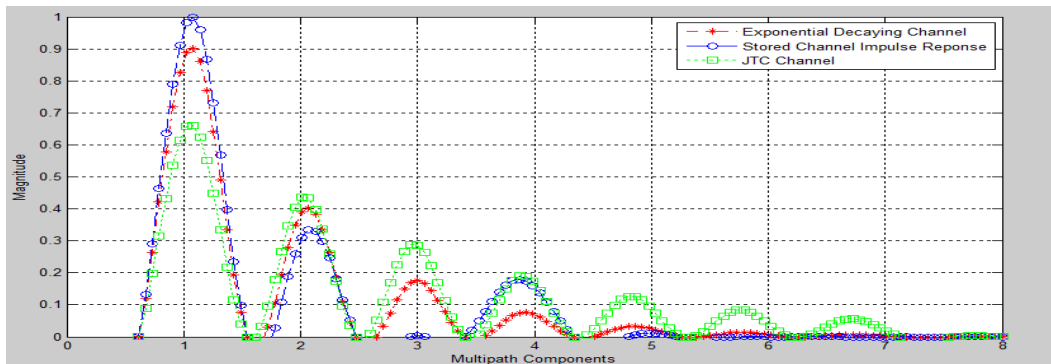


Figure 5.3: Channels impulse response for raised cosine[31,49,50]

Sampler: - take sample or samples from the received pulse operating at the symbol rate of n/T for n number of samples in period.

Blind Adaptive Equalization:- the blind adaptive equalization techniques used for the simulation (CMA, MMA & FS CMA).

Digital Demodulation: - extract the original information-bearing signal, binary bits from the received digital modulated signal.

Derandomization:- remove the randomness from the bits introduced by the randomizer at the transmitter using the same polynomial used at the transmitter.

Dequantization: reconstruction of the sampled audio signals from the bits received from the derandomizer.

The main flow chart for the simulation of the adaptive blind equalizers is shown in Figure 5.4. The detail processes and flow charts for each of the adaptive blind equalization methods are presented in their respective section.

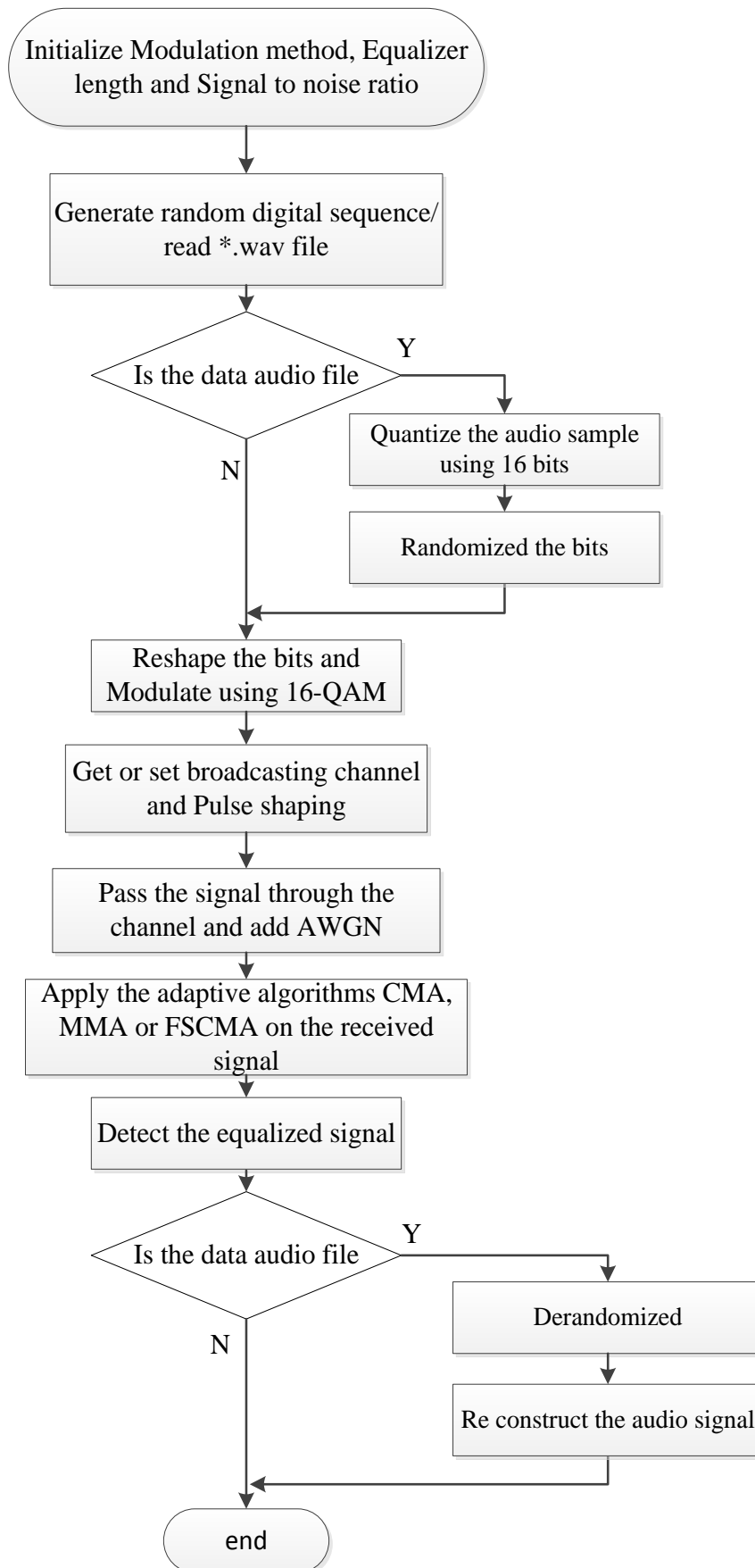


Figure 5.4: Flow chart for audio and random bit stream simulation.

5.3 Simulation Results

The simulation results are organized with top priority given to the adaptive blind equalization techniques with separate sections provided for channel models under it, and then the result for two data sources are presented for each of the three channel model.

5.3.1 Constant Module Algorithm Results

The CMA was discussed in section 4.6, for its simulation a flow chart is prepared and shown in Figure 5.5. The simulation result of it is presented in the next sections.

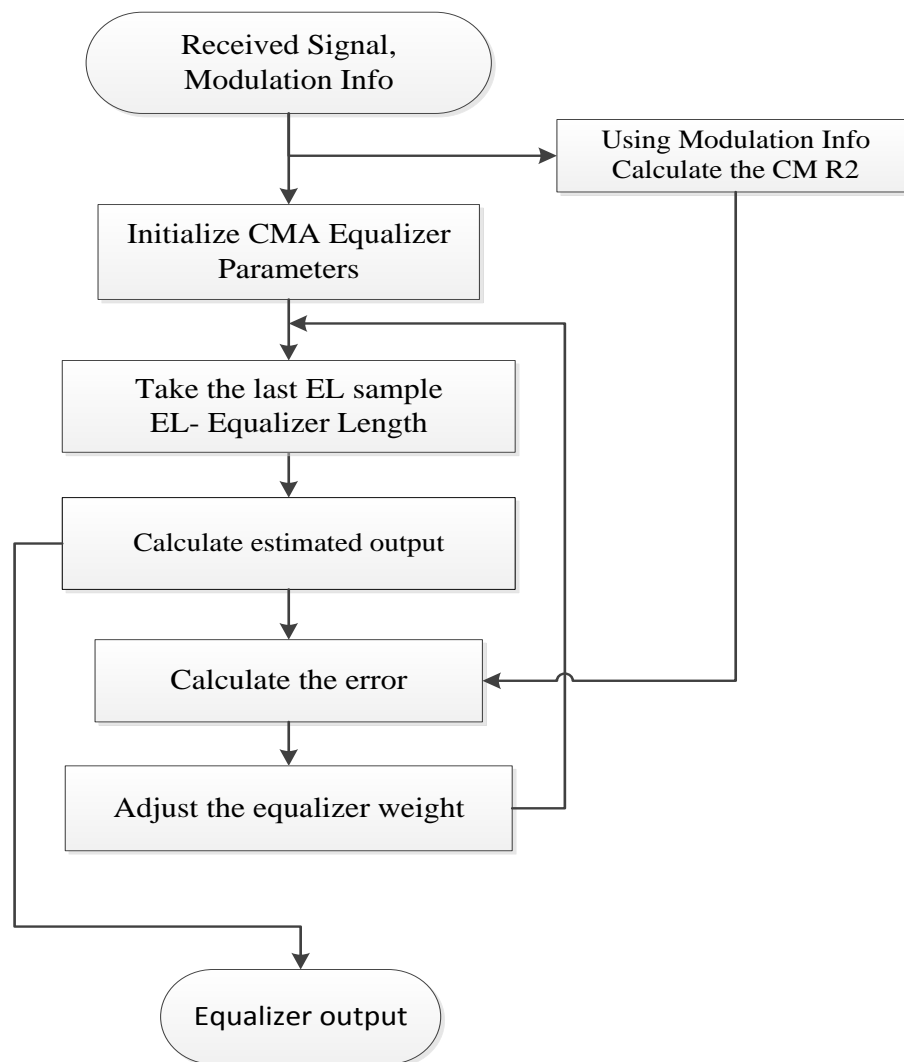


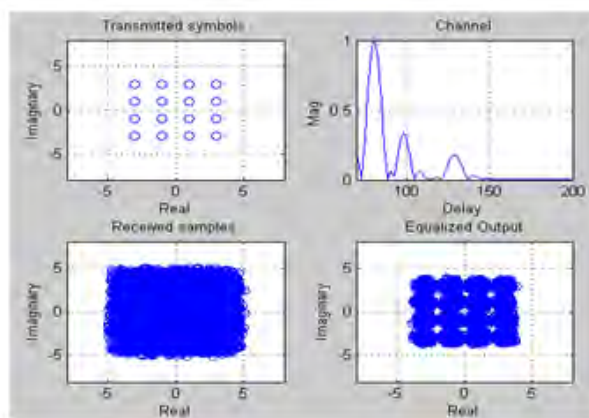
Figure 5.5: CMA Implementation flow chart.

5.3.1.1 Stored channel impulse response

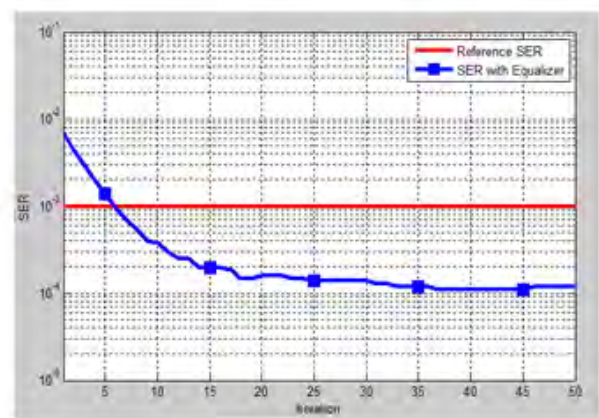
A. Random Data Source

The simulation is done using randomly generated binary data and stored channel impulse response show in Figure 5.3 with an iteration of up to 1,000, with each iteration contain 10,000 symbols of randomly generated bits. The resulted equalized signal constellation points with transmitted, channel, and received signal at 6th iteration illustrated in Figure 5.4 (a) for 10 dB SNR. The result indicates that CMA algorithm able to achieve SER of 10^{-4} at this iteration. The SER at the first iterations is very high and SER decline rapidly towards its steady state and the steady state achieved at 6th iteration.

The SER is calculated at each 1,000 symbol interval using step size of 0.0001 and 10^5 symbols. The SER result is shown in Figure 5.4 (b). The CMA converges for step-sizes of 0.0001 and stays stable after it converges.



(a) Constellation points



(b) SER

Figure 5.6: CMA Equalizer for stored channel and random generated data source.

B. Audio File Data Source

One iteration with 48k samples is used for the simulation and the result constellation points for an audio *.wav source without using randomizer is shown below in Figure 5.5 (a). When a randomizer is used the result indicates better separation as shown in Figure 5.5 (b). The better separation is also expressed in the actual SER the algorithm achieves, $\sim 5 \times 10^{-4}$ SER without using randomizer and $\sim 1 \times 10^{-4}$ using randomizer.

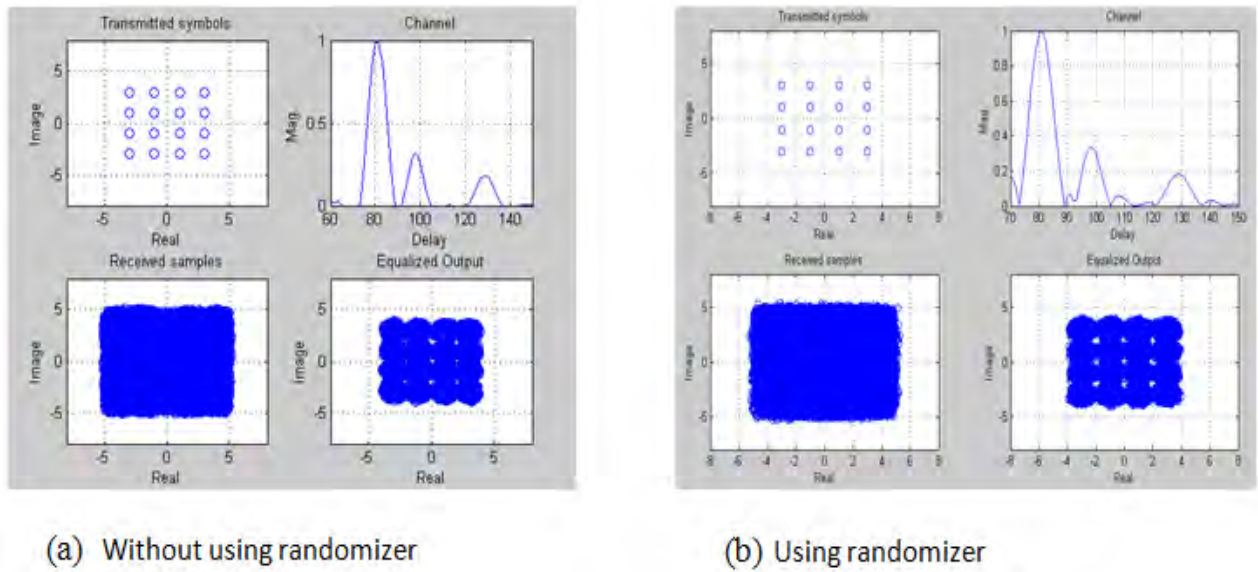


Figure 5.7: CMA Equalizer for stored channel response for an audio data source.

5.3.1.2 Joint Technical Committee Model

A. Random Data Source

For randomly generated data source the CMA equalization technique requires 13.5 dB SNR to recover a signal exposed to JTC channel shown in Figure 5.3 and achieve SER better than 10^{-3} . The CMA converge to SER of 4×10^{-4} and stays stable after that, the result is show in Figure 5.6 (b) , in addition the constellation of the source, channel, received and equalization illustrated in Figure 5.6 (a).

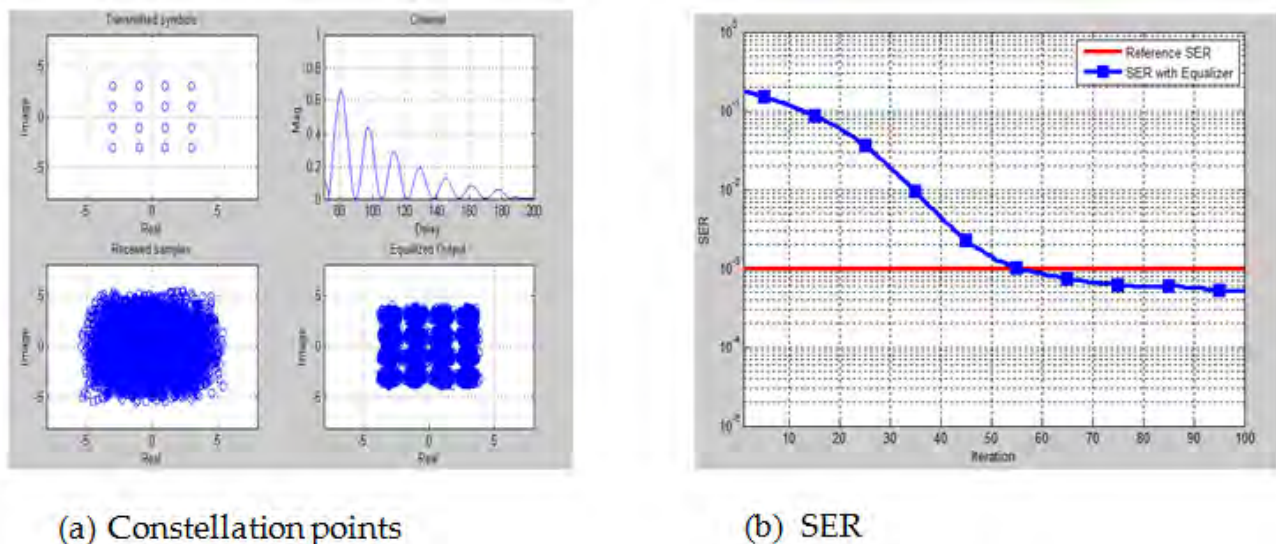
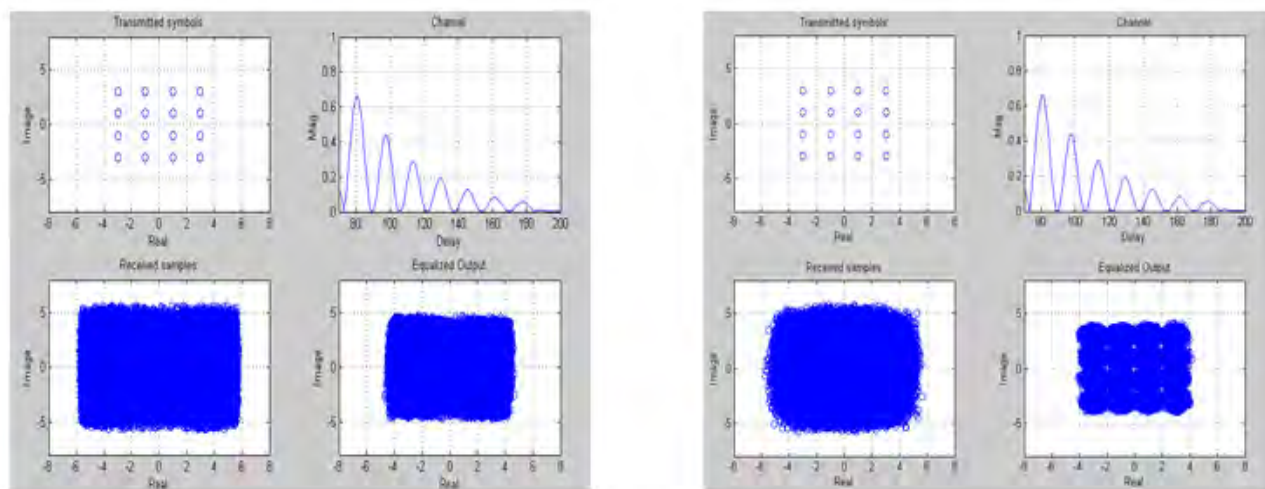


Figure 5.8: CMA Equalization for JTC channel for random data source.

B. Audio File Data Source

When the input is an audio file the CMA equalization method do not able to recover the transmitted signal without using a randomizer in the JTC channel condition shown in Figure 5.3 but when a randomizer is used the equalization method able to recover the transmitted signal at 13.5 dB with SER of 7×10^{-4} , the same SNR as the algorithm requires to recover randomly generated source. The constellation points are illustrated in Figure 5.7 (a) and (b), seeing the CMA equalizer needs a randomizer to compensate the effect of the JTC channel for an audio source.



(a) Without randomizer at 20 dB SNR

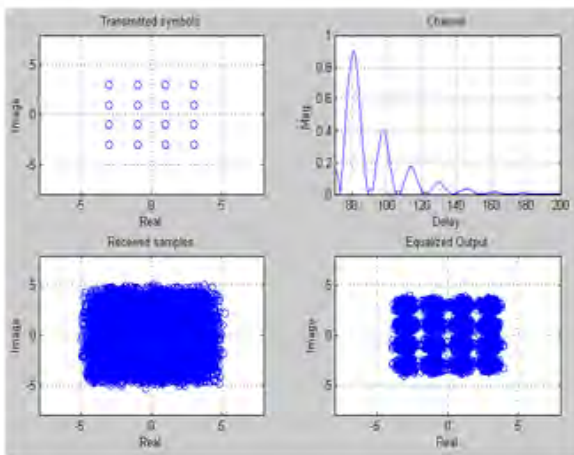
(b) Using randomizer at 13.5 dB SNR

Figure 5.9: CMA Equalizer for JTC channel with an audio data source.

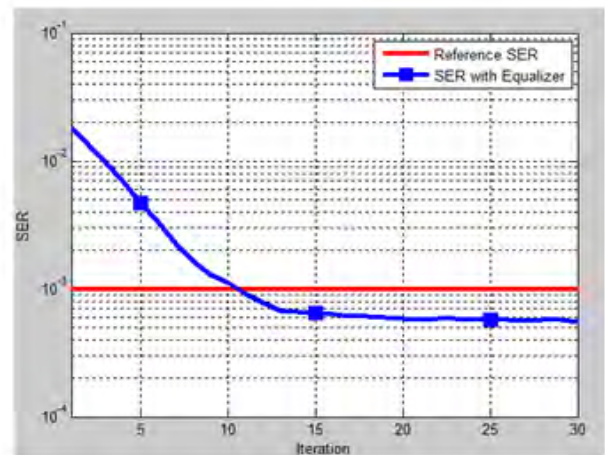
5.3.1.3 Exponential Decaying Channel

A. Random Data Source

In an exponentially decaying channel shown in Figure 5.3 the CMA equalization method is able to recover the transmitted signal with SER of 4×10^{-4} at 10 SNR for random data source. The algorithm converges at the 3rd iteration for step-size of 0.0001, the result is illustrated in Figure 5.8 (a). As the step-size is increased it converges with SER less than 10^{-3} until it reaches 0.0004 and diverges for large step size, more than 0.001.



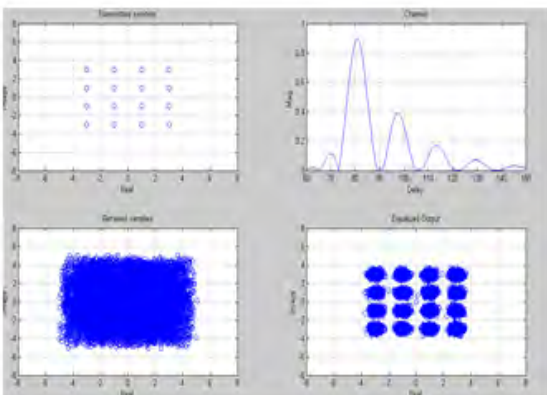
(a) Constellation points



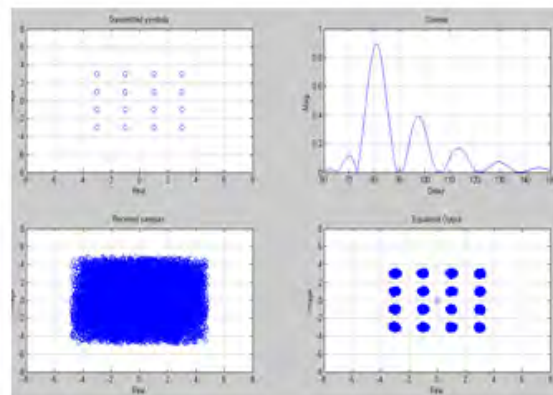
(b) SER

Figure 5.10: CMA Equalizer for exponential decaying channel.

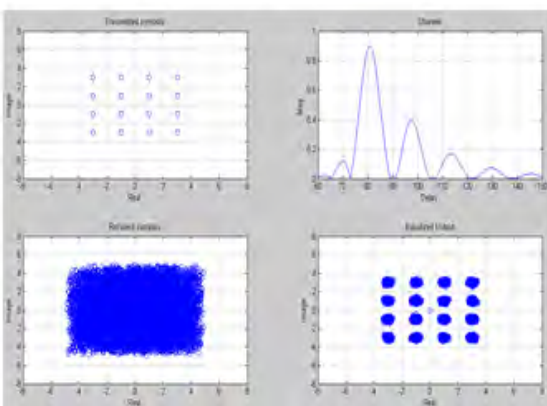
In addition to the multiple iterations, the result for different SNR are investigated and found that the concentration to the desire value increases as the SNR increases, Figure 5.9(a) to (d).



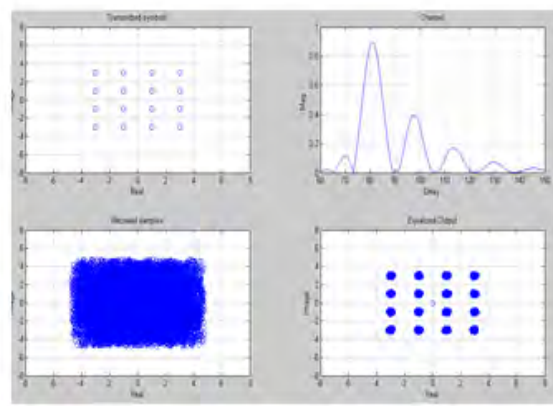
(a) At 12 dB SNR



(c) At 24 dB SNR



(b) At 18 dB SNR

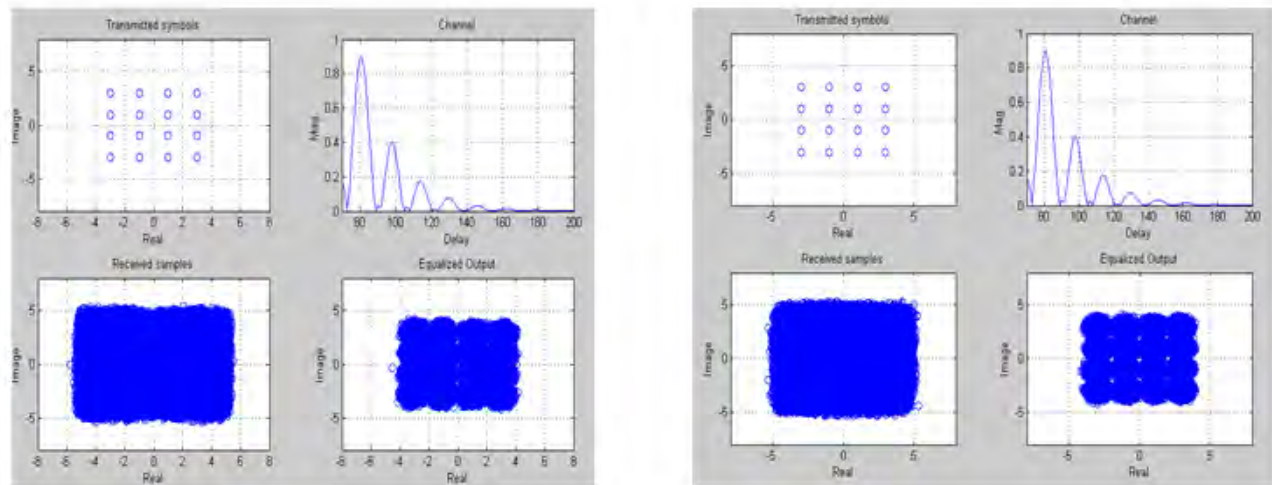


(d) At 32 dB SNR

Figure 5.11: CMA Equalized signal at 4th iteration for different SNR.

B. Audio File Data Source

The result when the input is an audio file is shown below in Figure 5.10 (a). Even though the separation in the constellation is not clear, the equalizer is able to recover the transmitted signal with $\text{SER} \sim 2 \times 10^{-3}$, a better constellation separation is achieved using a randomizer which is shown in Figure 5.10 (b) with SER of $\sim 6 \times 10^{-4}$.



(a) Without using randomizer

(b) Using randomizer

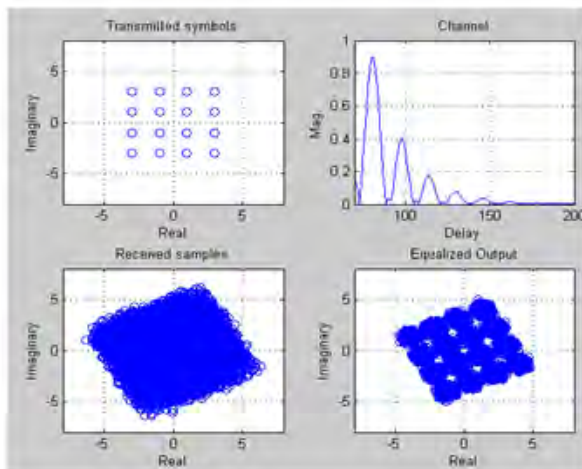
Figure 5.12: CMA Equalizer for exponentially decaying channel for audio data source.

5.3.1.4 Additional CMA Performance Matrix

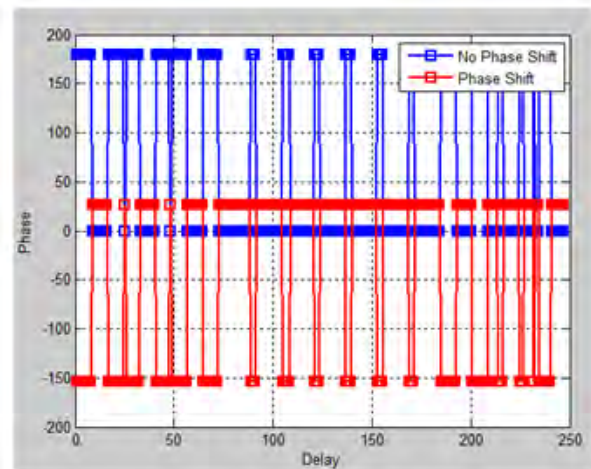
As indicated in Chapter III there are different matrixes used to measure the performance of equalizer. We have seen the result for some of the matrixes in previous section in the next section we will see the phase shift recovery, complexity and audibility.

A. Phase Shift Recovery

When the channel introduce a phase shift the CMA equalization do not have a capability to recover the phase shift, the simulation result and the phase shift introduced by the channel is illustrated in Figure 5.11 (a) and (b) respectively.



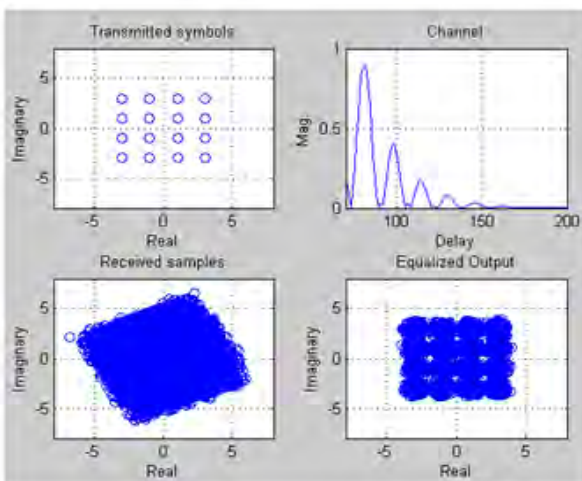
(a) Constellation points



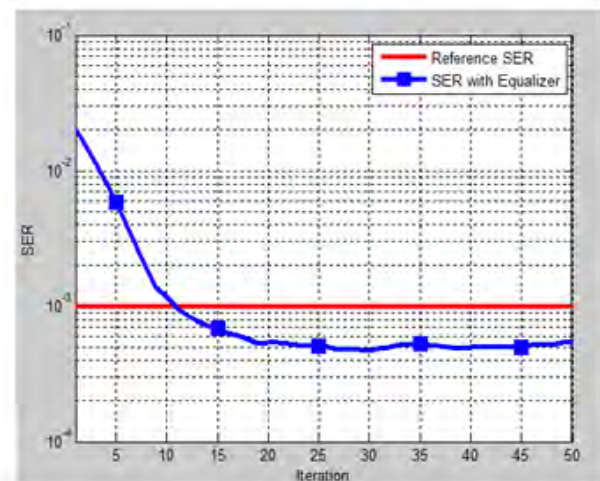
(b) Channel phase shift

Figure 5.13: CMA Equalizer for a complex channel at 10 dB SNR.

In order to recover the signal an additional phase recovery loop is required otherwise the signal will not be recovered at all. Using a phase recovery loop the signal can be recovered with SER 5×10^{-4} , Figure 5.12 (a) and (b).



(a) Constellation points



(b) SER

Figure 5.14: CMA Equalizer using phase recovery loop.

B. Complexity:

The CMA algorithm uses 1 sample per period; the total number of samples the algorithm process for 1second audio data sampled at 48k is 192000. On the other hand the CMA algorithms only consider the magnitude component of variables in the process to find the equalizer weights which minimize the processing time. In order to process the 1 second

audio data the CMA algorithm takes an average of 430 ms using the laptop used for the simulation.

C. Audibility:

An audible audio signal is recovered when the channel does not introduce phase shift at 10 dB but when the channel introduce phase shift the CMA requires a phase recovery loop to recover the audio signal and produce and audible signal.

5.3.2 Multi Module Algorithm Result

In Section 4.7 we have seen the MMA equalization technique; the flowchart for its simulation is shown in Figure 5.15. Similar to the CMA simulation the results of MMA equalization method for the three broadcasting channels and the different performance matrixes are presented in the next sections.

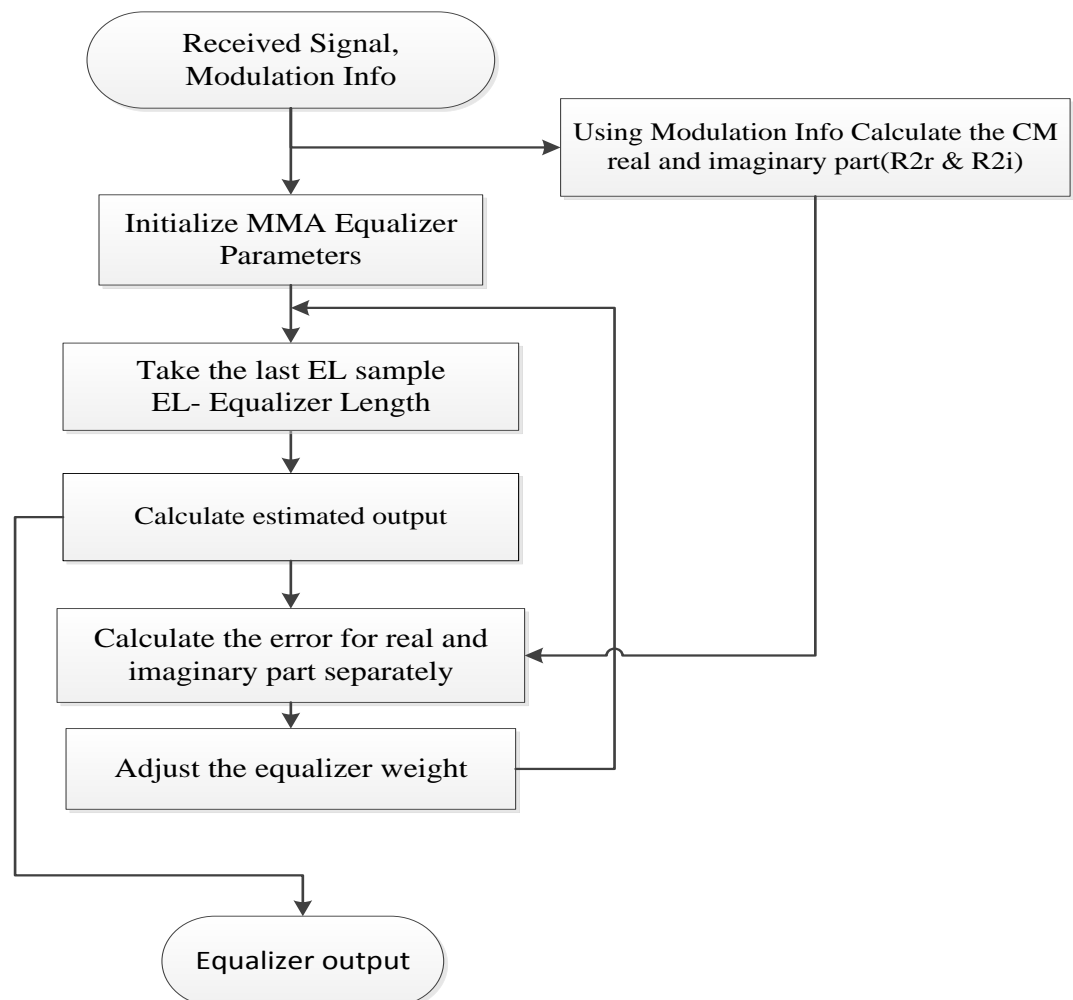


Figure 5.15: MMA Simulation flow chart.

5.3.2.1 Stored channel impulse response

A. Random Data Source

In stored channel impulse response channel condition indicated in Figure 5.3 and using randomly generated data source the simulation result for MMA algorithm shows that the algorithm able to recover the signal at SNR of 10 dB with SER of 8×10^{-5} , the output constellation points and SER are presented in Figures 5.13 (a) and (b).

The MMA algorithm achieves SER less than 1×10^{-3} at 4th iteration, after algorithm reaches its steady state it remains stable for all iterations beyond that.

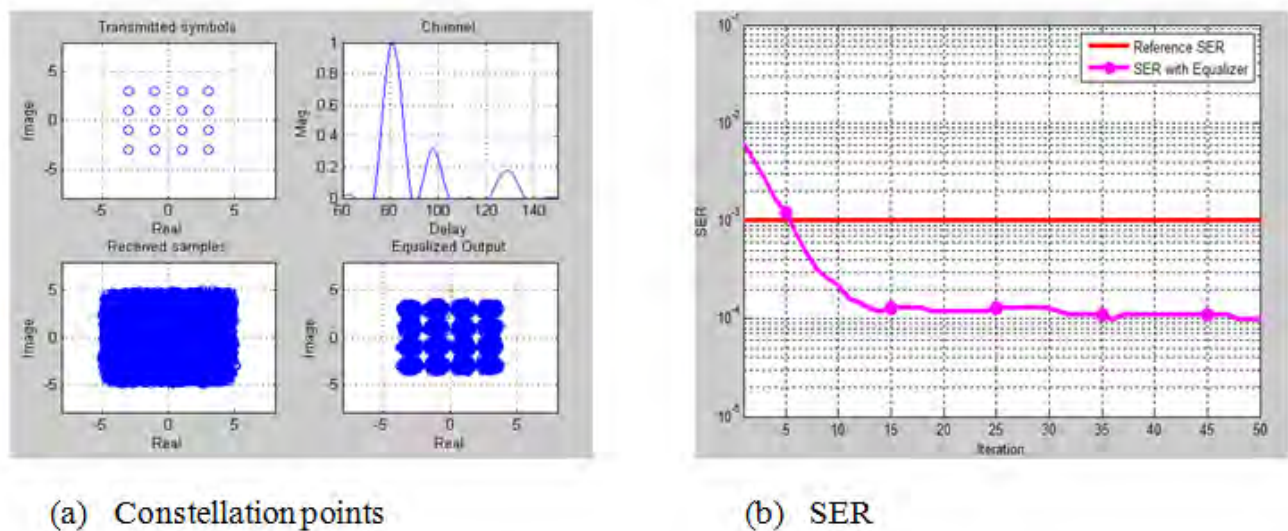


Figure 5.16: MMA Equalizer for stored channel response for random data source.

B. Audio File Data Source

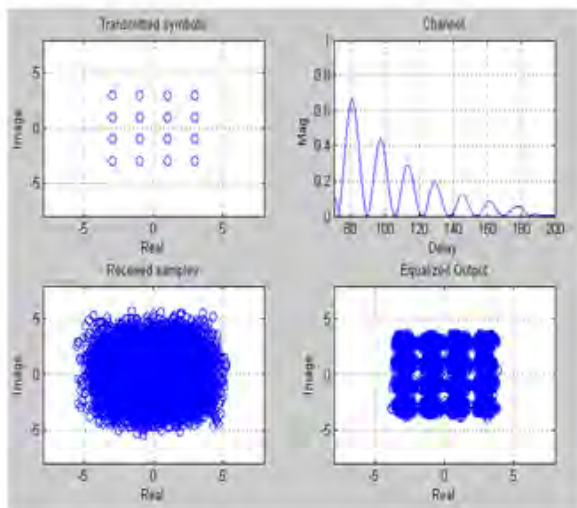
The MMA equalization is able to recover when for an audio data source without the need for randomizer with SER of 1×10^{-3} . When a randomizer is used the equalization technique achieves better performance result, SER of $\sim 4 \times 10^{-4}$.

5.3.2.2 Joint Technical Committee Model

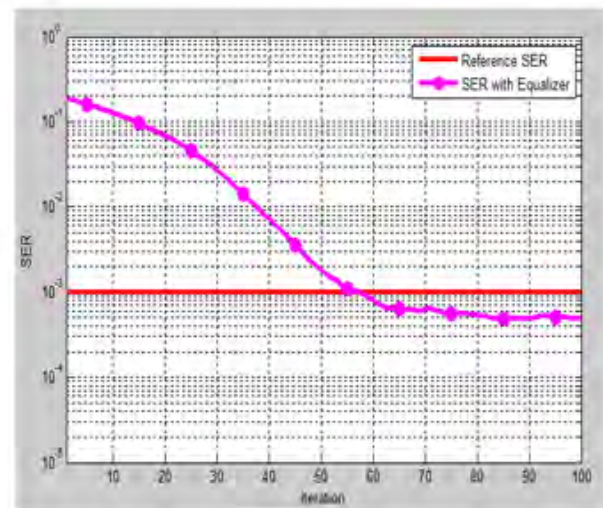
A. Random Data Source

Although the MMA algorithm has good performance at 10 dB SNR for the previous channel the algorithm requires 13.5 dB to achieve 4×10^{-4} SER for randomly generated data

source in JTC channel condition. The algorithm converged and stays stable after it converges, Figure 5.14 (a) and (b).



(a) Constellation points

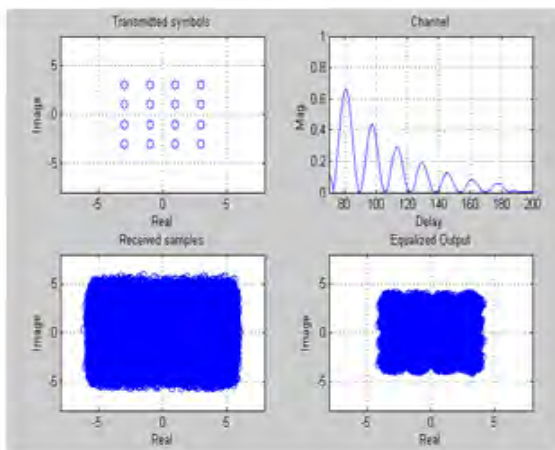


(b) SER

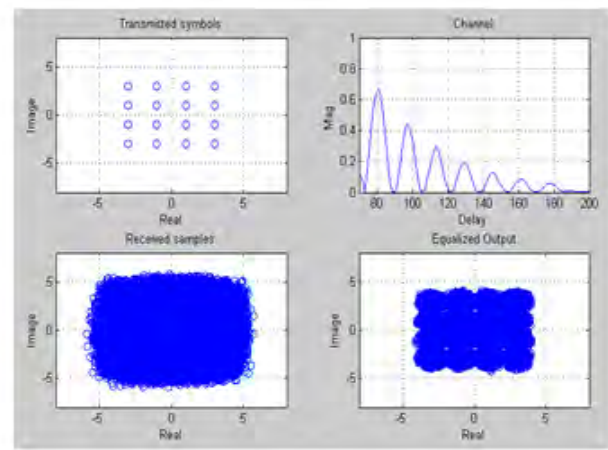
Figure 5.17: MMA Equalizer for JTC channel taken with random data source.

B. Audio File Data Source

The result for an audio source at 13.5 dB SNR is presented in Figure 5.15 (a), the algorithm recovers the audio signal at this SNR without the need for a randomizer, SER of $\sim 1.5 \times 10^{-3}$. A randomizer is also used for comparison purpose and the result indicates that better concentrations to the desired value and SER of $\sim 4.5 \times 10^{-4}$ found at same SNR, Figure 5.15 (b).



(a) Constellation without randomizers



(b) Constellation with randomizers

Figure 5.18: MMA Equalizer for JTC channel at 13.5 dB for an audio data source.

5.3.2.3 Exponential Decaying Channel

A. Random Data Source

When a signal from a randomly generated data source passed through an exponentially decaying channel shown in Figure 5.3, the MMA equalization technique recover the data and able to converge with SER of 3×10^{-4} using 10 dB SNR. The constellation points of the output and the SER is illustrated in Figure 5.16 (a) and (b) respectively. Once the algorithm converged the SER stays stable at of 3×10^{-4} .

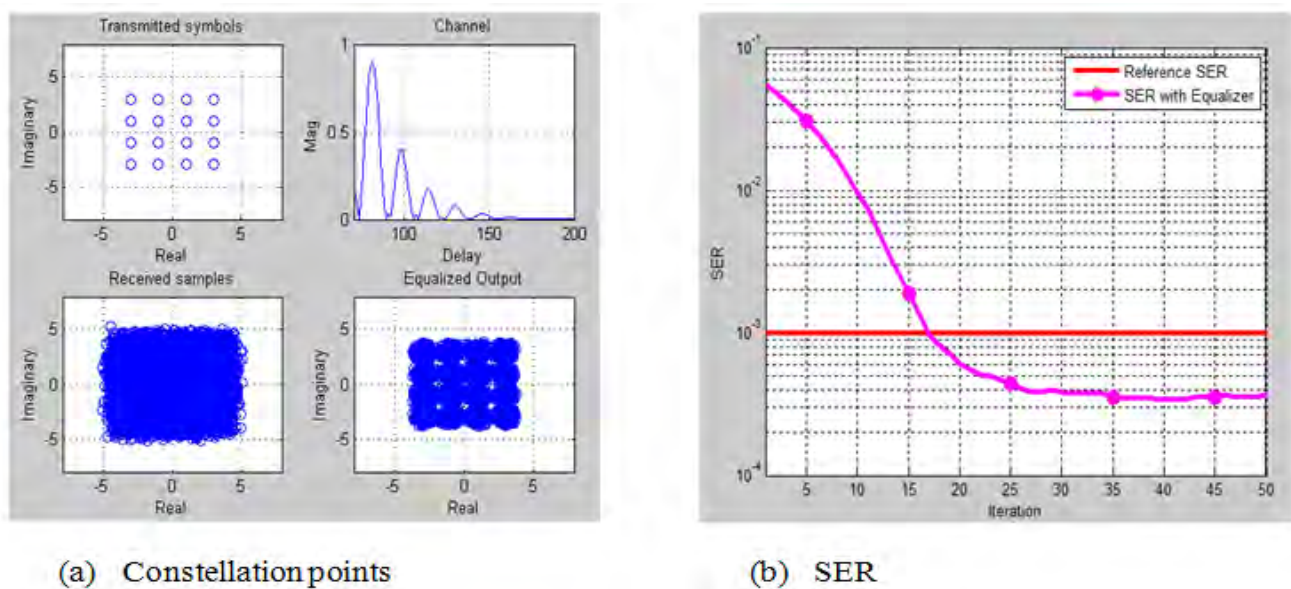


Figure 5.19: MMA Equalizer for exponentially decaying channel.

Using different SNR the performance of the MMA algorithm is also investigated and the result shows that the concentration to the desire value increases as the SNR increases, Figure 5.17 (a) to (d).

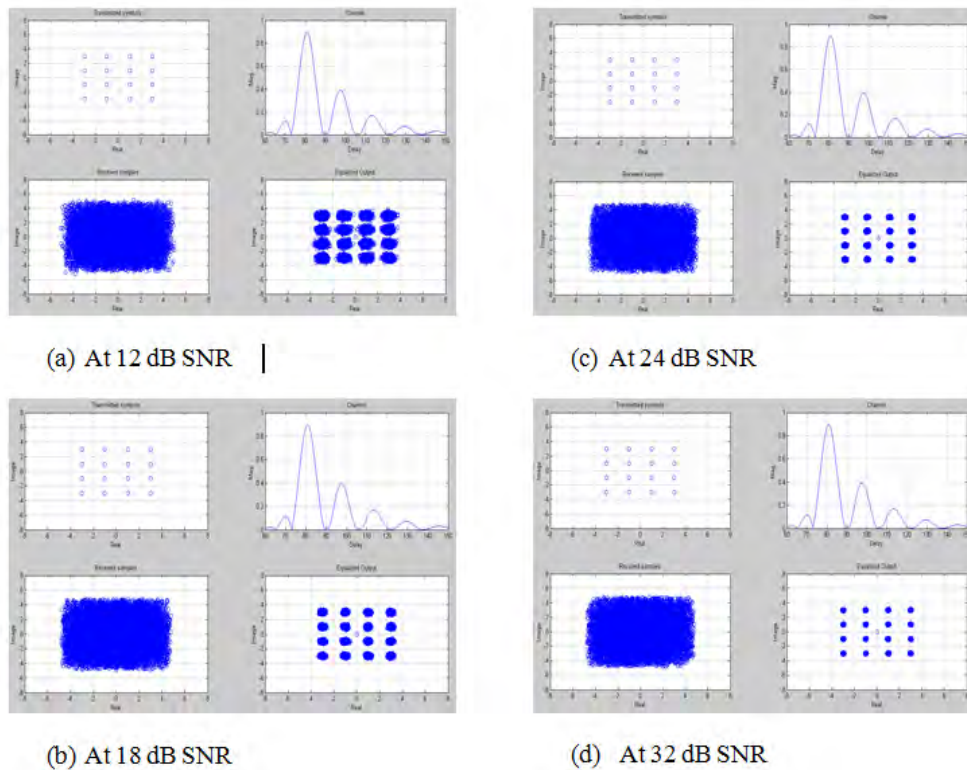


Figure 5.20: MMA Equalized for different SNR.

B. Audio File Data Source

When the data source is an audio file, the MMA equalization method is able to recover the audio signal at 10 dB SNR without the need for a randomizer in an exponentially decaying channel condition with SER of $\sim 1 \times 10^{-4}$, without a randomizer the equalization technique able to achieve SER of $\sim 4 \times 10^{-4}$. The constellation points with and without randomizer are shown in Figure 5.18 (a) and (b) respectively.

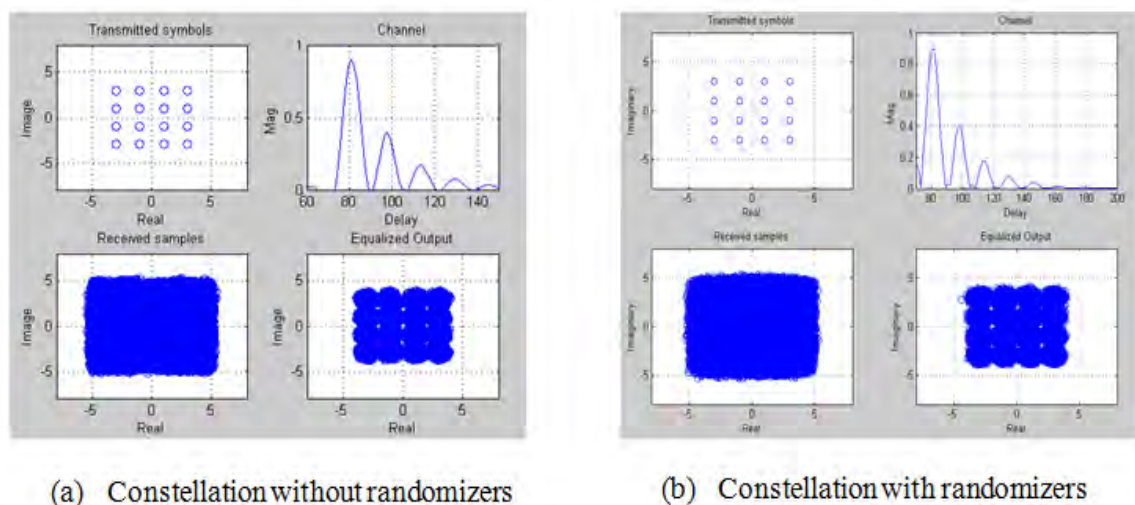


Figure 5.21: MMA Equalizer for exponentially decaying channel for audio source.

5.3.2.4 Additional MMA Performance Matrix

In the next section the result of the different matrixes for MMA Equalization method are summarized.

A. Phase Shift Recovery

The result from the simulation of MMA equalizer technique show that when the channel introduce phase shift, MMA equalizer method able to recover the transmitted signal. The output constellations points before and after equalization are shown in Figure 5.19(a) with converged SER of 3×10^{-4} , Figure 5.19 (b).

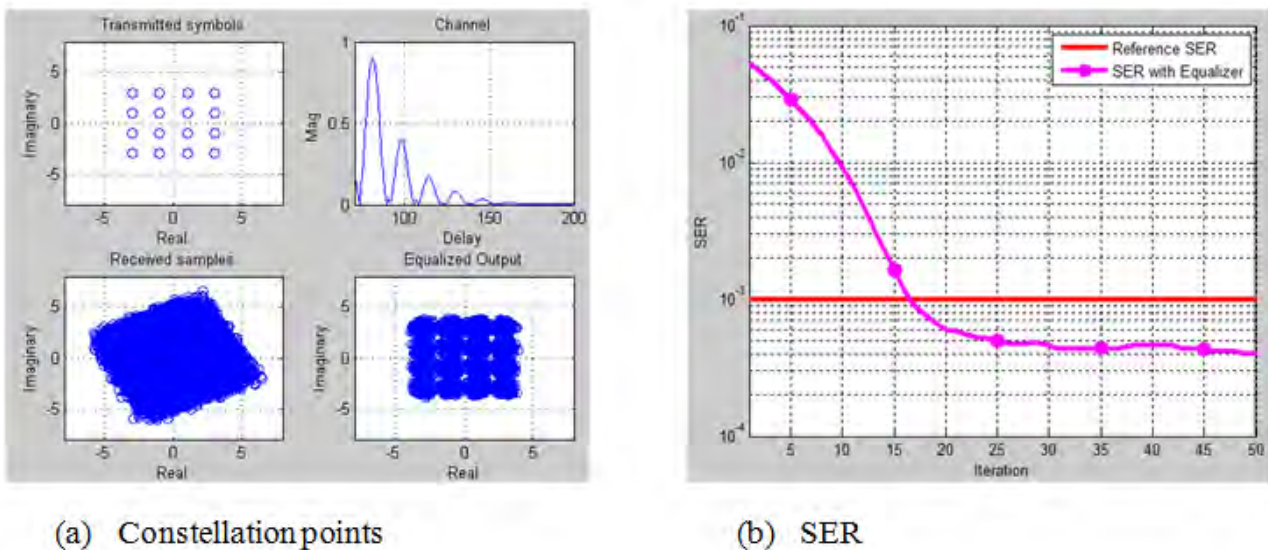


Figure 5.22: MMA phase recovery for exponentially decaying channel.

B. Complexity

In the same way as CMA the MMA algorithm uses 1 sample per period but in MMA algorithms an additional parameter is included to consider the phase component during the process of finding the equalizer weight which adds complexity. The effect of the additional parameter is reflected in the time the MMA algorithm takes to process 1 second audio data, it takes on average 532 ms.

C. Audibility

The MMA equalization method able to recover an audible audio signal in the three channel conditions including the channel which introduce phase shift.

5.3.3 Fractional Space Constant Module Algorithm Result

The FS CMA simulation is done using $T/2$ sampler (taking two samples per period) similar to previous two equalization methods the three channel models are used to investigate the performance of the equalizer. The simulation flow diagram is shown in Figure 5.23 and the detail simulation results for each of the channel are presented in the next sections.

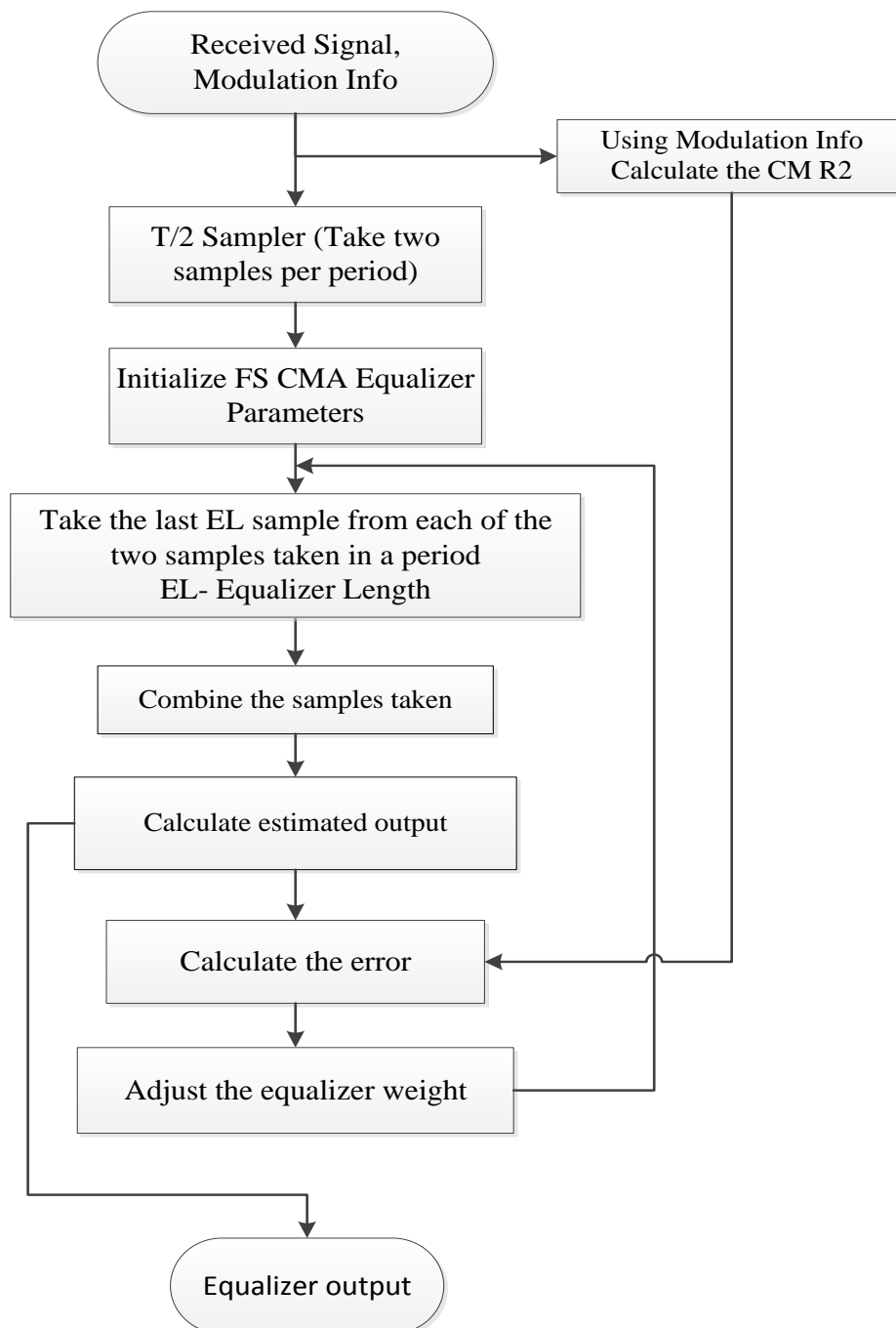
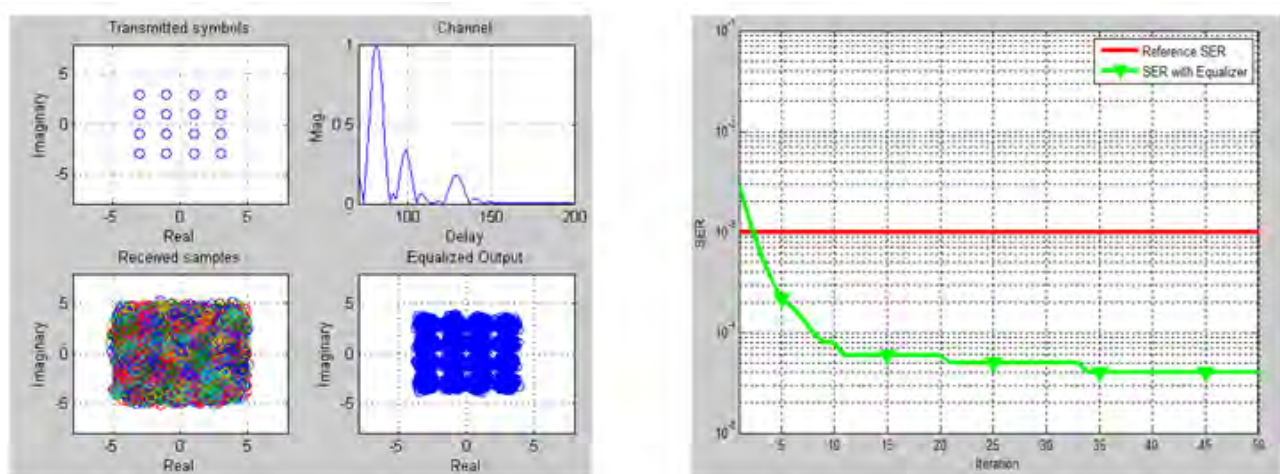


Figure 5.23: FS CMA Simulation flow chart.

5.3.3.1 Stored channel impulse response

A. Random Data Source

When the source is a randomly generated bits signal in a stored channel impulse response channel condition indicated in Figure 5.3, the FS CMA equalization method is able to recover the transmitted signal with clear distinction between the different constellation points at 9 dB SNR, Figure 5.20 (a). The equalization technique achieve SER of 4×10^{-5} at the 10th iteration and converges to SER of 2×10^{-5} , moreover it stays stable after it converged, Figure 5.20 (b).



(a) Constellation points

(b) SER

Figure 5.24: FS CMA Equalizer for randomly generated data source.

B. Audio File Data Source

When an audio file is used as source, the equalizer achieves SER of 5×10^{-5} SER at 10 dB SNR using a randomizer and it requires a 13 dB SNR to achieve the same SER without using equalizer.

5.3.3.2 Joint Technical Committee Model

A. Random Data Source

The result from the simulation of FS CMA method indicate that the equalizer is able to recover randomly generated source exposed to JTC channel with SNR of 12 dB with SER of 5×10^{-4} and converged at this iteration and stays stable afterwards, Figure 5.21 (a) & (b).

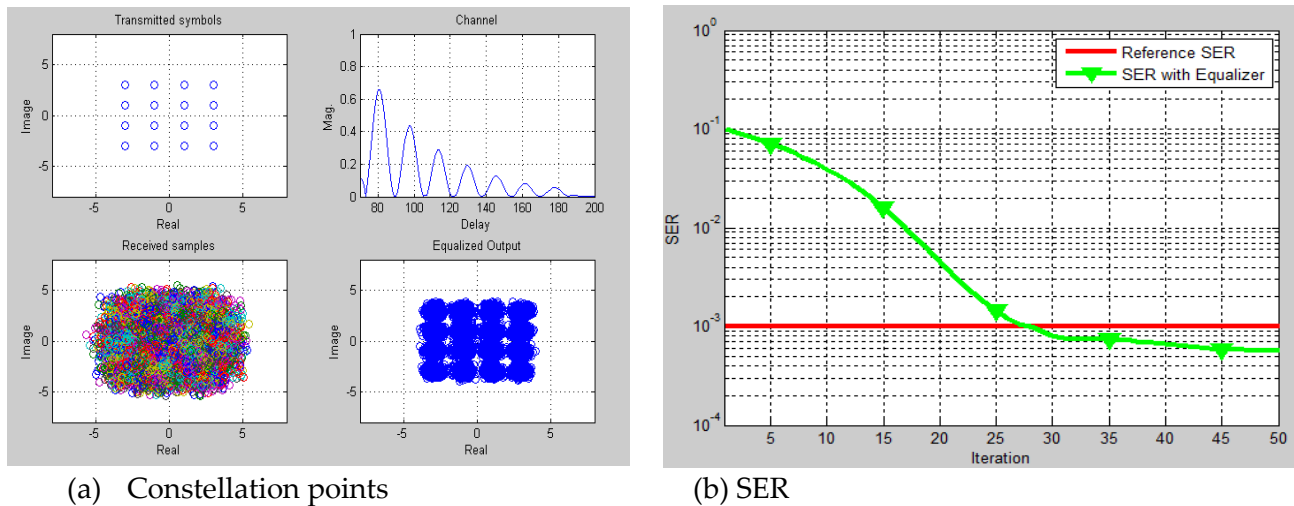


Figure 5.25: FS CMA Equalizer for randomly generate source in JTC channel.

B. Audio File Data Source

When the source is an audio file exposed to a JTC channel the FS CMA is not able to recover the signal even at high SNR, 20 dB but when a randomizer is used the equalizer able to recover the audio signal at 12 dB with SER of $\sim 7 \times 10^{-4}$. In Figure 5.22 the constellation for both without & with randomizer are presented.

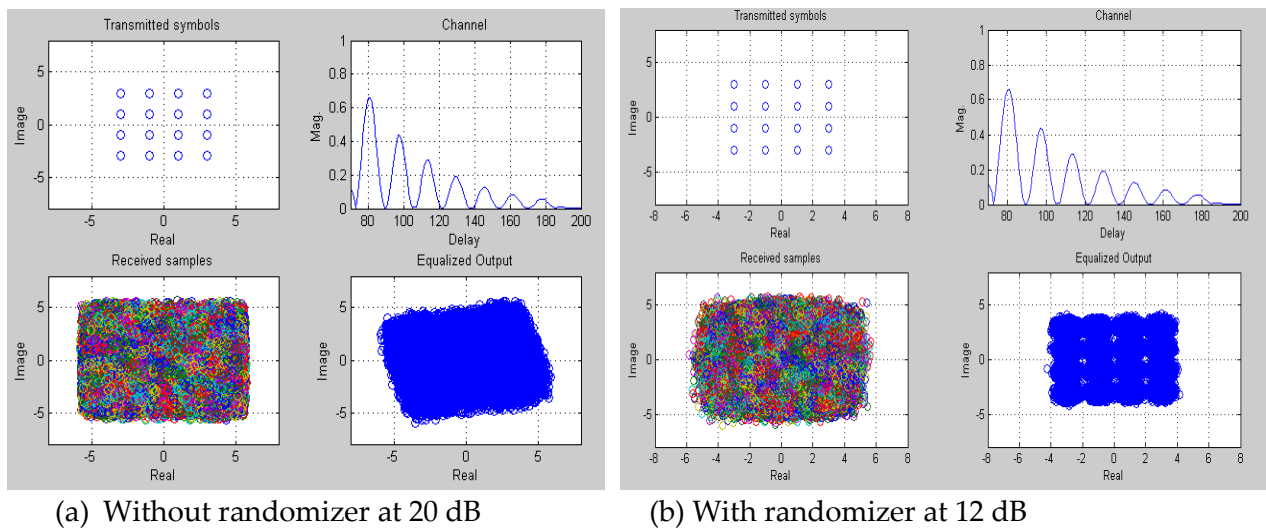


Figure 5.26: FS CMA Equalizer for JTC channel for audio Source.

5.3.3.3 Exponential Decaying Channel

A. Random Data Source

In an exponentially decaying channel and randomly generated source, the FS CMA algorithm able to recover the random generated bits with SER of 2×10^{-4} . The constellation

points of the received symbols are shown in Figure 5.23 (a) and Figure 5.23 (b) illustrates algorithm convergence to its steady state at 8th iteration and stays stable afterwards.

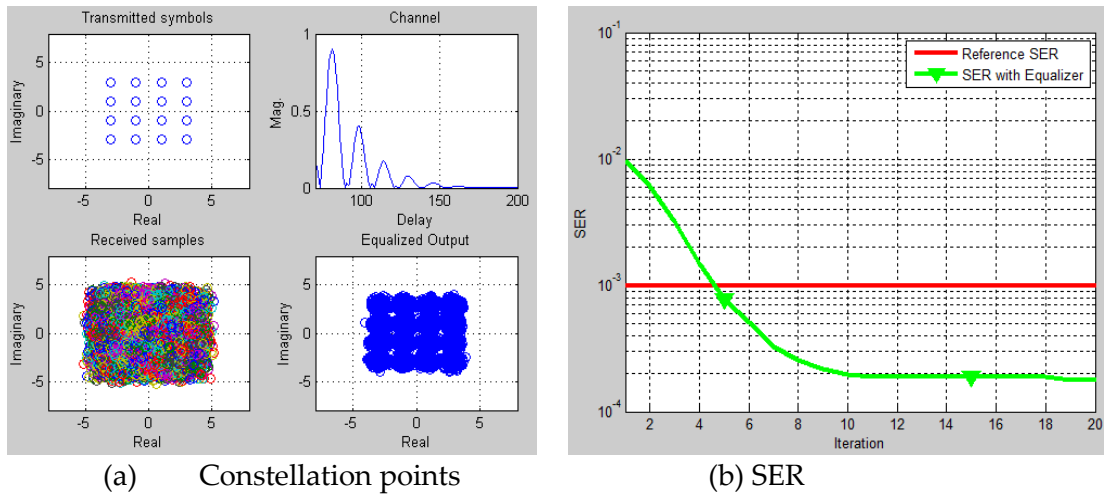


Figure 5.27: FS CMA in exponentially decaying channel for random data source.

When we see the FS CMA equalization technique for different SNR, as shown in Figure 5.24 (a) to (d), as the SNR increased the constellation points concentrate towards the ideal points.

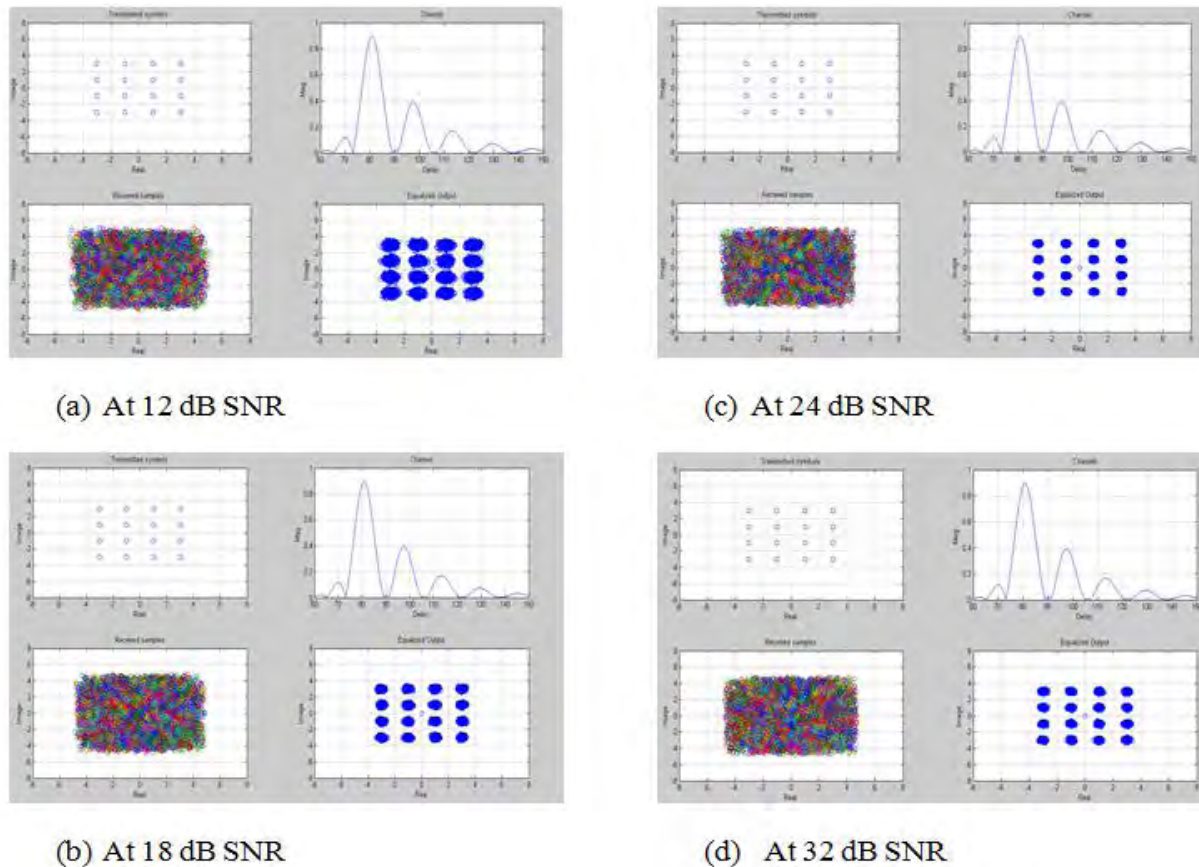


Figure 5.28: FS CMA Equalizer at different SNR.

B. Audio File Data Source

The result for audio data source shows that the equalization method is able to recover the audio signal in the exponentially decaying channel show in Figure 5.3 with SER of 1×10^{-4} at 10 dB using a randomizer and fail to achieve SER of 10^{-3} at 20 dB.

5.3.3.4 Additional FS CMA Performance Matrix

The result of the different performance measurement matrixes for FS CMA Equalization method is presented in the next section.

A. Phase Shift Recovery

When the randomly generated bits or an audio file pass through the channel which introduce phase shift, even though the FS CMA algorithm able to concentrate the symbols it is not able to recover the phase shift as shown in Figure 5.25.

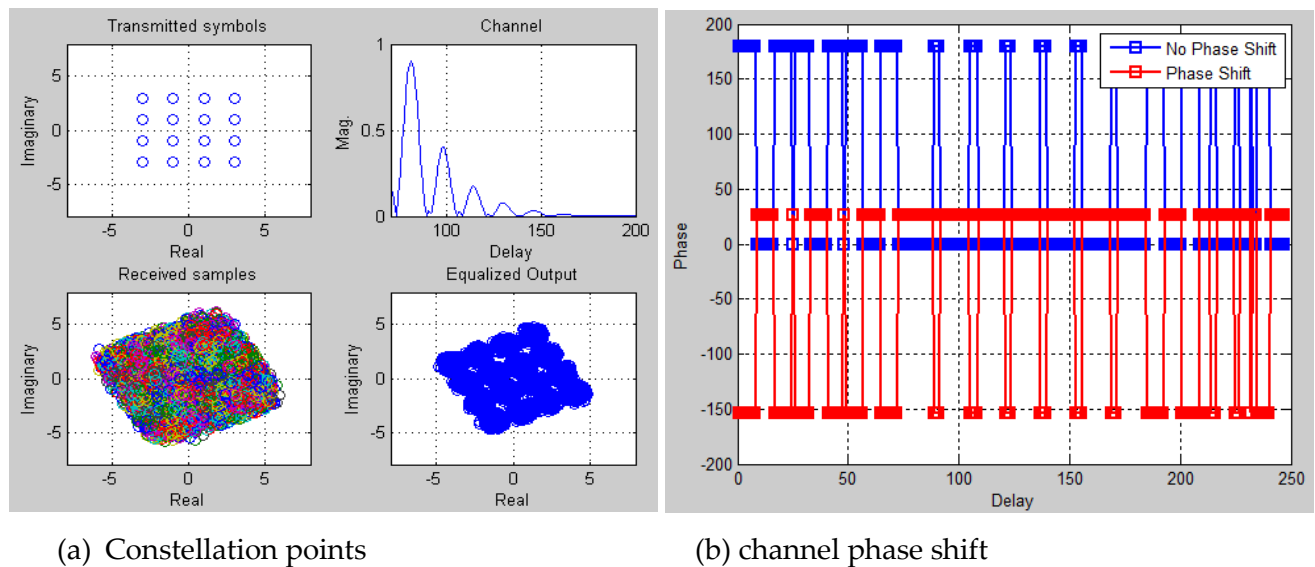


Figure 5.29: FS CMA Equalizer for a complex channel at 10 DB SNR.

Using a phase recovery loop the FS CMA can achieve SER 2×10^{-4} , Figure 5.26 (a) and (b).

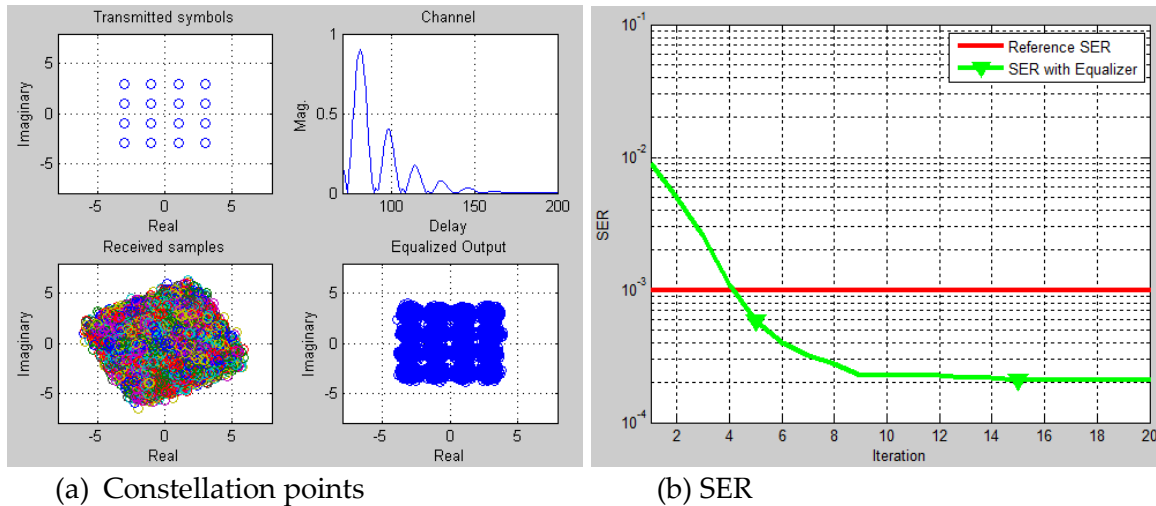


Figure 5.30: FS CMA with phase recovery for exponentially decaying channel.

B. Complexity:

The FS CMA uses 2 or more samples per period, as indicated previously in this thesis 2 samples per period is used. Thus, the total numbers of samples processed by FS CMA is double that of CMA and MMA. In the same was as CMA the algorithm considers the magnitude component to find the equalizer weights. In order to process a 1 second audio data the algorithm takes on average 636ms using the laptop used for the simulation.

C. Audibility:

A clear audible sound is constructed from the equalized signal for the three channels except when the channel introduce phase shift.

5.4 Summery

In order to compare the performance of the three blind adaptive equalizer techniques the result for different matrices are summarized in the following sub section.

A. Symbol Error Rate

The SER simulation result for the three algorithms is shown in Figure 5.27 (a), the result indicate that the FS CMA has much better SER performance than the other two equalization methods consistently from the first iteration to the last, moreover when we see the SER for different SNR the FS CMA out performance CMA & MMA, Figure 5.27(b).

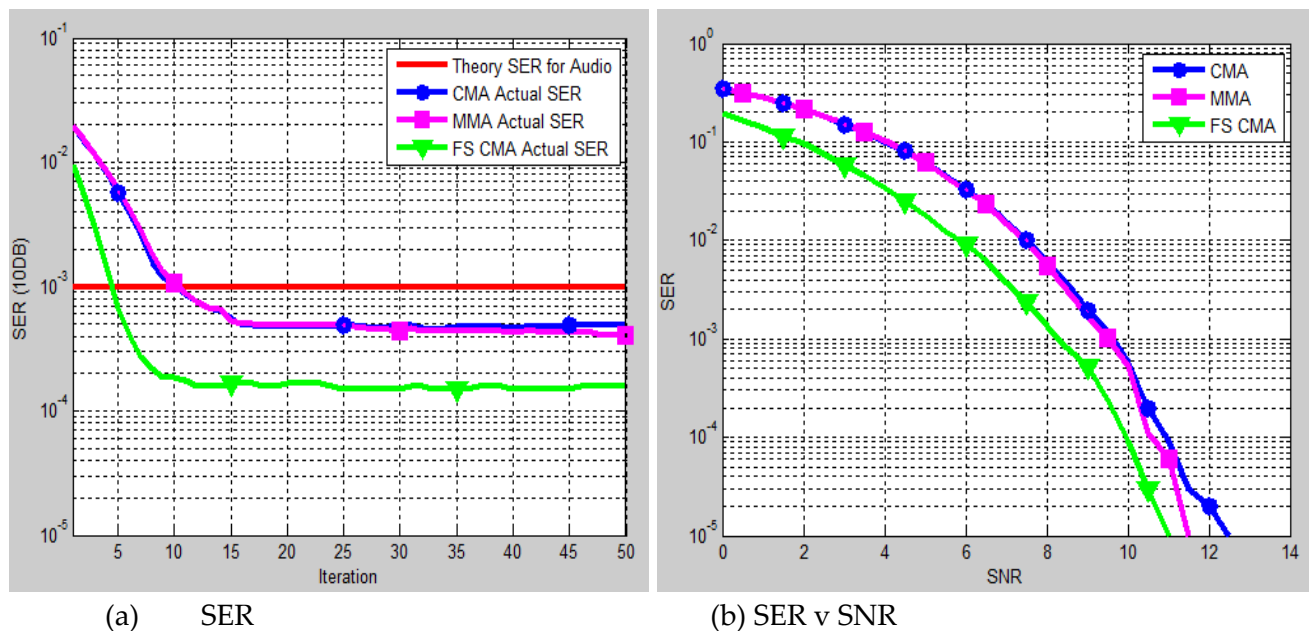


Figure 5.31: SER v Iteration for CMA, MMA & FS CMA at 10 dB, exponential decaying channel.

B. Audibility

In order to check the audibility of the output signal, the audio output from the equalizers are compare with DAB threshold of audibility (ToA). The ToA for DAB is defined as 10^{-4} BER [2,60], this ToA is taken as reference and compared with the result found from the simulation and summarized in Figure 5.28 and Table 5.2 using the worst channel condition used for the simulation, JTC channel. The FS CMA able to achieve the required BERs at 12 dB SNR while CMA & MMA requires ~14 to achieve the BER, thus FS CMA has better performance than the CMA & MMA.

Equalization Method	DAB ToA BER	SNR (dB) Required
CMA	10^{-4}	14
MMA	10^{-4}	14
FS CMA	10^{-4}	12

Table 5.2: Equalizers BER compared to DAB ToA.

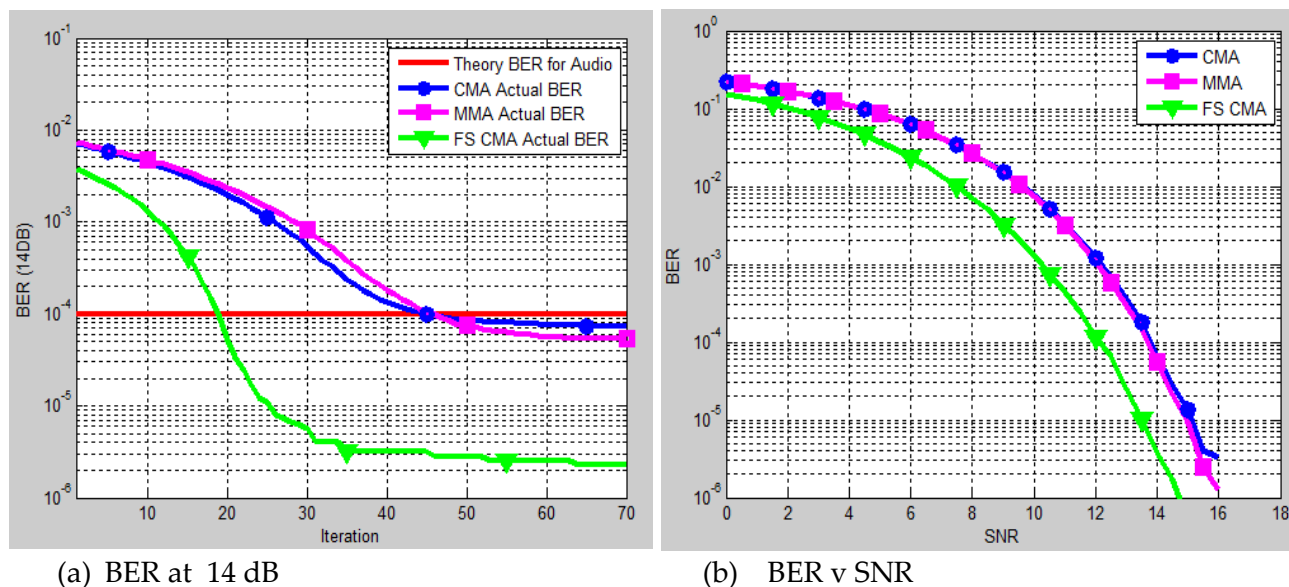
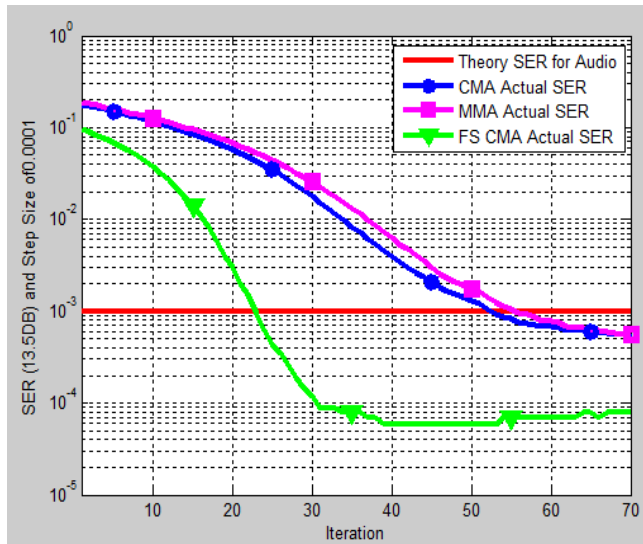


Figure 5.32: BER v Iteration/SNR for CMA, MMA & FS CMA for JTC channel.

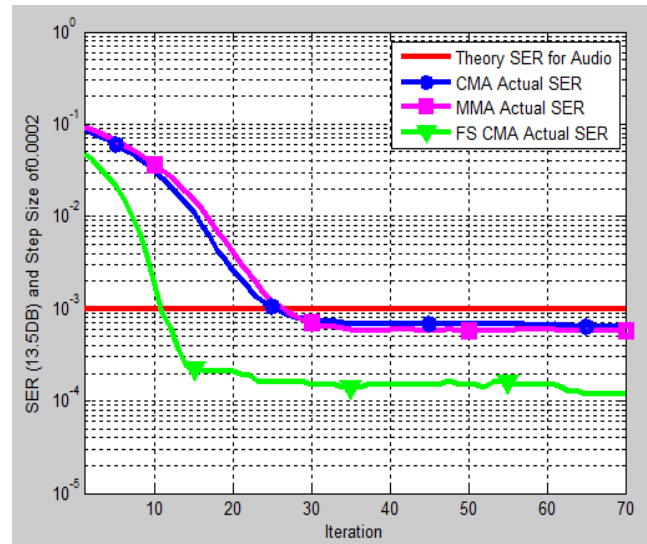
C. Convergences

The rate of convergence depends on the step size. In JTC channel condition and SNR of 13.5 dB by increasing the step size from very small value the convergence is evaluated. All the three algorithms converge for the three channels used in the simulation at step size of 0.0001 or less, although there is a difference in the rate in which the algorithms converged. A very small step size assures convergence but it is at the cost of the rate in which the algorithms converge.

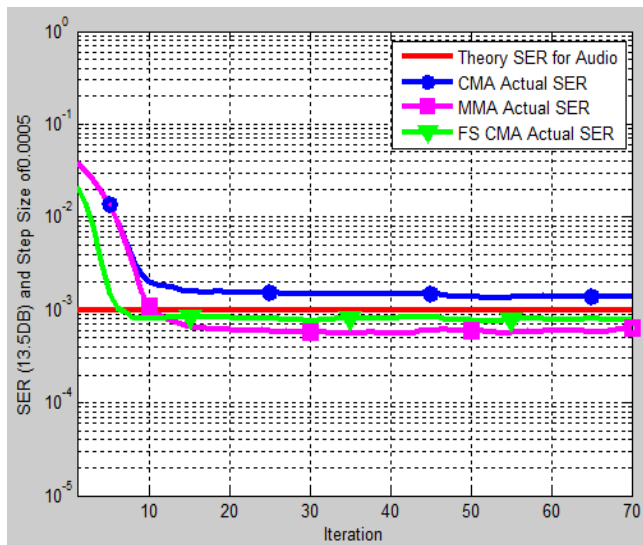
The FS CMA has much less SER starting from the first iteration even though it converges to steady state slower than the CMA and MMA, CMA and MMA have almost the same rate of convergence Figure 5.27 (a) and Figure 5.28 (a). Once the algorithms converged they stay stable for the rest of the iteration. When the step size increase from 0.0001 the equalizers methods converge faster, Figure 5.29 (a) & (b), as the step size increase further it start to diverge and it diverges at 0.001. FS CMA diverges faster than CMA & MMA, as shown in Figure 5.25 (c) & (d).



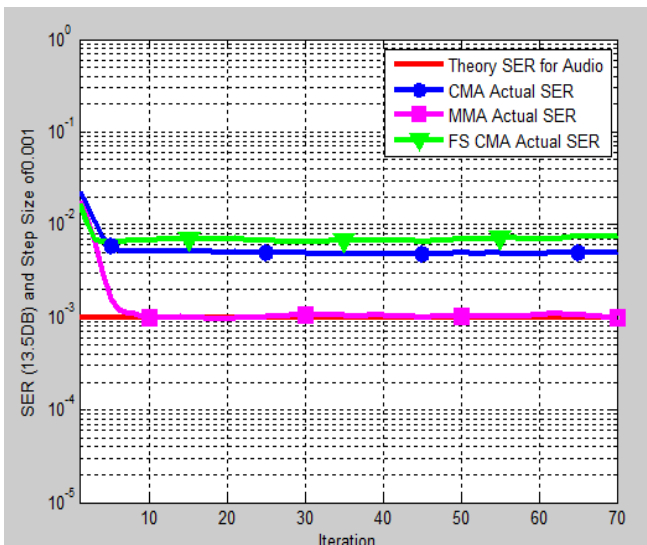
(a) Step size 0.0001



(b) Step size 0.0002



(a) Step size 0.0005



(b) Step size 0.001

Figure 5.33: SER at different step size for JTC channel at 13.5 dB

D. Complexity

When checking the complexity of the algorithm taking the processing time as measurement for complexity FS CMA takes more time than the other two methods. The FS CMA takes more time than the other two due to the double size of the data required by the algorithm to equalizer the signal. The extraction of the phase information in MMA makes the algorithm to have two terms in the process of finding the equalizers weight. This process makes MMA to take more time for processing than CMA., the result is summarized in Table 5.3.

E. Phase Shift Recovery

On channel condition which introduce phase shift the MMA algorithm able to recover the signal without the need for phase recovery loop but the CMA & FS CMA requires an additional block for phase recovery. Using phase recoveries for CMA & FS CMA the result indicate that FS CMA has better performance than the CMA & MMA even though it needs an additional block for the phase.

Finally the different matric results are summarized in Table 5.3.

Equal. Method	Complexity (Processing Time)	Convergence to required SER	Phase Shift Recovery	SER	Stability
CMA	430ms	~2 nd iteration	Require phase recovery loop	~4X10 ⁻⁴	Stable once converge
MMA	532ms	~2 nd iteration	Yes	~3X10 ⁻⁴	Stable once converge
FS CMA	636ms	~1 st iteration	Require phase recovery loop	<10 ⁻⁴	Stable once converge

Table 5.3: Equalizations Methods Performance Summery

CHAPTER VI

Conclusion and Future Works

6.1 Conclusion

In this thesis three blind adaptive equalization techniques are simulated and their performance is analyzed. Successful simulation results are obtained for different type of both real and complex channels. The three equalization methods are able to recover the transmitted signal in different channels used in the thesis the exception happens when the channel is complex and the MMA is the only equalization technique which able to recover the transmitted signal without the need for phase recovery loop.

In all of the performance measuring parameters except the phase recovery CMA & MMA the performance techniques is nearly identical for the same initial conditions and step size. CMA and MMA coverage's faster than FS CMA although FS CMA performance in terms of SER is much better than the two techniques starting from the first iteration. As simulation result indicates FS CMA SER performance is much better than the performance of CMA & MMA from the first iteration until it converges both at lower SNR and higher SNR.

When we compare the performance of FS CMA with CMA & MMA, FS CMA has better overall performance than the two except the phase shift recovery which can be address by phase recovery loop and with the addition of phase recovery FS CMA out performance CMA & MMA, moreover the FS CMA has capability to recover transmitted signal at 1 to 1.5 dB lower than the other two methods therefore considering the recommendation is for a security firm where data recovery is much critical than cost and the availability of alternate option to address the phase recovery gap of FS CMA. From the three equalization techniques the thesis recommends FS CMA for implementation.

6.2 Future Works

The flow chart and the simulation used in the thesis is organized in such a way that it can be extended for video broadcasting with change in modulation index of the QAM modulation, associated SNR required for video broadcasting and some of the parameters used in the simulation. Anyone interested in implementing blind adaptive equalization technique can extend their work from this thesis.

In the course of analyzing the performance of the equalization techniques it is clearly indicated that FS CMA & MMA has their strong sides, specifically high SER performance and phase recovery respectively. This two positive characteristics of FS CMA and MMA conceptually can be achieved using equalizations techniques called FS MMA, thus blind equalization technique for audio broadcasting system can also be extended include these equalization technique.

REFERENCES

- [1] U. Reimers, *DVB: The Family of International Standards for Digital Video Broadcasting*, 2nd ed., Berlin: Springer, 2005.
- [2] W. Hoeg and T. Lauterbach, *Digital Audio Broadcasting: Principles and Applications of Digital Radio*, 2nd ed., England: John Wiley & Sons Ltd, 2003.
- [3] Y. Sato, "A method of self-recovering equalization for multi-level amplitude modulation", *IEEE Trans. on Commn.*, COM-23:679–682, June 1975.
- [4] A. Benveniste, M. Goursat, and G. Ruget, "Robust identification of a non-minimum phase system", *IEEE Trans. Autom. Control*, AC-25:385–399, June 1980.
- [5] D.N. Godard, "Self-recovering equalization and carrier tracking in two-dimensional data communication systems", *IEEE Trans. on Communications*, COM- 28: 1867–1875, 1980.
- [6] J. R. Treichler and B. G. Agee, "A new approach to multipath correction of constant modulus signals", *IEEE Trans. on Acoust., Speech, Signal Processing* ASSP-31:349–372, 1983.
- [7] J. Yuan and T. Lin, "Equalization and Carrier Phase Recovery of CMA and MMA in Blind Adaptive Receivers," *IEEE Transactions on Signal Processing*, Vol. 58, No. 6, June 2010.
- [8] R. Babu and R. Kumar, "Blind Equalization using Constant Modulus Algorithm and Multi-Modulus Algorithm in Wireless Communication Systems," *International Journal of Computer Applications: 0975 – 8887*, Vol. 1, No. 3, 2010.
- [9] J. Yang, J.-J. Werner, and G. A. Dumont, "The multi modulus blind equalization and its generalized algorithms", *IEEE Journal on selected areas in communication*, COM- 20: 997–1015, 2002.

- [10] J. Yuan and K. Tsai, "Analysis of the Multimodulus Blind Equalization Algorithm in QAM Communication Systems", *IEEE Trans. on Commn.*, Vol. 53, No. 9, September 2005.
- [11] V. Swathi, K. Rajani , and K. Padmaja , "Blind Equalization Based on Modified Constant Modulus Algorithm," *International Journal of Advanced Research in Computer and Communication Engineering*, Vol. 3, Issue 5, May 2014.
- [12] R. Vanka, B. Murty, and C. Mouli, "Adaptive Blind Equalization of QAM Transmitted Constellations across Linear Band-Limited Channel," *IOSR Journal of VLSI and Signal Processing*, Vol. 4, Issue 3, May-June 2014.
- [13] D.R. Srinivas and S. Murthy, "Blind Adaptive Equalization of Complex Signals based on the Constant Modulus Algorithm," *International Journal of Computer Applications*, Vol. 11, No. 5, December 2010.
- [14] K. Oh and Y. Chin, "Modified constant modulus algorithm: Blind equalization and carrier phase recovery algorithm," *IEEE International Conference on Communications*, pp. 498–502, June 18–22, 1995.
- [15] J. Yang, J.-J. Werner, and G. A. Dumont, "The multi modulus blind equalization algorithm", *Digital Signal Processing*, 1997, pp. 127–130.
- [16] S. Arivukkarasu and R. Malar , "Multi Modulus Blind Equalizations for Quadrature Amplitude Modulation," *International Journal of Innovative Research in Computer and Communication Engineering*, Vol. 3, Issue No. 3, March 2015.
- [17] A. Nasir, S. Durrani , and A. Kennedy, "Blind Fractionally Spaced Equalization and Timing Synchronization in Wireless Fading Channels," *IEEE International Conference on Future Computer and Communication*, May 2010.
- [18] Y. Li and Z. Ding, "Global convergence of fractionally spaced Godard (CMA) adaptive equalizers," *IEEE Trans. Signal Process.* , Vol. 44, No. 4, pp. 818–826, April 1996.
- [19] I. Fijalkow, A. Touzni, and R. Treichler, "Fractionally Spaced Equalization Using CMA: Robustness to Channel Noise and Lack of Disparity," *IEEE Trans. on Signal Process.* , Vol. 45, No. 1, January 1997.

- [20] rthk.hk, "Systems of DAB:Eureka 147," http://rthk.hk/about/dab/systems_e.htm, Checked on: June 26, 2016
- [21] wikipedia, "microSD," <https://simple.wikipedia.org/wiki/MicroSD>, Checked on: December 24, 2016
- [22] wikipedia, "MP3," <https://simple.wikipedia.org/wiki/MP3>, Checked on: December 24, 2016
- [23] Farncombe, "Benefits of digital broadcasting," *London: Plum Consulting*, January 2014.
- [24] A. Williams, A. Jones, H. Layer and G. Osenkowsky, *National Association of Broadcasters ENGINEERING HANDBOOK*, 10th ed., USA: Focal Press, 2007.
- [25] Ittiam Systems, "Audio Compliance with ISDB-T," https://www.ittiam.com/wp-content/knowledge-center/whitepapers/WP007_isdb-t-audio-compliance.pdf, Checked on: December 22, 2016.
- [26] Wikipedia, "Digital Radio Mondiale," https://en.wikipedia.org/wiki/Digital_Radio_Mondiale, Checked on: July 1, 2016.
- [27] Y. Lee, S. Park, S. W. Kim, C. Ahn, and J. S. Seo, "ATSC Terrestrial Digital Television Broadcasting Using Single Frequency Networks," *ETRI Journal*, Vol. 26, No. 2, April 2004.
- [28] Advanced Television Systems Committee A/52, *ATSC Standard: Digital Audio Compression (AC-3, E-AC-3)*, Advanced Television Systems Committee, Inc. Washington, DC, December 2012.
- [29] G. N. Henderson, E. Bretl, S. Deiss, A. Goldberg, B. Markwalter, M. Muterspaugh, and A. Touzni, "ATSC DTV Receiver Implementation," *Proceedings of the IEEE*, Vol. 94, No. 1, January 2006.
- [30] Advanced Television Systems Committee A/53, *ATSC Digital Television Standard Part 1-6*, Advanced Television Systems Committee, Inc. , Washington, DC, January 3, 2007.
- [31] W. Fischer, *Digital Video and Audio Broadcasting Technology*, 3rd ed., Germany: Rohde & Schwarz GmbH & Co. KG, 2010.

- [32] D. Sparano, "WHAT EXACTLY IS 8-VSB ANYWAY?," <https://pdfs.semanticscholar.org/c91d/c2af16cb0c4dc519b7f521e87>, Checked on: December 24, 2016.
- [33] Advanced Television Systems Committee A/54A, *Recommended Practice: Guide to the Use of the ATSC Digital Television Standard, including Corrigendum No. 1*, Advanced Television Systems Committee, Inc. ,Washington, DC, December 20, 2006.
- [34] A. F. Molisch, *Wireless Communications*, 2nded., USA: John Wiley & Sons Ltd, 2011.
- [35] T. S. Rappaport, *Wireless Communications: Principles and Practice*, 2nded. Singapore: Pearson Education, Inc., 2002.
- [36] National Instruments, "Pulse-Shape Filtering in Communications Systems," <http://www.ni.com/white-paper/3876/en/>, Checked on: September 3, 2016.
- [37] G. Kalivas, *Digital Radio System Design*, 2nded., UK: John Wiley & Sons Ltd, 2009.
- [38] R. Jain, "Channel Models A Tutorial," http://www.cse.wustl.edu/~jain/cse574-08/ftp/channel_model_tutorial.pdf, Checked on: December 3, 2016.
- [39] A. Goldsmith, *Wireless Communications*, 1st ed., Cambridge University Press, 2005.
- [40] IDC Technologies, "FUNDAMENTALS OF FADING," http://www.idc-online.com/technical_references/pdfs/electronic_engineering/Fundamentals_of_Fading.pdf, Checked on: July 30, 2016.
- [41] H. Hijazi, "High Speed Radio-Mobile Channel Estimation in OFDM Systems," <http://hussein.hijazi.free.fr/research.php>, Checked on: September 3, 2016.
- [42] T. K. Sarkar, Z. Ji, K. Kim, A. Medour, and M. Salazar-Palma, "A Survey of Various Propagation Models for Mobile Communication," *IEEE Antennas and Propagation Magazine*. Vol. 45, No. 3, June 2003.
- [43] North Western, "What is the Doppler effect?," <http://www.qrg.northwestern.edu/projects/vss/docs/communications/3-what-is-the-doppler-effect.html>, Checked on: September 3, 2016.
- [44] Wikipedia, "Rayleigh fading." https://en.wikipedia.org/wiki/Rayleigh_fading, Checked on : September 3, 2016.

- [45] International Telecommunication Union, "Method for point-to-area predictions for terrestrial services in the frequency range 30 MHz to 3 000 MHz," *Radiowave propagation*, 2013.
- [46] D. Luengo and L. Martino, "Statistical Simulation of Multipath Fading Channels for Mobile Wireless Digital Communication Systems," *Simulation Technologies in Networking and Communications*, October 7, 2014.
- [47] J. Zhuang, L. Jalloul, R. Novak, and J. Park, "IEEE 802.16m Evaluation Methodology Document (EMD)", *IEEE 802.16 Broadband Wireless Access Working Group*, July 3, 2008.
- [48] W. G. Newhall, T. S. Rappaport, and D. G. Sweeney, "A Spread Spectrum Sliding Correlator System for Propagation Measurements," *RF Design Magazine*, April 1996, pp. 40-54.
- [49] K. Pahlavan and A. H. Levesque, *Wireless Information Networks*, 2nded. New Jersey: John Wiley & Sons, Inc., 2005.
- [50] S. Halford, K. Halford, and M. Webster, "Evaluating the Performance of HRb Proposals in the Presence of Multipath,"
http://www.ieee802.org/11/Documents/DocumentArchives/2000_docs/0282r18S-Evaluating%20the%20Performance%20of%20HRb%20Proposals%20in%20the%20Presence%20of%20Multipath.ppt, Checked on: July 11, 2016.
- [51] V. K. Madiseti, *The Digital Signal Processing Handbook*, 2nded. NW: CRC Press, 2009.
- [52] L. G. Morales, *ADAPTIVE FILTERING APPLICATIONS*, Croatia: InTech, June 2011.
- [53] S. Abrar, A. Zerguine, and A. K. Nandi, "Adaptive Blind Channel Equalization",
<http://cdn.intechopen.com/pdfs/31294.pdf>, Checked on: December 25, 2016.
- [54] F. Alberge, P. Duhamel, and M. Nikolova, Adaptive Solution for Blind Identification/Equalization Using Deterministic Maximum Likelihood, *IEEE Transactions on Signal Processing*, Vol. 50, No. 4, April 2002.
- [55] S. V. Vaseghi, *Advanced Digital Signal Processing and Noise Reduction*, 2nded., John Wiley & Song,, 2000.
- [56] Wong and Lok, *Theory of Digital Communications*, 2nd ed., John Wiley & Song, 2000.

- [57] A. Zaouche, I. Dayoub, J. M. Rouvaen, and C. Tatkeu, "Blind Channel Equalization Using Constrained Generalized Pattern Search Optimization and Reinitialization Strategy", *EURASIP Journal on Advances in Signal Processing*, Vol.: 2008, Article ID: 765462, August 26, 2008.
- [58] S. Abrar and Roy A. Axford, "Sliced Multi-modulus Blind Equalization Algorithm," *ETRI Journal*, Vol. 27, No. 3, June 2005.
- [59] Manoj, M. Kumar, and K. Rohilla, "Adaptive Equalization of Fractionally Spaced Equalizer Based on Activity Detection and Tap Decoupling," *International Journal of Engineering and Innovative Technology (IJEIT)*, Vol. 3, Issue 12, June 2014.
- [60] P. Roy and A. A. Beex, "Fractionally Spaced Blind Equalizer Performance Improvement," *The Bradley Department of Electrical and Computer Engineering*, January 2000.
- [61] ETSI TR 101 758, "Digital Audio Broadcasting (DAB); Signal strengths and receiver parameters ;Targets for typical operation," V2.1.1 (2000-11), 2000.
- [62] Intuitive Guide to Principles of Communications, "Inter Symbol Interference(ISI) and raised cosine filtering," <http://complextoreal.com/wp-content/uploads/2013/01/isi.pdf>,
Checked on: August 27, 2016.

Appendix A

Raised Cosine Pulse Shaping Filter

Raised cosine pulses are one class of pulses proposed by Nyquist due to they are realizable and had the same good qualities as the sinc pulse. A raised cosine pulses are a modification of the sinc pulse. Where the sinc pulse has a bandwidth of W , where W is specified as

$$W = 1/2T_s \quad (A.1)$$

The raised cosine pulses have an adjustable bandwidth which can be varied from W to $2W$. We want to get as close to the Nyquist bandwidth, W as possible with a reasonable amount of power. The factor α relate the archived bandwidth to the ideal bandwidth W as

$$\alpha = 1 - \left(\frac{W}{W_0}\right) \quad (A.2)$$

Where W is the Nyquist bandwidth and W_0 the utilized bandwidth

The factor α is called the roll off factor. It indicate how much bandwidth is being used over the ideal bandwidth. The smaller this factor, the more efficient the scheme. The percentage over the minimum required W is called the excess bandwidth. It is 100% for roll off 1.0 and 50% for roll of 50%. The alternate way to express the utilized bandwidth is

$$W_0 = (1 + \alpha)R_s \quad (A.3)$$

Where R_s , The symbol rate given by $R_s = 1/T_s$, T_s symbol time

The typical roll off values used for wireless communication ranges from 0.2 to 0.4.

The raised cosine pulse is defined in time domain as

$$h(t) = \text{sinc}(t/T_s) \frac{\cos(\pi\alpha t/T_s)}{1-(2\alpha t/T_s)^2} \quad (A.4)$$

The first part is the sinc pulse. The second part is a cosine correction applied to the sinc pulse to make it behave better. The sinc pulse insures that the function transitions at integer multiples of symbol rate which makes it easy to extract timing information of the signal. The cosine part works to reduce the excursion in between the sampling instants. The

bandwidth is now adustable. It can be any where from $\frac{1}{2} R_s$ to R_s . It is greater than the Nyquist bandwidth by factor $(1+ \alpha)$. For $\alpha=0$, the above equation reduce to the sinc pulse, and for $\alpha=1$, the equaltion becomes that of pure square pulse[61], Figure A.1 (a).

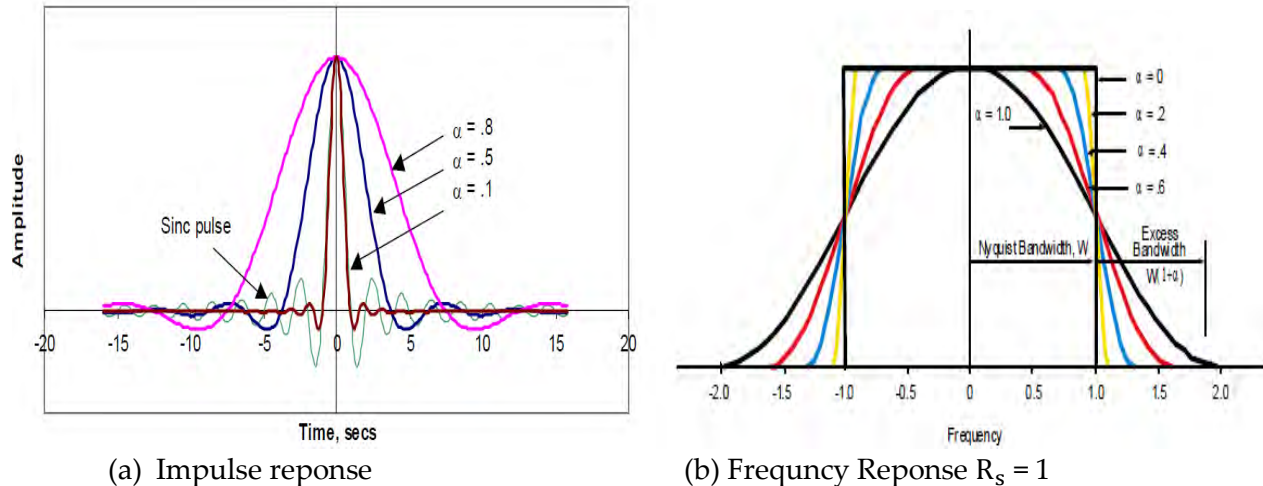


Figure A.1: Raised cosine impulse & frequency reponse

In frequency domain, the relationship is given by

$$H(f) = \begin{cases} 1 & \text{for } |f| \leq \frac{1-\alpha}{2T_s} \\ \left\{ \cos^2 \frac{\pi T_s}{2\alpha} \left(|f| - \frac{1-\alpha}{2T_s} \right) \right\} & \text{for } \frac{1-\alpha}{2T_s} \leq |f| \leq \frac{1+\alpha}{2T_s} \\ 0 & \text{for } |f| > \frac{1+\alpha}{2T_s} \end{cases} \quad (\text{A.5})$$

The frequency response looks somewat like a square pulse. A randge of bandwidths are possible depending on the chosen α . The bandwidth can be anywhere from $\frac{1}{2} R_s$ (the same as W) for the sinc pulse to R_s for the square pulse [61], Figure A.1 (b).

The duty cycle states just how wide the sampling pulse is compared to the symbol time. A large duty cycle implies a really big(or a square pulse) and a small duty cycle implies a very narrow pulse.

$$\text{duty cycle} = \frac{\tau}{T} \quad (\text{A.6})$$